NEW MAPPING IN THE EAST RANGE, NEVADA: IMPLICATIONS FOR THE WINNEMUCCA AND FENCEMAKER DEFORMATION BELTS

by

JAMES NUTAITIS

(Under the Direction of Sandra Wyld)

ABSTRACT

The East Range, located in north-central Nevada is an excellent location to study the relationship between the Early to Middle(?) Jurassic east-vergent Luning-Fencemaker fold-thrust belt (LFTB) and the Jurassic west-vergent Winnemucca Deformation belt (WDB). Many aspects of the WDB are poorly understood and controversial. Because of their proximity to one another, continued study of the WDB will help further constrain the age and extent of the LFTB. This study involved detailed mapping of units and structure in the central East Range, which lead to the conclusion that the interpretation of the WDB is incorrect, and its principal features are a product of east-vergent deformation. Folding and faulting previously associated with the WDB is explained by eastward propagation of deformation into the footwall of the Fencemaker thrust. New mapping of the central East Range in addition to previous fossil data has lead to alternative interpretations age and extent of Paleozoic and Triassic rocks in this area.

INDEX WORDS: **East Range, Luning-Fencemaker fold-thrust belt, Winnemucca deformation belt, North-central Nevada.**

NEW MAPPING IN THE EAST RANGE, NEVADA: IMPLICATIONS FOR THE WINNEMUCCA AND FENCEMAKER DEFORMATION BELTS

by

JAMES NUTAITIS

B.S., West Virginia University, 2007

A Thesis Submitted to the Graduate Faculty of The University of Georgia in Partial Fulfillment of the Requirements for the Degree

MASTER OF SCIENCE

ATHENS, GEORGIA

2010

NEW MAPPING IN THE EAST RANGE, NEVADA: IMPLICATIONS FOR THE WINNEMUCCA AND FENCEMAKER DEFORMATION BELTS

by

JAMES NUTAITIS

Major Professor: Sandra Wyld

Committee: Jim Wright
Douglas Crowe

Electronic Version Approved:

Maureen Grasso
Dean of the Graduate School
The University of Georgia
December 2010

TABLE OF CONTENTS

LIST OF FIGURES

Page

CHAPTER 1: INTRODUCTION

The Winnemucca Deformation Belt (WDB; Figs. 1.1 and 1.2) was defined by Elison (1987), Heck (1987), Speed et al. (1988), Elison and Speed (1989), and Stahl (1989) as a belt of major west-vergent shortening of Jurassic age in the north-central, Nevada. Principal structures associated with the WDB are the Willow Creek thrust (WCT; Figs. 1.2 and 1.3) and folds that are associated spatially with the thrust. The total amount of shortening within the belt is estimated to be on the order of 10"s of kilometers (Elison. 1987). Age of shortening is inferred to be Late(?) Jurassic based on apparent cross-cutting relations with the Jurassic Luning-Fencemaker fold-thrust belt (LFTB; Figs. 1.1 and 1.2) and a post-tectonic pluton dated at circa 153 Ma (Elison and Speed, 1989; Elison et al., 1990).

The WDB is important for several reasons. First, it is anomalous from a regional perspective because other Mesozoic shortening belts in this part of the Cordillera are east-vergent, including the Jurassic LFTB to the west(Oldow, 1984; Elison and Speed, 1989; Wyld, 2002;) and the Cretaceous Sevier fold-thrust belt (SFTB) to the east as depicted in figure 1.1 (DeCelles, 2004). Why a belt of back-thrusting should have developed in this restricted area is unclear. Second, the WDB is believed to be responsible for bringing lower Paleozoic rocks to the surface far west of their principal area of exposure in eastern Nevada, a relation that appears to require considerable vertical offset on the WCT (Fig. 1.3; Elison, 1987; Speed et al., 1988). Third, the WDB provides

a crucial upper limit on the age of deformation in the LFTB, which is otherwise unknown (Elison and Speed, 1989; Wyld, 2002; Wyld et al., 2003). Lastly, its age and location are important to ongoing controversies regarding whether Jurassic and Cretaceous shortening in the U.S. Cordillera represent separate orogenic events (e.g., Miller et al., 1988; Smith et al., 1993; Wyld, 2002; Martin et al., 2010) or part of a continuum (e.g., DeCelles, 2004; DeCelles and Coogan, 2006).

Despite its importance, the WDB is also controversial and poorly understood, in terms of both the structures that define it and the age and affinity of the geologic units affected by it. Many conflicting interpretations have been presented over the last five decades, some of which even question whether the WCT exists (Ferguson et al., 1951; Silberling and Roberts, 1962; Whitebread, 1978, 1994; Elison, 1987; Stahl, 1989; Speed et al., 1988; Ketner, 2008).

The current project aims to address these problems by providing new, detailed structural data from the East Range (Figs. 1.2 and 1.3), one of the principal areas where WDB structures are found. Crucially, it is in the East Range where some of the most important relations and controversies about the WDB were identified by earlier workers. It was here where the clearest evidence was found for west-vergent structures and major shortening along these structures (Elison, 1987), and where the WCT was first defined (Silberling and Roberts, 1962) and then later questioned (Ketner, 2008). Two major deformation belts converge here (Fig. 1.3): the east-vergent LFTB and the west-vergent WDB, making the East Range an ideal, and possibly the only location to examine cross cutting relations of the two thrust belts (Elison, 1987). Finally, the East Range is the only known location where the age of the WDB can be limited by cross-cutting relations with

Mesozoic plutons; this is the location of the critical ca. 153 Ma pluton noted earlier (Elison et al., 1990).

Regional Geologic Setting

The East Range, of north-central Nevada (Figs. 1.2, 1.3), lies along the boundary between two major early Mesozoic geologic provinces - a shelf terrane to the east, dominated by shallow marine carbonates and clastics, and a basinal terrane to the west, dominated by deep marine clastics (Speed, 1978; Elison and Speed, 1989; Wyld, 2002). These terranes represent parts of a single related depositional system of Triassic age (Speed, 1978; Lupe and Silberling, 1985; Wyld, 2000), but they were juxtaposed along the Fencemaker thrust during development of the Jurassic LFTB (Figs. 1.2, 1.3; Oldow, 1984; Elison and Speed, 1989; Wyld, 2002).

Shortening in the northern LFTB resulted in two principal phases of deformation. D1 deformation is widespread and represents the event that is responsible for closing the back arc basin in which the basinal strata were deposited (Wyld, 2002). This deformation resulted in tight to isoclinal folding at various scales, widespread cleavage-development under low-grade metamorphic conditions, and reverse faulting (Elison and Speed, 1989; Wyld et al., 2001; Wyld, 2002). This phase accommodated at least 55-75% NW-SE shortening and SE transport. It predates intrusion of a pluton dated at 165 Ma (Speed, 1974; Wyld and Wright, 2000; Wyld, 2002; Wyld et al., 2003). A D2 phase of deformation is associated with emplacement of deformed basinal terrane rocks over the shelf terrane along the Fencemaker thrust and is characterized by folds and local foliation in both terranes near the thrust (Fig. 1.4; Elison, 1987; Wyld et al., 2001, 2003; Wyld,

2002). This phase postdates the 165 Ma pluton and is assumed to be of Middle or Late Jurassic age (Wyld and Wright, 2000; Wyld, 2002).

Paleozoic rocks in the East Range and nearby areas have a more complex history, and depending on unit, either form depositional basement for the early Mesozoic rocks or are faulted over the younger rocks along Mesozoic thrusts. In general, Paleozoic rocks in central Nevada are grouped into one of two allochthonous terranes, either the early to middle Paleozoic Roberts Mountains allochthon (RMA) or the middle to late Paleozoic Golconda allochthon (Fig. 1.2; Burchfiel et al., 1992). Both consist of deep marine volcanic and sedimentary strata that were internally deformed prior to being thrust eastward over the continental margin. The RMA was emplaced during the Early Mississippian Antler orogeny along the Roberts Mountains thrust, now exposed in central to eastern Nevada (Burchfiel et al., 1992). The Golconda allochthon is interpreted to have been thrust over the RMA during the Permian-Triassic Sonoma orogeny along the Golconda thrust, now exposed in central Nevada (Burchfiel et al., 1992). Based on this structural arrangement, the RMA should be buried at depth beneath the Golconda allochthon at the latitude of the East Range; however, it is instead widely exposed here and in the nearby Sonoma Range (Fig. 1.2). Jurassic shortening within the WDB and back-thrusting along the WCT are interpreted to be responsible for uplift and exposure of the RMA in this area (Fig. 1.3; Speed et al., 1988).

Geology of the East Range and Prior Work

The East Range is a N-S trending block, (Fig. 1.5) uplifted by Cenozoic Basin and Range province normal faulting, that lies 30 miles SW of Winnemucca, NV (Fig. 1.2). It

can be divided into two parts, a northern part underlain by Triassic strata and a central part underlain mostly by Paleozoic rocks (Fig. 1.5). The boundary between these two parts generally follows Rockhill Canyon (Fig. 1.5). Interpretations of geologic relations in the northern Triassic rocks have been fairly consistent through time, but interpretations of the geology of the central East Range are more controversial. Unit affiliations and their ages, their contact types and locations have been interpreted differently through time (Ferguson et al., 1951; Silberling and Roberts, 1962; Whitebread, 1978, 1994; Elison, 1987; Ketner, 2008).

Stratigraphy and Intrusive Rocks

Triassic strata north of Rockhill Canyon comprise the different assemblages (Figs. 1.5 and 1.6). The Koipato, Star Peak, and Auld Lang Syne groups are part of the Triassic shelf terrane (Ferguson et al., 1951; Whitebread, 1978; Speed, 1978; Oldow, 1984; Lupe and Silberling, 1985; Elison, 1987). Detailed descriptions of these units are found in figure 1.6. The Lower Triassic Koipato Group consists mostly of felsic volcanogenic strata deposited in a subaerial setting, and is >1,500 m (Ferguson et al., 1951; Whitebread, 1978; Speed, 1978). The Middle to early Late Triassic Star Peak Group is almost 1 km thick and consists primarily of shallow marine carbonates with minor siliciclasitcs (Ferguson et al., 1951; Nichols and Silberling, 1977; Whitebread, 1978). The Star Peak Group is overlain by the 1,700 m thick, and consisting of fine-grained siliciclastic deltaic strata. The Late Triassic (Norian) Auld Lang Syne Group (Ferguson et al., 1951; Lupe and Silberling, 1985; Whitebread, 1978). The Star Peak and Auld Lang Syne Group have been divided into a number of formations, which are described in more

detail in figure 1.6. The Raspberry Formation in the northwest tip of the East Range (Fig. 1.5) was originally considered to be part of the Auld Lang Syne Group (Ferguson et al., 1951; Silberling and Roberts, 1962; Johnson, 1977), but was more recently reinterpreted as deep marine facies rocks of the coeval basinal terrane (Elison, 1987). This formation is a 3 km thick package of middle Norian strata consisting of slate, phyllite, and fine-grained siliciclastics (Ferguson et al., 1951; Elison, 1987).

In general, four different Paleozoic units have been identified in the central East Range: the Valmy Formation, Inskip Formation, Havallah Sequence, and an unnamed sequence of metasedimentary rocks located in the area around Lee Peak (Fig. 1.5). The Valmy and Inskip Formations have been identified since the earliest studies (Ferguson et al., 1951, Silberling and Roberts, 1962). The Valmy Formation, which is at least 1 km thick, consists primarily of dark chert, argillite, quartzite, and minor greenstone, and is well dated by fossils as early Early to Middle Ordovician (Ferguson et al., 1951; Roberts et al., 1958; Whitebread, 1978; Ketner, 2000). It is considered to be part of the RMA (Miller et al., 1992). Overlying the Valmy Formation to the west is the Inskip Formation, which consists of over 3,400 m of fine to coarse-grained siliciclastics, including distinctive quartz grit and quartz pebble conglomerate, with less common greenstone, and limestone (Roberts, 1958; Ferguson et al., 1951; Whitebread, 1978; Ketner, 2008). This unit, which contains Mississippian age fossils (Whitebread, 1978), has been speculatively interpreted to be part of the Antler overlap (Stewart, 1980), an assemblage of Mississippian to Pennsylvanian siliciclastic strata derived from and deposited on the RMA (Speed and Sleep, 1982; Miller et al., 1992). The contact between the Valmy and

Inskip Formations has been interpreted as either depositional (Ferguson et al., 1951; Whitebread, 1978) or faulted (Silberling and Roberts, 1962).

Paleozoic rocks north of the Valmy Formation in Rockhill Canyon consist of light to dark chert, argillite, siliceous argillite, and phyllite, with minor limestone, quartzite, conglomerate, greenstone, and volcanoclasitics, and are overlain unconformably by the Koipato Group (Silberling and Roberts, 1962). These rocks have been interpreted very differently through time (Fig. 1.7). They were originally included in the Inskip Formation (Ferguson et al., 1951), but were later reassigned to the Havallah Sequence, a Mississippian to Permian unit of the Golconda allochthon, by Silberling and Roberts (1962). Subsequent mapping by Whitebread (1978) and Elison (1987) supported this conclusion but indicated that an even larger area previously mapped as the Inskip Formation, is the Havallah Sequence. Ketner (2008) later concluded that all of the Paleozoic rocks north of the Valmy Formation in Rockhill Canyon are part of the Inskip Formation, as originally mapped by Ferguson et al. (1951). This conclusion was based on similarity of rock types and new fossil evidence from south of Rockhill Canyon indicating that the Inskip Formation is Mississippian to Permian and therefore overlaps in age with the Havallah Sequence.

The unnamed metasedimentary rocks are found in an elliptical shaped area around Lee Peak and are surrounded by the Valmy Formation and intruded by the Lee Peak pluton (Fig. 1.5). The metasedimentary rocks are divided into a carbonate, and a siliciclastic unit (Ferguson et al., 1951; Whitebread, 1978). The stratigraphic affinity of these units has been interpreted very differently though time (Fig. 1.7). They have been interpreted as Triassic shelf terrane (Ferguson et al., 1951; Silberling and Roberts, 1962),

as an unidentified Early Ordovician unit (Whitebread, 1978), and as the Preble Formation (Ketner, 2008). The structural relations between these units and the rest of the East Range have also been interpreted different ways (Fig. 1.7). The metasedimentary units were initially interpreted to be a structural window (Ferguson et al., 1951) and then interpreted to be in depositional contact with the overlying Valmy Formation (Ketner, 2008).

Rocks in the central East Range are intruded by a pluton that underlies Lee Peak (Lee Peak pluton), several stocks, and a number of dikes and sills. The intrusions have a compositional range from granite to diorite. These intrusions are inferred to be Jurassic on the basis of a K-Ar hornblende age of 153 ± 3 Ma from the Lee Peak pluton and a Rb/Sr age of 168.8 ± 25 from the Rockhill Canyon stock (Elison et al., 1990).

Luning-Fencemaker and Winnemucca Belt Deformation in the East Range

East vergent thrusting has been recognized in the northwestern East Range since the earliest studies (Ferguson et al., 1951), but it was not until Elison (1987) that this area was recognized to contain the Fencemaker thrust boundary between the basinal and shelf terranes (Fig. 1.5). On the basis of that study, Triassic rocks in the northern East Range were divided into allochthonous basinal strata and autochthonous shelf strata of the Fencemaker thrust (Elison, 1987). Elison (1987) further demonstrated that SE-vergent structures related to the LFTB are found throughout the northern East Range, in both the autochthon and the allochthon. These structures include tight to isoclinal folds, NW-dipping axial planar foliation, and NW-dipping thrust faults (Fig. 1.4). Two sets of these structures were identified in the allochthonous basinal strata and only one set in the autochthonous shelf strata, but all are considered to reflect progressive deformation along

the eastern margin of the LFTB during emplacement of the Fencemaker thrust (Elison, 1987; Elison and Speed, 1989). The principal LFTB structures in Triassic strata of the northern East Range is a spaced to penetrative foliation (S1), and NE-SW trending east-vergent folds and faults.

No studies have previously addressed the question of whether any LFTB deformation is recorded in the central East Range. Foliations, folds and faults have been identified in this area, but have generally not been assigned to any particular regional deformation event. The only exceptions are two controversial fault boundaries, an east-west trending high-angle fault along Rockhill Canyon and a low angle fault around the unnamed metasedimentary rocks of Lee Peak. Interpretation of these faults has changed significantly through time (Fig. 1.7) and played a critical role in defining the WDB (Stahl, 1987, Speed et al., 1988, Elison and Speed, 1989). The fault in Rockhill Canyon was originally shown as two separate fault segments that were not necessarily related (Ferguson et al., 1951). Silberling and Roberts (1962) concluded that these segments were actually one connected fault boundary that separated Triassic strata and the newly identified Havallah Sequence to the north from the Inskip and Valmy Formations to the south (Fig.1.7). They named this fault the Willow Creek thrust (WCT) and interpreted it to be a south-dipping fault that connected with the low angle fault around the Lee Peak metasedimentary rocks. At that time, the Lee Peak metasedimentary rocks were believed to be equivalent to Triassic strata of the shelf terrane (Ferguson et al., 1951; Silberling and Roberts, 1962), leading to the view that the metasedimentary rocks were exposed as a footwall window below the WCT (the Lee Peak window). Later mapping by Whitebread

(1978) and Elison (1987) supported this structural architecture despite new fossil evidence suggesting that the unnamed metasedimentary rocks were actually Ordovician.

Elison (1987) was the first to suggest that west-vergent folding in the northern East Range (Fig. 1.8) was related to emplacement of the WCT. Stratigraphic layering and the S1 foliation in the northern East Range are deformed into NE-SW trending folds in the area north of Rockhill Canyon (Ferguson et al., 1951; Silberling and Roberts, 1962; Elison, 1987). This includes a large syncline located in Triassic strata north of Rockhill Canyon (Fig. 1.8). These folds subsequently became a defining element of the west-vergent WDB (Fig. 1.3; Heck, 1987; Elison, 1987; Stahl, 1989; Speed et al., 1988). Evidence for a kinematic relation between folding and the WCT includes an increasing strain rate towards the WCT, and tighter folding to the SE (Elison, 1987). Elison (1987) was also the first to recognize that the geometry of faulting in the Rockhill Canyon area was very different from that around the Lee Peak window (Fig. 1.9). He speculated that the steeply-dipping Rockhill Canyon segment of the fault was a lateral ramp of the WCT and that the WCT around the Lee Peak window may have been domed upwards during emplacement of the Lee Peak pluton.

More recently, Ketner (2000, 2008) proposed a completely different explanation of structural relations in the central East Range based on reinterpretation of stratigraphy (Fig. 1.7F). He argued that the unnamed metasedimentary rocks of the Lee Peak window are in part depositional with the overlying Valmy Formation, and that their apparent Early Ordovician age (Whitebread, 1978) removes any need to invoke a major thrust fault in this area. Ketner (2000, 2008) restricts the WCT to the boundary in Rockhill Canyon,

which he interprets to be a high-angle reverse fault of minor displacement associated with the doming of the Lee Peak pluton.

Field Area and Methods

To shed light on the controversies noted above, the central East Range was remapped at a scale of 1:24,000. The field area is located between Koipato Group, north of Rockhill Canyon and Inskip Canyon (Fig. 1.5). Many of the controversial units and their boundaries are located within the field area. Important geographic features with in the field area are: Rockhill, Willow Creek, Inskip, Rawhide, and Spaulding Canyons; and Lee Peak (Fig. 1.10).

All units were examined for defining characteristics and this resulted in some significant changes to their map distribution in comparison with previous studies, as well as the identification of a new unit. Structural features within and between units were examined, compared, and evaluated in terms of cross cutting relations of deformation structures. The main structures identified within the field area are folds, foliations, lineations, a variety of high and low angle faults, and a previously unrecognized ductile shear zone on the western side of the range (Fig. 1.10). Faults were mapped in detail and structure contoured. Rock samples were collected throughout the field area for lithologic descriptions, micro-structural analysis, and identification of shear sense indicators in the ductile shear zone. Samples of key igneous rocks were collected for U-Pb geochronology.

Several new names are proposed here for some of the major structures. The ductile shear zone is named the Buena Vista shear zone, after the adjacent valley. The E-W trending fault in Rockhill Canyon has previously been called the WCT (Whitebread,

1978, Elison, 1987), but is here renamed the Rockhill Canyon fault to avoid ambiguity, and because it is a high angle fault and not a thrust. The low angle fault between the unnamed metasedimentary units and the Valmy Formation around Lee Peak has also previously been called the WCT (Whitebread, 1978, Elison, 1987), however it is here renamed the Lee Peak fault because results of this study indicate that it has a very different origin than previously proposed (Silberling and Roberts, 1962; Whitebread, 1978; Elison, 1987; Ketner, 2000, 2008). The term Lee Peak window is used to refer to the lower plate metasedimentary rocks bounded by the Lee Peak fault.

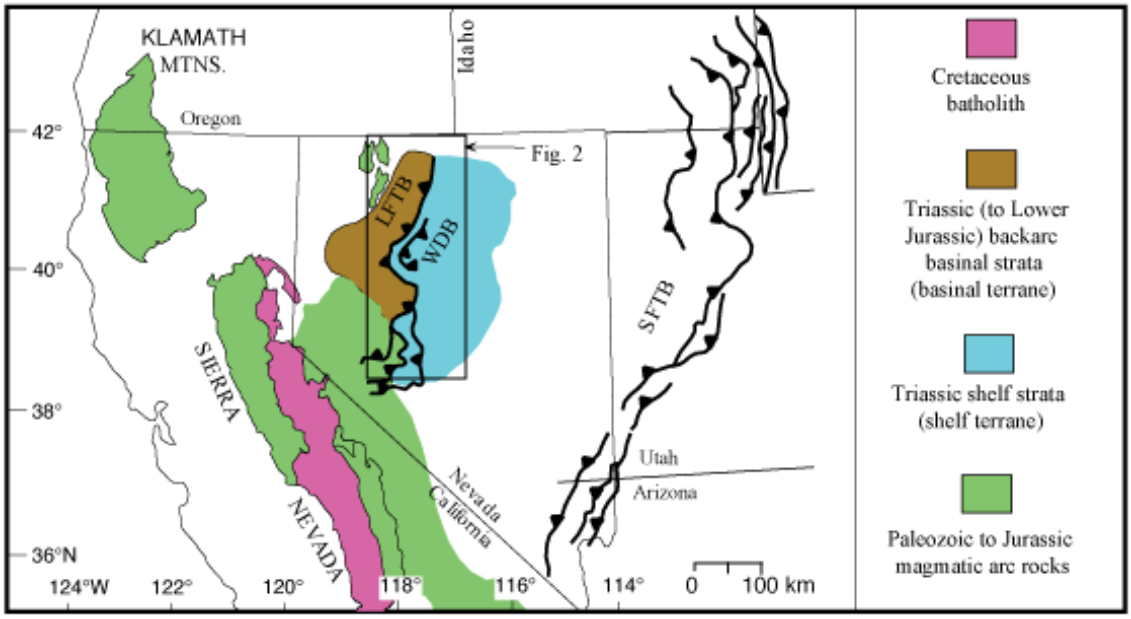

Fig. 1.1. Early Mesozoic rocks of the western US Cordillera, and locations of major Mesozoic fold and thrust belts. LFTB: Jurassic Luning-Fencemaker fold and thrust belt (Oldow, 1984; Elison and Speed, 1989; Wyld, 2002); only frontal thrusts are shown. SFTB: Cretaceous Sevier fold and thrust belt (DeCelles, 2004). WDB: Jurassic Winnemucca Deformation belt.

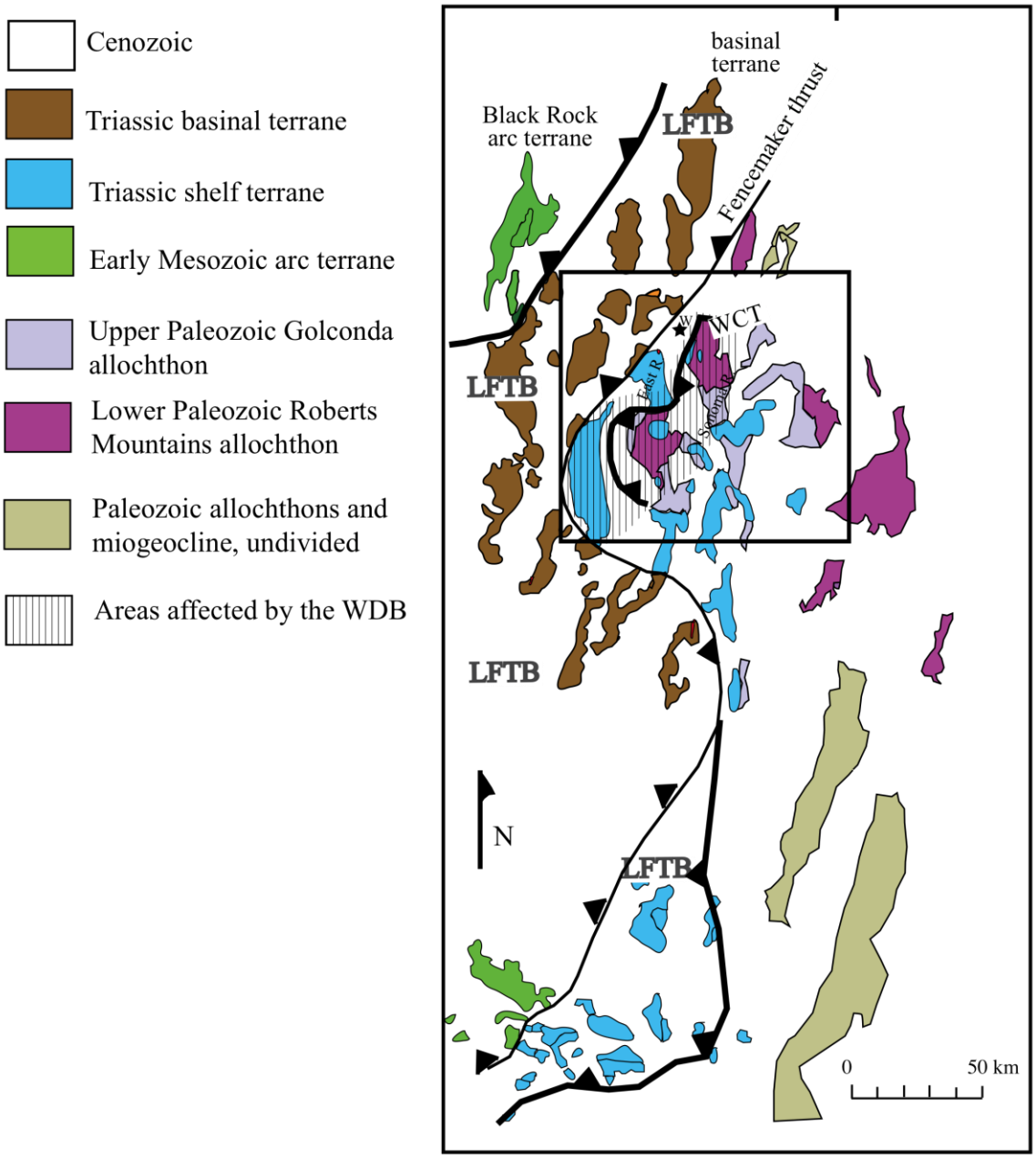

Fig. 1.2. Map showing terranes of north-central Nevada (see figure 1.1 for location). The northern LFTB is largely confined to basinal terrane. The Fencemaker thrust reflects final emplacement of deformed basinal terrane eastward onto shelf terrane. Structures associated with WDB are known only in northern shelf terrane, just east of the Fencemaker thrust. WCT is Willow Creek thrust. W is location of Winnemucca.

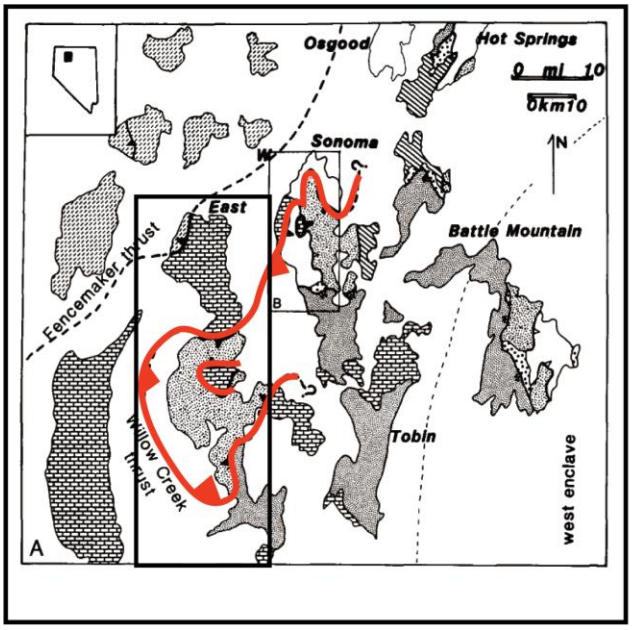

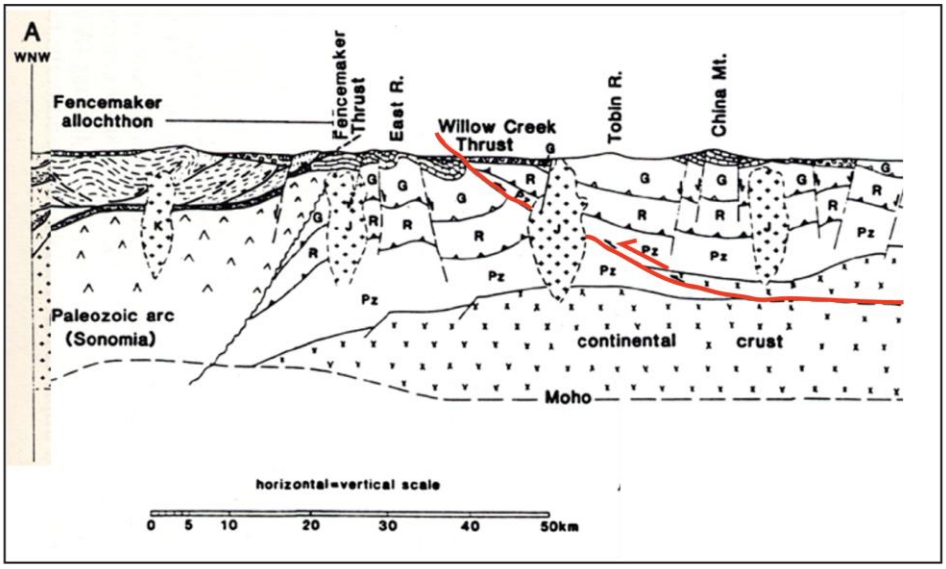

Fig. 1.3. Map and cross section view showing the extent of the Willow Creek thrust. (A) Map view showing the Jurassic west-vergent Willow Creek thrust (WCT, shown in red) emplacing Paleozoic basement over Triassic shelf terrane. (B) Cross section showing possible relationship between Fencemaker thrust and the WCT. This figure is modified from Stahl (1987), Speed et al. (1988), and Elison and Speed (1989).

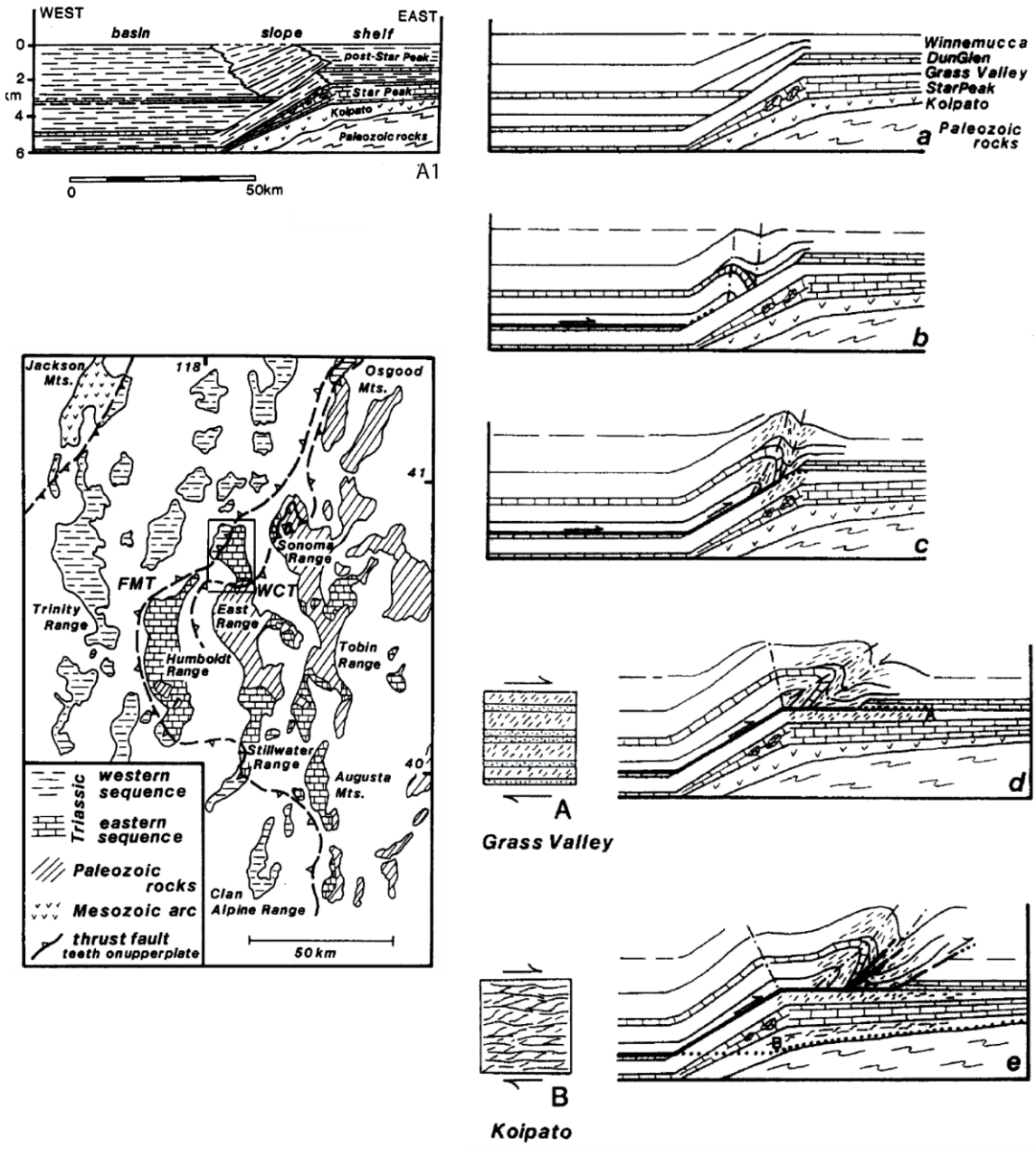

Fig. 1.4. Structural development along the Fencemaker thrust in the northern East Range (Modified from Elison and Speed, 1989). a-e) Show the progressive development of the LFTB and the associated folding and foliation. Note (A1) and (a) show original stratigraphy before LFTB deformation and correspond to the box in map view.

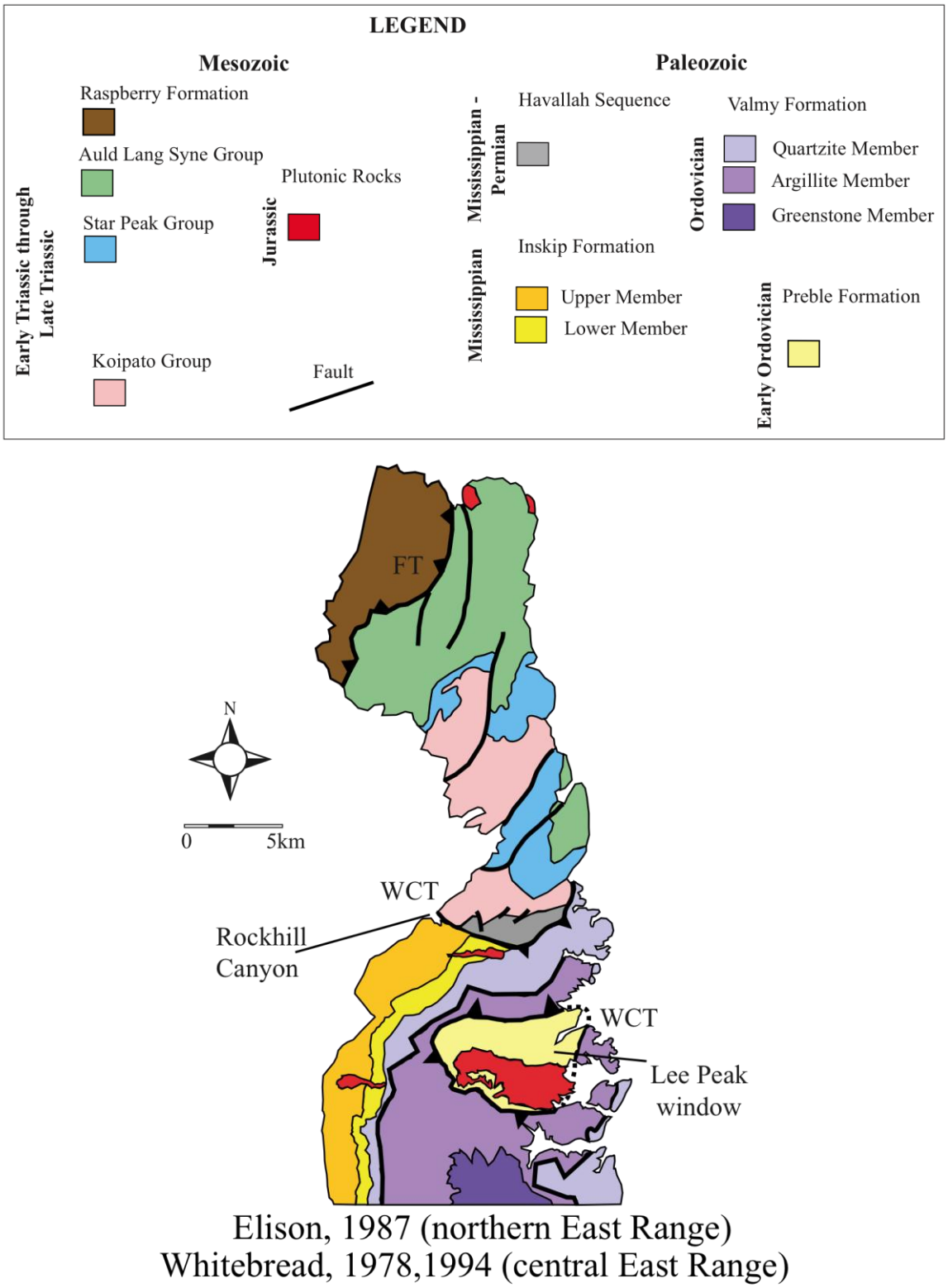

Elison, 1987 (northern East Range)
Whitebread, 1978,1994 (central East Range)

Fig. 1.5. Simplified geologic map of the East Range with the mapping of Elison (1987) north of Rockhill Canyon and Whitebread (1971) south of Rockhill Canyon.

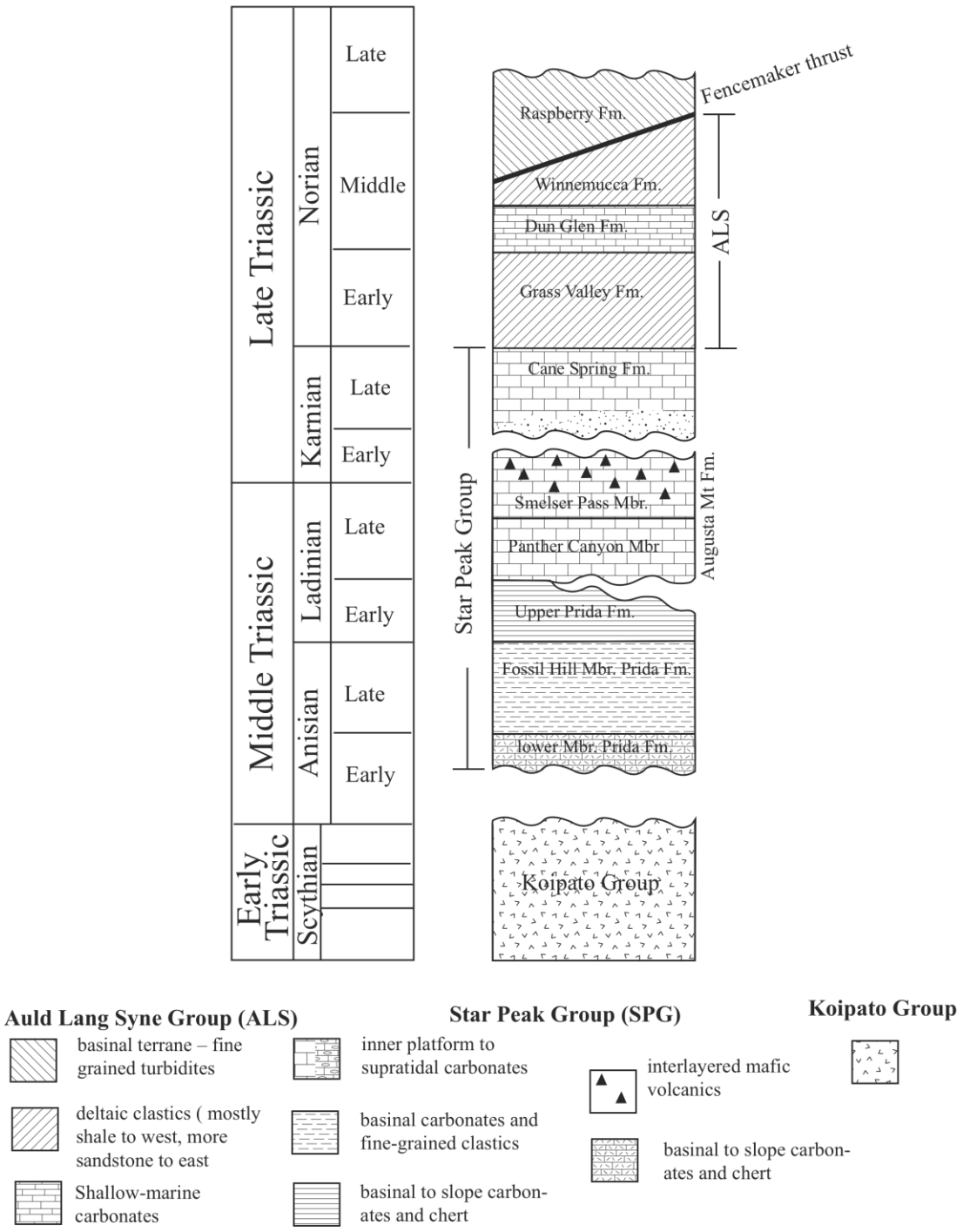

Fig. 1.6. Stratigraphic column of the northern East Range. Note emphasis on depositional environments, episodes of erosion, and stratigraphic variations. Note that the Raspberry Formation represents the Triassic basinal terrane, and is separated from the ALS by the Fencemaker thrust (Elison, 1989). This figure is modified from Wyld (2000).

Fig. 1.7. Simplified maps of the East Range showing interpreted geologic relations over time. (A) Based on Ferguson et al. (1951). Note Willow Creek Thrust (WCT) surrounding rocks inferred to be correlative with the Start Peak Group in the Lee Peak window (black arrow). (B) Based on Silberling and Roberts (1962). Note extension of WCT north of Rockhill Canyon, and addition of the Havallah Sequence to the stratigraphy in eastern Rockhill Canyon (red arrow). Note addition of fault between Inskip and Valmy Formations (red arrow). (C) Based on Johnson (1977). Note expansion to the south of the WCT and Lee Peak window rocks. Revision of southern areas to include Havallah Sequence, but not Inskip Formation (orange arrows). (D) Based on Whitebread (1978; reissued in color, 1994). Note increased detail in stratigraphy (upper and lower members of Inskip, and three members in the Valmy Formation). Also increased extent of Havallah Sequence north of Rockhill Canyon, changed boundaries of Lee Peak window, and revised interpretation of the rocks of the Lee Peak window are Early Ordovician (purple arrows). (E) Based on Elison (1987). Note identification of Fencemaker thrust and basinal strata of the Raspberry Formation in the NW East Range (green arrow). (F) Based on Ketner (2008). Note consolidation of Inskip Formation and Havallah Sequence, and removal of WCT (blue arrows).

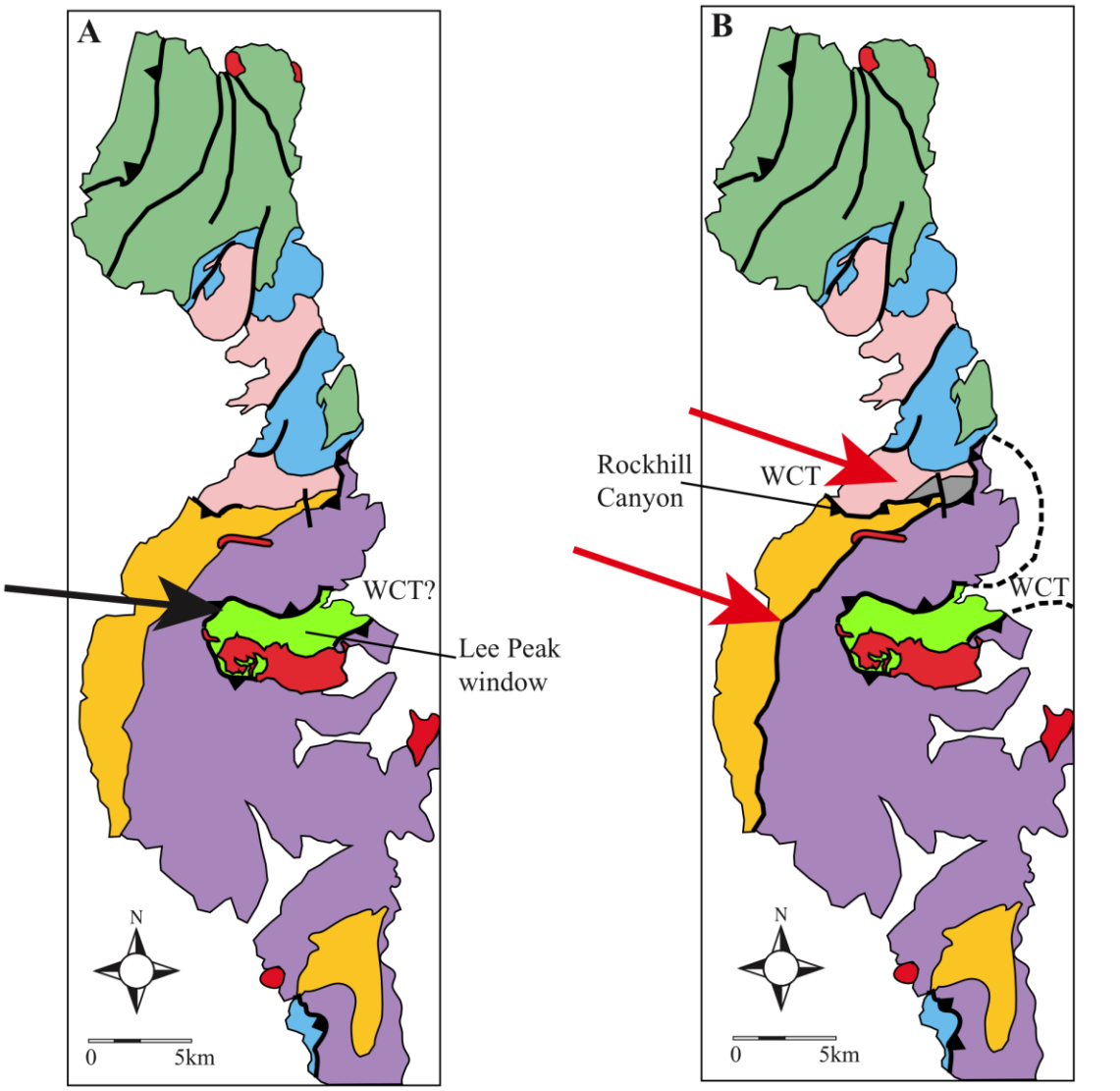
A
WCT?
Lee Peak
window
N
0
5km
B
Rockhill
Canyon
WCT
WCT
N
0
5km
Ferguson et al., 1951
Silberling and Roberts, 1962
LEGEND
Mesozoic
Paleozoic
Auld Lang Syne Group
Plutonic Rocks
Star Peak Group
Jurassic
Early Triassic through
Late Triassic
Triassic?
Fault
Koipato Group
Mississippian -
Permian
Havallah Sequence
Ordovician
Valmy Formation
Mississippian
Inskip Formation

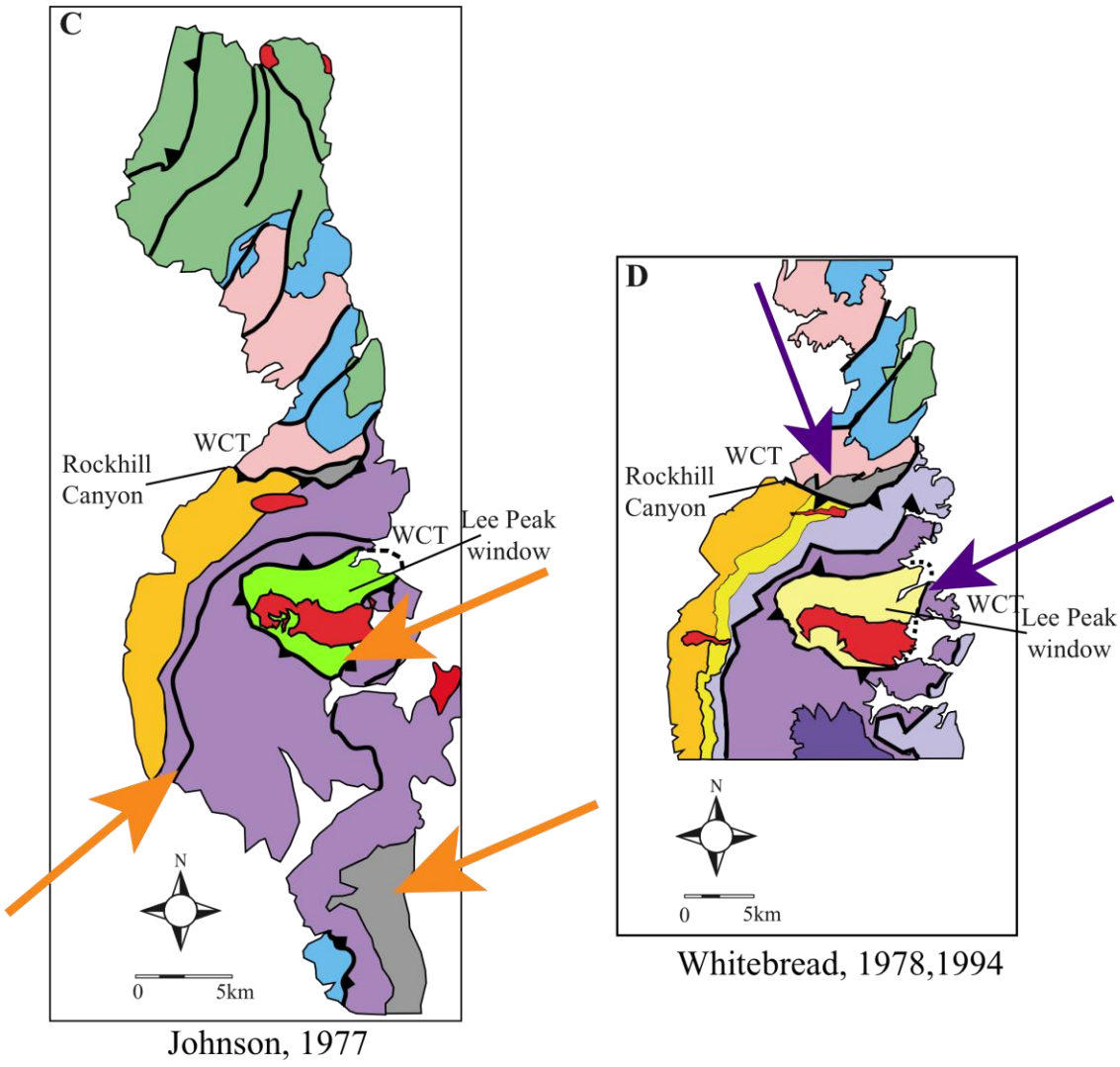
C
WCT
Rockhill
Canyon
WCT
Lee Peak
window
N
0
5km
Johnson, 1977
D
WCT
Rockhill
Canyon
WCT
Lee Peak
window
N
0
5km
Whitebread, 1978,1994
LEGEND
Mesozoic
Paleozoic
Auld Lang Syne Group
Plutonic Rocks
Star Peak Group
Jurassic
Triassic?
Early Triassic through
Late Triassic
Koipato Group
Fault
Havallah Sequence
Mississippian -
Permian
Valmy Formation
Ordovician
Quartzite Member
Argillite Member
Greenstone Member
Inskip Formation
Mississippian
Upper Member
Lower Member
Early Ordovician
No unit afinity
identified

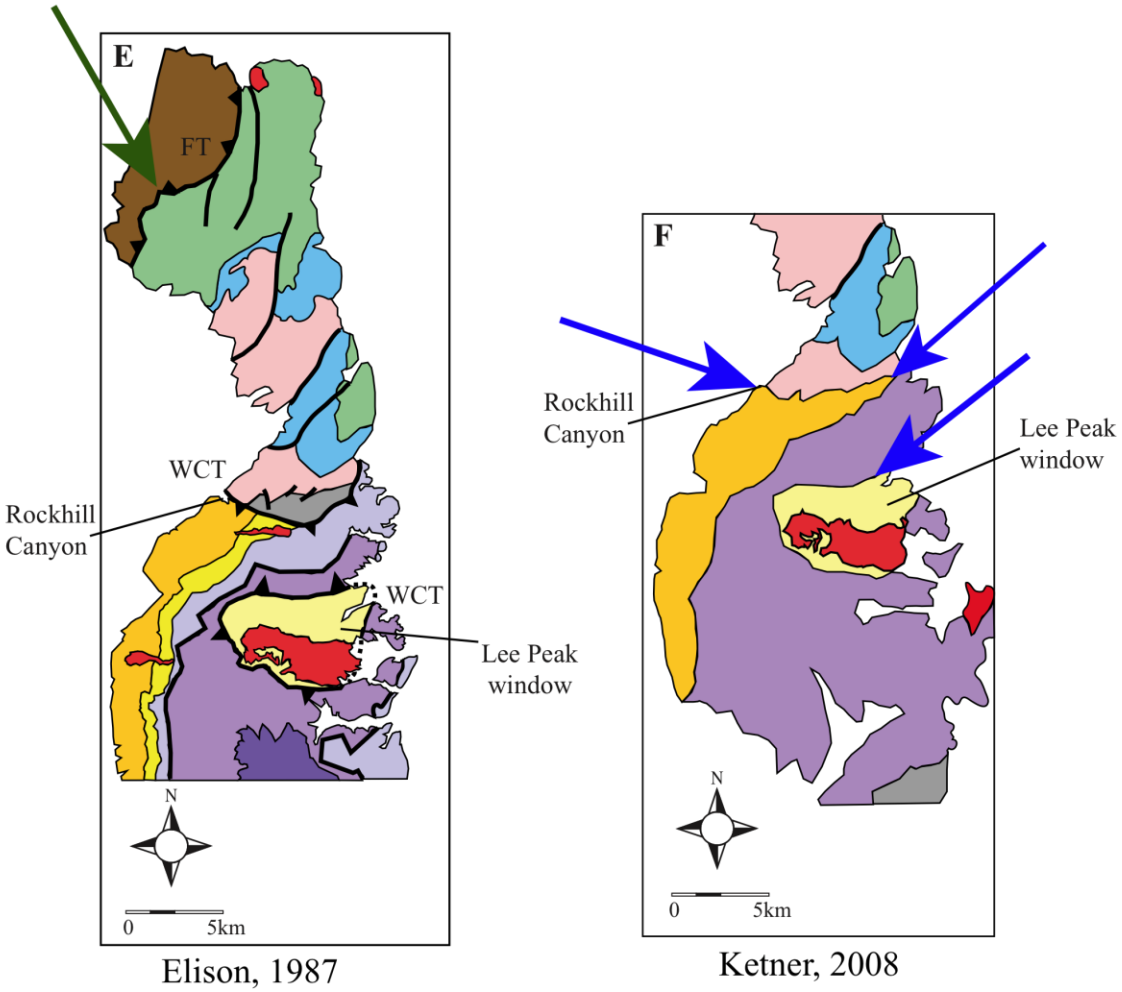
E
FT
WCT
Rockhill
Canyon
WCT
Lee Peak
window
N
0
5km
Elison, 1987
F
Rockhill
Canyon
Lee Peak
window
N
0
5km
Ketner, 2008
LEGEND
Mesozoic
Raspberry Formation
Auld Lang Syne Group
Star Peak Group
Koipato Group
Early Triassic through
Late Triassic
Plutonic Rocks
Jurassic
Fault
Paleozoic
Mississippian -
Permian
Havallah Sequence
Valmy Formation
Ordovician
Quartzite Member
Argillite Member
Greenstone Member
Mississippian
Inskip Formation
Upper Member
Lower Member
Early Ordovician
Preble Formation (?)

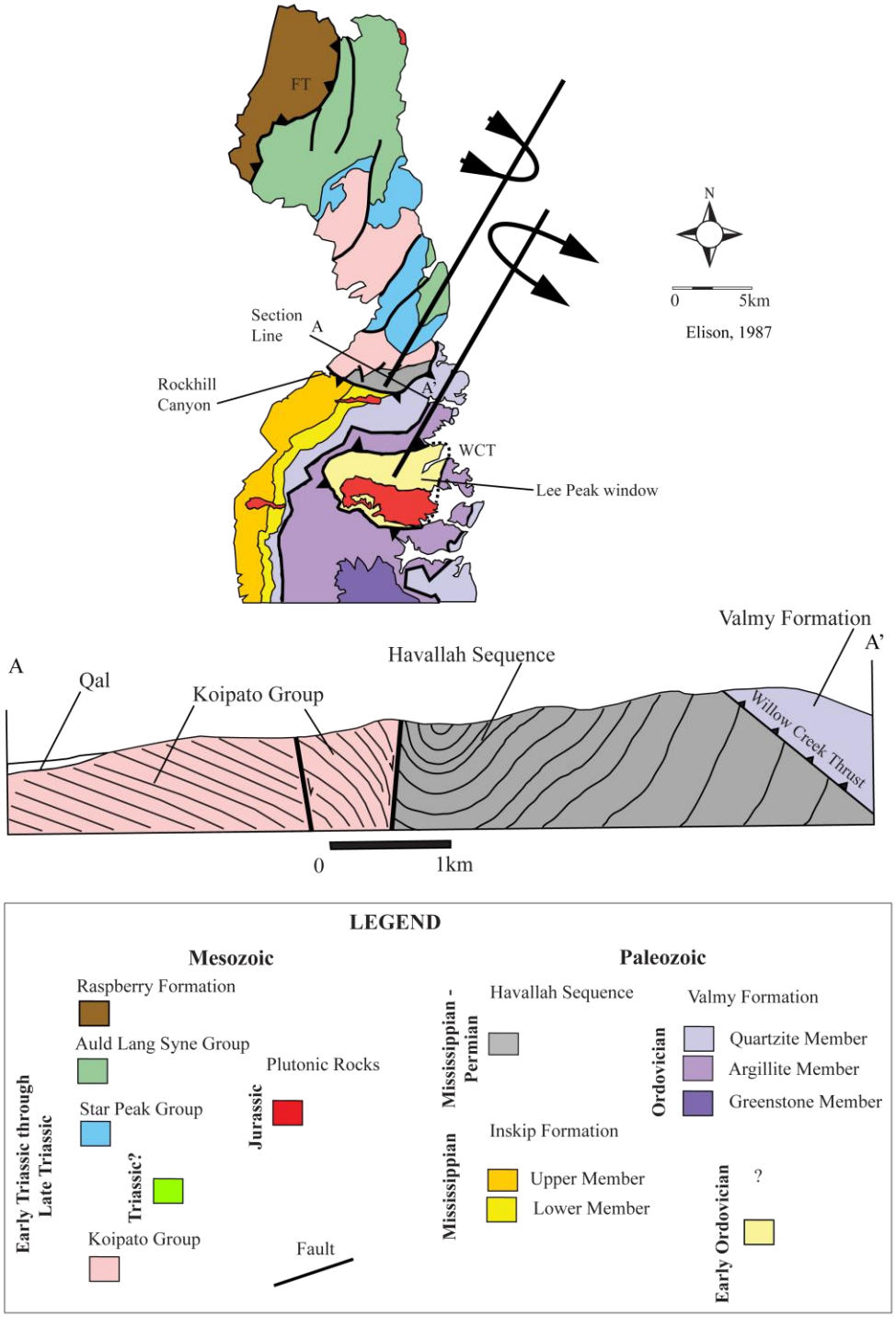

Fig. 1.8. Major folding interpreted in the East Range. NW overturned syncline in Triassic strata, and NW overturned anticline in Paleozoic strata. Cross-section A-A' shows interpretation of folding (modified from Elison, 1987).

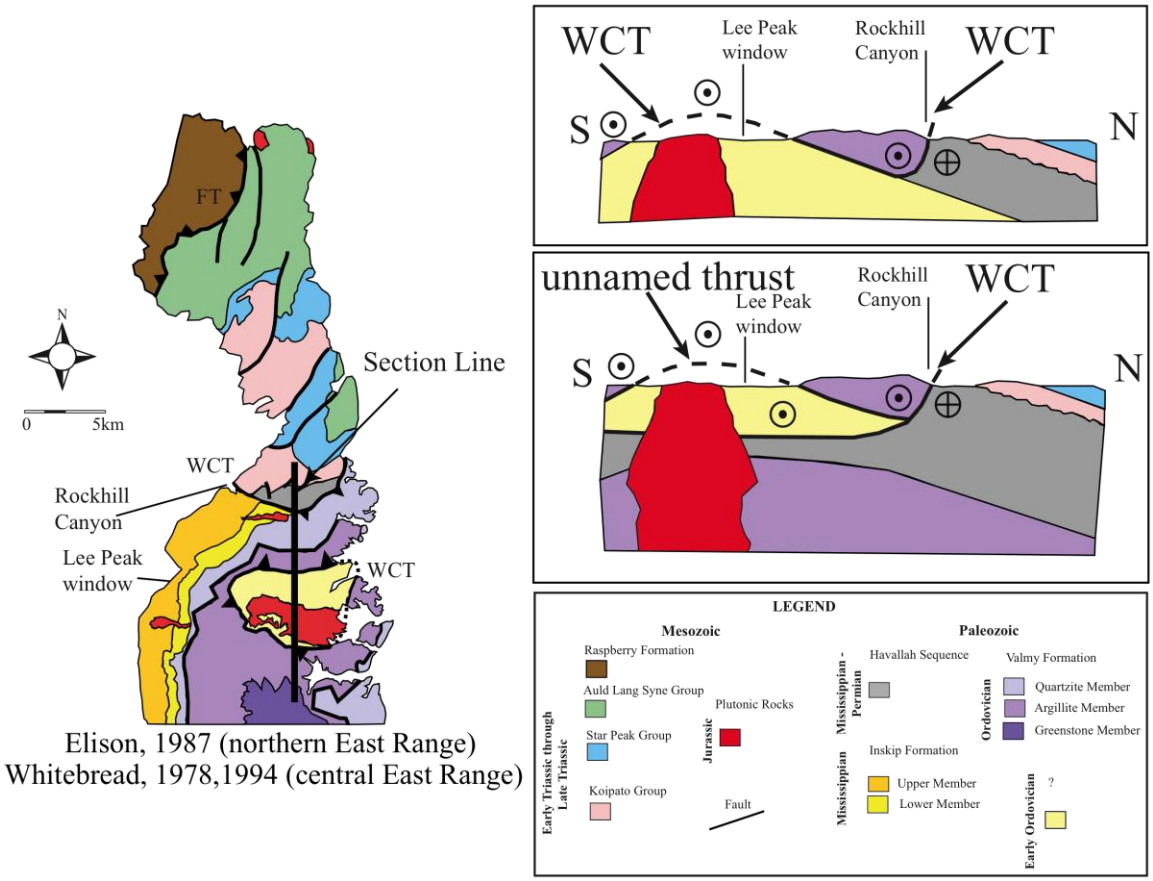

Fig. 1.9. Two possible interpretations for the relationship of faults in Rockhill Canyon and around the Lee Peak window (modified from Elison, 1987). In both (B) and (C), the faults are interpreted to reflect transport to the west: the steeply dipping segment of the WCT in Rockhill Canyon is a right-lateral tear fault. In (B) there is only one fault (WCT) and it is folded. In (C) the WCT underlies the central East Range and cuts a separate folded fault around the Lee Peak window.

Fig. 1.10. New mapping in the central East Range (see Plate 1 for more detail).

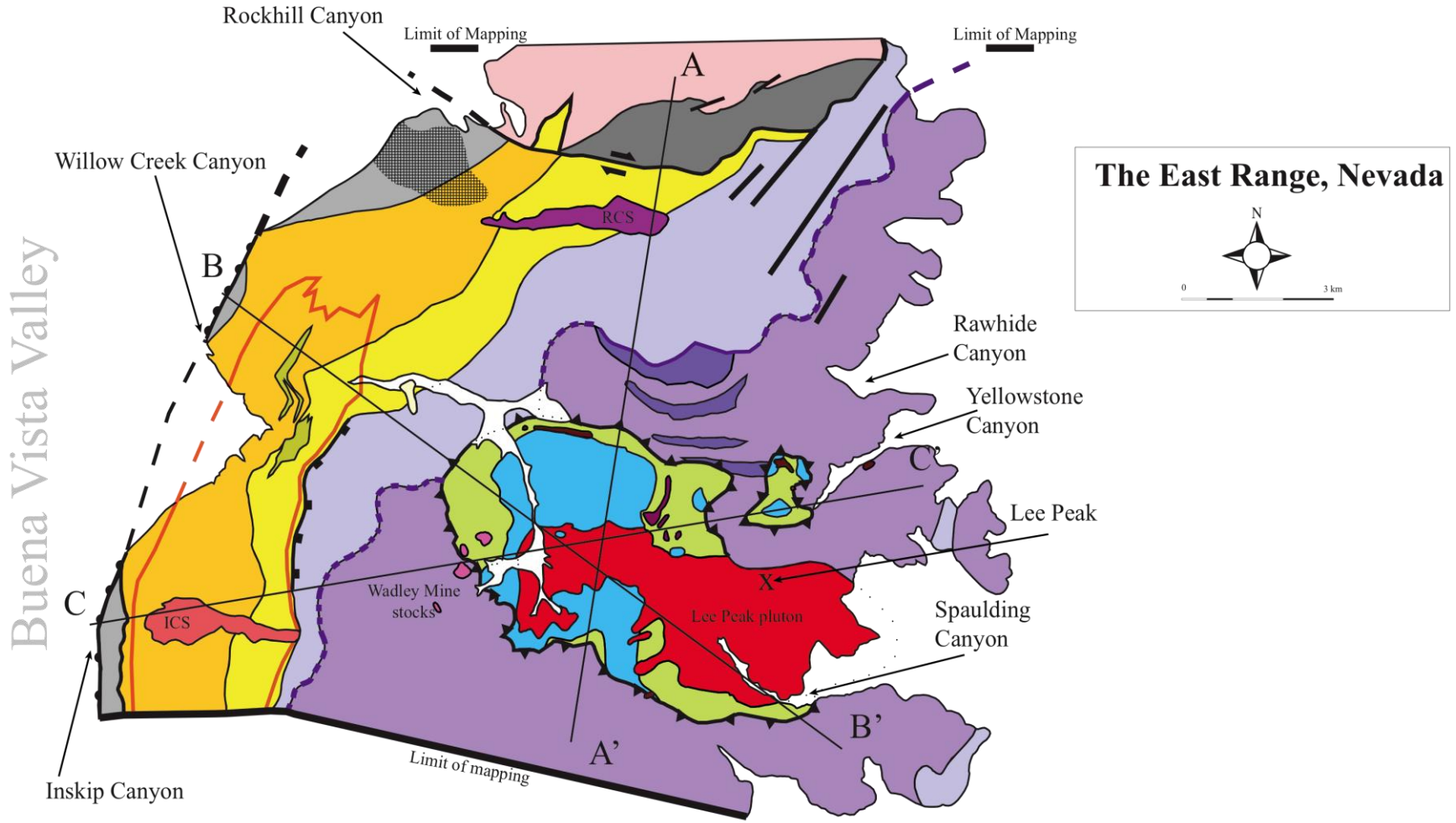
Rockhill Canyon
Limit of Mapping
Limit of Mapping
A
Willow Creek Canyon
B
RCS
Buena Vista Valley
The East Range, Nevada
N
0
3 km
Rawhide
Canyon
Yellowstone
Canyon
C'
Lee Peak
X
C
ICS
Wadley Mine
stocks
Lee Peak pluton
Spaulding
Canyon
B'
A'
Limit of mapping
Inskip Canyon

CHAPTER 2: STRATIGRAPHIC UNITS

Prior studies in the central East Range were focused on mapping and fossil collection. There have been no prior detailed studies of the stratigraphy of this area. The only previous published descriptions of units are found in the legends of geologic maps (Ferguson et al., 1951; Whitebread; 1978) and brief summaries in overview papers (e.g., Stewart, 1980; Gehrels et al., 2000; Ketner, 2000, 2008). Many of these are in conflict, as noted above. An accurate analysis of structural relations in the central East Range therefore requires an improved understanding of the stratigraphy of this area.

Mapping of units in the area was approached from the perspective that prior studies provide a guide to the stratigraphy, but that revisions might be required. Characteristic features of different units, contact types and contact locations were therefore evaluated as objectively as possible based on detailed field observations and supplemented with thin section petrography. In the following sections, units are defined and described, based on this study, and results are compared with those presented in earlier studies. A stratigraphic column, based on results of this study, is presented in figure 2.1. Sandstone samples from all relevant formations were collected for detrital zircon U-Pb geochronology, but were not processed for this study. Sample locations are shown on Plate1.

Valmy Formation

The Valmy Formation (Fig. 2.1) forms the lowest part of the main stratigraphic assemblage of the East Range (exclusive of the window units). It was divided by Whitebread (1987) into three members - the Greenstone, Argillite, and Quartzite members, and this division was used for mapping in this study. The base of the Valmy Formation is not exposed as the unit sits structurally above the window units along the Lee Peak fault. The stratigraphic top of the Valmy Formation is the contact with the Inskip Formation, which appears to be an unconformity. Maximum thickness of the Valmy Formation in the central East Range is difficult to calculate because the unit is internally folded and faulted, and because depth of the Lee Peak fault beneath the Valmy Formation in much of the area is speculative. Estimates based on cross-sections through the Valmy Formation south and west of the Lee Peak window suggest a maximum thickness of at least 1,000-2,000m (Fig. 2.1 and Plate 2).

Map relations suggest that the Greenstone member forms the lowest part of the Valmy Formation and the Quartzite member forms the highest part, with the Argillite member in between (Fig. 2.1). The contact between the Quartzite member and the underlying members is a fault (Fig. 1.10 and Plate 1), based on widespread evidence for truncation of bedding within adjacent units (Fig. 1.10 and Plate 1). This fault, which does not extend beyond the Valmy Formation to cut any younger units, is folded on a scale not seen with any other faults in the field area. The Valmy Quartzite basal fault therefore most likely predates deposition and deformation of younger units in the central East Range, and is possibly related to the Paleozoic RMA (Miller et. al., 1992). Whitebread (1978) also mapped this contact as a fault (Fig. 1.5.).

Greenstone and Argillite Members

The Greenstone member in the field area was found only as local map scale lenses contained within the Argillite member (Fig. 1.10 and 2.1). These lenses consist entirely of mafic metavolcanic rocks, identifiable in many places as fine-grained volcaniclastic strata or pillow lava. Volcaniclastic rocks include breccia with clasts from 1-12 cm in size and a carbonate matrix. Pillow lavas contain cm - m scale pillows in a carbonate matrix. Finer-grained greenstone/greenschist was probably derived from fine-grained volcaniclastic strata. Bedding is rarely seen within the Greenstone member, but where found is <1m thick and not laterally continuous. In thin section, samples from the Greenstone member are generally subophitic to poikilitic, fine-grained and consist of 40% plagioclase, 40% actinolite (replacing hornblende), and 10% chlorite, with minor sphene, calcite, and clinozoisite. Plagioclase forms laths up to 4mm, commonly engulfing actinolite and forming a poikilitic texture. This mineral assemblage is consistent with a basaltic protolith (Fig. 2.3).

The Argillite member is the most widely exposed unit in the central East Range (Fig. 1.10 and Plate 1). It consists mostly of argillite, siliceous argillite, and chert; other rock types are much less abundant and include quartzite, limestone, argillaceous limestone and greenstone. Due to the abundance of argillite, the Argillite member tends to have poor exposure, especially on the east side of the range.

Argillites in the member are dark grey to black and variably siliceous. Where well exposed they show laterally continuous, 1-10cm thick bedding. Local interbeds of dark grey to black chert are characteristic of the argillites. Where well exposed, these are also found to be 1-10 cm laterally continuous beds inter-layered within more abundant argillite (Fig. 2.2). Where exposure is poor, float consists of dark grey chips of argillite with subordinate dark fragments of chert.

Other rock types in the Argillite member are only present locally. Limestone ranges from light to dark grey, and varies from relatively thin (<10cm) interbeds to discontinuous lenses commonly found within greenstone. Bedding in these outcrops is not laterally continuous. Quartzite within the Argillite member is lithologically identical to the Quartzite member described below. The bedding of this quartzite is on the scale of meters but is not laterally continuous and does not form the large distinctive outcrops characteristic of the Quartzite member.

Volcanic rocks of the Greenstone member and within the Argillite member (Fig. 2.3) have a fractured texture with a mineral assemblage consisting of 15% plagioclase, up to 80% actinolite (replacing pyroxene), 10% quartz, and 5% chlorite, biotite, clinozoisite, and oxides. Plagioclase commonly forms laths up to 2mm. Veins within this fractured rock are filled with quartz, oxides, calcite, chlorite, and clinozoisite. This composition is similar to what is found in the greenstone member, and are consistent with a basaltic protolith.

Quartzite Member

The Quartzite member consists mostly of quartzite, with less abundant argillite, chert, and greenstone. The rock types in the Quartzite member are similar in appearance to quartzite, argillite and chert in the underlying Argillite member.

Massive outcrops (typically 3-10 m thick) of quartzite dominate the Quartzite member and often form laterally continuous beds that can be traced long distances across the field area (Figs. 2.2 and 2.4). The protolith of the quartzite is a fine to medium-grained (0.1-0.9mm), moderate to well-sorted, sub-rounded to rounded quartz arenite (Fig. 2.5). It is distinctively vitreous in appearance due to the abundance of quartz (95%), and dark, typically nearly black, due to the presence (<5%) of metamorphic biotite, chlorite, and oxides in the matrix. Trace muscovite is also present. Quartz veins are common. Outcrops of quartzite do not show any internal stratification. Channelization structures between quartzite and underlying chert-argillite beds (Fig. 2.2) suggests that the quartzite beds may have been mass flow deposits.

Comparison with Prior Studies and Biostratigraphic Age Relations

The distribution of the Valmy Formation in the central East Range as defined by this study is similar to that defined in prior studies, except in the area north of the Lee Peak pluton on the east side of the range (the area dissected by the Rawhide and Yellowstone Creek drainages; Fig. 1.10 and Plate 1). In prior studies, this area is shown to be underlain by metasedimentary rocks of the Lee Peak window. Detailed new mapping for this study indicates that only a small part of this area is underlain by the metasedimentary strata of the Lee Peak window (Fig. 1.10 and Plate 1). The rest of the

Rawhide-Yellowstone drainage was found to be underlain by the Valmy Formation, mostly the Argillite member but also including lenses of the Greenstone member. A detailed explanation of criteria used to distinguish the Argillite member from the window metasedimentary rocks, and rationale for revised mapping in the Rawhide-Yellowstone drainage, is provided in a later section on the Lee Peak window.

The new mapping has important implications for biostratigraphically-defined ages of units in the central East Range. Six conodont samples collected from the Valmy Formation south of the Lee Peak pluton indicate the unit ranges in age from early Early Ordovician through early Middle Ordovician (Fig. 2.6; Whitebread, 1994), or ca. 488-465 Ma according to the time scale of Gradstein et al. (2004). One conodont sample from carbonate in the lowermost part of Rawhide Canyon has a similar age of early Early Ordovician (Fig. 2.6, Whitebread, 1994). Previous mapping suggested that this sample dated the phyllite-rich window unit, thereby leading to the proposal that the window unit rocks form stratigraphic basement to the Valmy Formation. Based on the new mapping, the fossil age from the lower Rawhide Canyon sample does not date the window units. It instead provides an additional fossil age for the Valmy Formation - one that is consistent with all the other fossil ages obtained from the Valmy Formation.

Inskip Formation

The Inskip Formation was divided into two members by Whitebread (1978), a lower and upper member (Fig. 2.1). This division is retained here although large conglomerate lenses found in both members are distinguished as a sub-member (Fig. 1.10 and Plate 1), and part of Whitebread's upper member is reassigned to a new unit called the Buena Vista unit (described in a later section). Total thickness of the Inskip Formation as defined here is approximately 2,750m (Plate 2).

Lower Member

The lower member of the Inskip Formation consists mostly of sandstone, wacke, conglomerate, and phyllite. It is easily recognized in the field by the abundance of large quartz, quartzite, and chert clasts in the sandstones and conglomerates (Fig. 2.7). Minor argillaceous limestone and volcanogenic rocks are also locally present. Total thickness of the lower member reaches a thickness of 750m.

Conglomerate and sandstone form discontinuous horizons up to 10m thick, separated mostly by phyllite (Fig. 2.8). A map-scale lens of cobble to pebble conglomerate is identified south of Willow Creek (Fig. 1.10 and Plate 1) and indicates the thickness of some conglomerate horizons. Conglomerates are poorly sorted, matrix-supported, and contain rounded clasts ranging in size from 1x2 cm to 12x27 cm (Fig. 2.7). Large clasts consist mostly of fine to medium-grained, moderately-sorted, sub-rounded quartz arenite, and closely resemble quartzites found in the Quartzite member of the underlying Valmy Formation. Other less common clasts consist of chert and siliceous

argillite, similar to that found in the Valmy Formation. Although there are chert clasts, there is no bedded chert found within the Inskip Formation.

The distinctive coarse grit sandstone/wacke of the lower member is found in beds ranging from 30cm-3m, and is interbedded with fine-grained sandstone, phyllite, and argillite, all of which have 1-3m beds (Fig. 2.8). These sandstones and wackes are fine to coarse-grained, poorly sorted, and are characterized by 2-3 mm quartz/quartzite grains. Limestone beds within the lower member are rare, and consist of dark grey and commonly sandy limestone with cm scale bedding.

Microscopic inspection of these rocks indicate that quartzite cobbles within the conglomerate lenses (found in the Lower member) are composed of 95% quartz framework grains ranging in size from 0.05-0.5mm. These grains are sub-angular to sub-rounded, and are moderately sorted. The matrix (<5%) consists of chlorite, muscovite, biotite, and oxides (Fig. 2.9). Quartz and feldspathic wackes within the lower member are characterized by large (0.25-3mm), sub-angular, poorly sorted feldspar and quartz grains. Quartz consists of equal parts of poly- and mono-crystalline quartz, and lesser amounts of crypto-crystalline quartz grains. These framework grains represent 20-50% of the volume of the wacke. Finer grains (<0.25mm) within the wackes consist of quartz and feldspar, micas, and oxides. These finer grains and matrix represent 80-50% of the wacke (Fig. 2.10).

Upper Member

The upper member of the Inskip Formation includes some strata similar to those found in the lower member, but it is mostly finer-grained and more distal than the lower

member. The contact is located at the last outcrop of coarse grit sandstone or wacke of the lower member; this coincides closely with where the contact was located by Whitebread (1978). Total thickness of the upper member, as defined in this study, varies from 1,200m in the south to 2,000m in the north.

The most common rock types in the upper member are phyllite, argillite, siltstone, wacke, and sandstone. Less common are grey, silty limestone, and mafic volcanic rocks. Siliciclastics are interbedded in beds ranging in thickness from 2-50cm (Fig. 2.11 A), and these form laterally continuous outcrops. Limestone is commonly found interbedded with siltstone and argillite at a cm scale (Fig. 2.11 B). Volcanic rocks consist of primarily of greenstone in the form of pillow basalt (Fig. 2.12).

Field observations indicate that sandstones vary from poorly sorted wackes similar to those found in the lower member, to well sorted, fine-grained quartz arenite. However, these rocks lack the distinctive coarse grains found in the lower member. Thin section petrography indicates that the quartz wackes are fine to coarse-grained, poorly sorted, and sub-angular to sub-rounded (Fig. 2.13). Larger grains within the wackes consist primarily of mono-crystalline quartz and lesser amounts of polycrystalline quartz grains. Smaller grains compose 75% of the wacke and are dominated by silt-sized quartz. Oxides (10-20%) and micas (10-20%) represent a large portion of the smaller grains. Quartz arenites within the upper member are fine to medium-grained, moderate to well-sorted, and sub-rounded. Framework grains consist entirely of quartz and the matrix represents <10% of the total rock, consisting of equal parts oxides and micas.

Mafic volcanic rocks of the upper member collected for thin section petrography are identified as basalt (Fig. 2.14). These fine-grained basalts have a texture ranging from subhedral granular to felty. The composition consists of 40% actinolite, 40% plagioclase, 15% epidote, biotite, chlorite, pyroxene, calcite, and sphene. Most actinolite is usually 0.5mm, but is found up to 1.25mm. Actinolite appears to have fully replaced hornblende in most samples, and plagioclase is mostly fine-grained, representing the majority of the groundmass. When coarse-grained, plagioclase engulfs amphibole creating a poikilitic texture.

Felsic volcanic rocks are common throughout the Inskip Formation. These rocks form 1-2m thick beds. The beds consist of fine-grained, recrystallized, and are laterally continuous. In the field these volcanic rocks are parallel to bedding and identified on the basis of distinctive biotite clusters with felsic groundmass.

Samples collected for this study come from the Inskip Formation in areas north of the Inskip Canyon stock and in the vicinity of Willow Creek canyon. Thin section petrography indicates that this rock is a fine-grained biotite-rich felsic volcanic rock (Fig. 2.15). The composition consists of 30-60% quartz, 30% plagioclase, 15-25% K-spar, 10-15% biotite, 5% muscovite, 5% calcite, with trace amounts of rutile and oxides. Quartz is commonly 0.1-0.25mm and represents the majority of the groundmass. Feldspar is mostly located within the groundmass, and occasionally forms phenocrysts. Clusters of mica consists mostly biotite, with lesser amounts of muscovite. Muscovite rarely forms clusters without biotite.

Comparison with Prior Studies and Biostratigraphic Age Relations

The extent of the Inskip Formation, based on this study, differs in three main ways from that of previous studies.

(1) Rocks typical of those found in the lower member occur in the small fault bounded wedge surrounded by Koipato Group north of the western part of Rockhill Canyon (Fig. 1.10 and Plate 1). This small area of rocks has been interpreted previously as part of the Koipato Group (Ferguson et al., 1951), part of the Havallah Sequence (Whitebread, 1978), and part of the Inskip Formation (Ketner, 2008). Rocks in this wedge consist of fine to coarse-grained siliciclastics, mostly thick-bedded sandstone/wacke and pebble conglomerate interbedded with phyllite and siliceous argillite, and sandstones that contain abundant large (up to 2mm) grains of quartz and feldspar (Fig. 2.10 C). These features are identical to those found elsewhere in the lower member of the Inskip Formation.

(2) The lower member of the Inskip Formation extends significantly farther to the east, south of the fault in Rockhill Canyon, than shown by Whitebread (1978) (Fig. 1.10 and Plate 1).

(3) Some of the rocks previously included in the Inskip Formation, along the western range front, are now separated out as a new unit (Buena Vista unit), due to distinct differences with the underlying upper member (Fig. 1.10 and Plate 1).

The new mapping has implications for biostratigraphically-defined ages of the Inskip Formation. Previous conclusions about the age of the Inskip were based on two conodont samples (Mississippian, middle Osagean) from the lower member, south of Inskip Canyon, and, more recently, a conodont sample (Permian, Leonardian) from rocks

near the range front just south of Rockhill Canyon (Fig. 2.6 ; Whitebread, 1978; Ketner, 2000). These data led Ketner (2000) to conclude that the age range of the Inskip Formation is Mississippian to Permian. The new mapping, however, indicates that the Permian fossils come from rocks now included in a different unit. The new mapping also indicates that a fossil locality from the small wedge of rocks surrounded by Koipato Formation north of Rockhill Canyon should be assigned to the lower member (Fig. 1.10 and Plate 1). Conodonts from this locality are dated as Mississippian (Whitebread, 1978). Based on these data, the age of the Inskip Formation is Mississippian.

Contact Relations

In most places, the Inskip Formation appears to be in depositional contact with the underlying Valmy Formation, based on concordant bedding across the contact (Plate 1) and lack of any evidence for major faulting. One exception (discussed in Chapter 3) is in a section north of Inskip Canyon, where clear evidence for faulting along the contact is evident (Fig. 1.10 and Plate 1). Where apparently depositional, the contact between the Inskip and Valmy Formations must be unconformable, based on the large amount of time missing across the contact (Late Ordovician through Devonian). An unconformity is also strongly suggested by the abundance of clasts in the lower member that appear to be derived from erosion of the Valmy Formation (Fig. 2.7).

Buena Vista Unit (new)

Mapping on the western margin of the central East Range indicates the presence of lithologically distinct assemblages of strata that clearly do not belong to the upper

member of the Inskip Formation, although this is how the rocks were mapped in all prior studies. These rocks are named the Buena Vista unit based on the name of the adjacent valley (Fig. 1.10 and Plate 1).

The Buena Vista unit, as defined here, is characterized by thinly bedded to laminated silty limestone, argillite, and siltstone. Minor interbedded sandstone (<3cm) and isolated dismembered limestone beds (10cm-1m) are also found within the unit. The Buena Vista unit is lithologically similar but distinct from the upper member. The distinguishing features are thin to laminated bedding, finer grain size dominated by siltstone and argillite, higher percentage of limestone that is thinly interbedded with siltstone and argillite, and no volcanic rocks.

A sample of metamorphosed calcareous sandstone collected from the Buena Vista unit was used for thin section analysis. This sample consists of fine-grained recrystallized limestone and quartz siltstone. Beds of limestone are 0.5-3mm and contain small amounts of silt sized quartz. The siltstone beds range from 0.5-5mm and contain less common oxides, calcite, and tremolite (Fig. 2.16).

A localized zone of silicic alteration (Fig. 1.10 and Plate 1) overprints the northern part of the Buena Vista unit, obscuring its contact with the upper member of the Inskip Formation and the thicknesses of the Buena Vista unit and Inskip Formation in this area. However, bedding within the Buena Vista unit is concordant with the underlying Inskip Formation and there is no evidence of faulting. This suggests that the contact is depositional. However, it appears that the whole Pennsylvanian is missing, and that the contact between the Havallah and Inskip is most likely an unconformity.

Conodonts collected from a limestone body within what is here defined as the Buena Vista unit yield a Permian (Leonardian) age (Fig. 2.6.; Whitebread, 1978; Ketner, 2000). This age is younger than fossil ages from the Mississippian Inskip Formation and supports the interpretation of a separate unit.

Havallah Sequence

The large eastern wedge of Paleozoic rocks north of Rockhill Canyon (Fig. 1.10 and Plate 1) is identified in this study as the Havallah Sequence based on lithology and stratigraphic position, in agreement with previous mapping (Silberling and Roberts, 1962; Whitebread, 1978), and consists of inter-bedded chert and argillite, silty or sandy limestone turbidites, greenstone and pillow basalts, volcanic strata, minor amounts of wacke and conglomerate. In general the Havallah Sequence, as defined by prior studies in other areas (Nichols and Silberling, 1977) is unconformably overlain by Triassic rocks. The rocks north of Rockhill Canyon are consistent with this lithologic makeup, and are likewise overlain unconformably by Triassic strata (Koipato Group; Fig 2.1) The Havallah Sequence in the East Range is distinguished from the Inskip Formation based on the presence of interbedded light to dark colored chert and argillite, which is not found in the Inskip Formation; greater abundance of volcanic strata; and relatively smaller percentage of siliciclastics.

In the East Range the Havallah Sequence does not outcrop as prominently as the Inskip Formation and is generally finer-grained. The principal rock types are chert interbedded with argillite, siliceous argillite, and phyllite. The chert is commonly tan,

grey, and/or black. Bedding within these outcrops ranges from 5mm to 17cm (Fig. 2.17). Bedding is laterally continuous only at outcrop scale.

Subordinate rock types in the Havallah Sequence are: limestone, quartz wacke, conglomerate, greenstone, and greenschist tuff breccia with flattened clasts. Coarse-grained siliciclastics represent a smaller portion of the Havallah Sequence. Conglomerates are found in <2m beds that are not laterally continuous. Clasts are 20cm thick, and consist of chert, argillite, quartzite, and what appear to be clasts of coarse-grit Inskip sandstone. Quartz rich sandstone and quartzite are found in beds <1m that are not laterally continuous. These beds are commonly interbedded with limestone, chert, and argillite.

A sample of quartz wacke (Fig. 2.17A) examined under microscope revealed that it is medium-grained, sub-angular, and moderately sorted. Large grains within the sample represent 50% of the total volume with the majority (35%) being mono-crystalline quartz, and minority (15%) being poly-crystalline quartz. The mono-crystalline quartz grains are 0.1-0.75mm, and consist of sub-angular moderately sorted grains. The poly-crystalline quartz grains are 0.25-1mm, and were much more elongate that the mono-crystalline grains. Smaller grains and matrix consisted of 10% silt sized quartz grains, 10% oxides, and 5% muscovite.

A sample of calcite-rich quartz wacke (Fig. 2.18B) that was examined has 25% large framework grains. These grains are characterized by mono-crystalline quartz (24%) and calcite (1%). Quartz grains are 0.1mm to 0.5mm and are poorly sorted. Whereas calcite grains are 1mm in diameter. The finer grains and matrix consisted of 30% quartz,

40% calcite, and 5% oxides and muscovite. The petrographic data described above indicate that these siliciclastic rocks are of the Havallah Sequence.

Comparison with Prior Studies and Biostratigraphic Age Relations

Based on this study, rocks that are clearly distinct from the Inskip Formation and that share common features with the Havallah Sequence elsewhere in Nevada are found in the area north of Rockhill Canyon. Distribution of these rocks is similar to that defined by Silberling and Roberts (1962; Fig. 1.7B) but less extensive than defined by Whitebread (1978; Fig. 1.7D), because some of the rocks assigned in the latter study to the Havallah Sequence are here assigned to the Inskip Formation, as explained in an earlier section.

Fossil collections from what is here defined as the Havallah Sequence include conodonts and fusilinids of Permian (Wordian and Leonardian) age (Fig. 2.6; Silberling and Roberts, 1962; Whitebread, 1978), and conodonts of uncertain but potentially Mississippian age. Some of the Mississippian fossils are considered to be potentially reworked (Ketner, 2008). This view is supported by the stratigraphic position of rocks containing Mississippian fossils, which is higher than rocks containing Permian fossils (Fig. 2.6). Mississippian fossils found in the fault bounded western wedge of Paleozoic rocks north of Rockhill Canyon were previously assigned to the Havallah Sequence (Whitebread, 1978), but these rocks are now recognized to be contained in rocks from the lower member of the Inskip Formation, as discussed previously - age data from these rocks therefore does not constrain the age of the Havallah Sequence in the East Range. Collectively these data indicate that the Havallah Sequence in the East Range appears to

be of Permian age consistent with the Mississippian to Permian age of the Havallah Sequence elsewhere in Nevada (Silberling and Roberts, 1962).

Ketner (2008) consolidates the Havallah Sequence and Inskip Formation on the basis of overlapping age ranges based on fossil data, their lithic composition, and their adjacent positioning. However, as described above, new mapping along with the possibility of reworked fossils, demonstrates that the age range of the Havallah and Inskip Formations do not overlap. Detailed petrographic analysis (discussed in chapter 5) indicates that although similar, the lithics in the Havallah Sequence are distinct from the Inskip Formation. The fault that separates the two is interpreted to be a dextral strike/slip fault (discussed in chapter 4), which explains the juxtaposition of the Havallah and Inskip Formations.

Koipato Group

Only the southernmost part of the Koipato Group was mapped in this study, in the area north of Rockhill Canyon (Figs. 1.10, Plate 1, and 2.19). In this area, the Koipato Group consists of felsic tuffs and flows, siliceous phyllite, and conglomerate. The felsic tuffs and flows are buff to white bedding that range from centimeter to meter scale. They are commonly plag-phyric, containing large feldspar crystals with siliceous matrix. Phyllite within the Koipato Group is silver to green and silicic. Conglomerates are found at the base of the Koipato Group. Clasts within the conglomerates are flattened, silicic tuffs, which range in size from 3mm-10cm.

The contact between the Koipato Group and Havallah Sequence is parallel to bedding and partially faulted, and is interpreted to be an unconformity. Thickness of the

Koipato Group is not well constrained by this study because of the limited extent of mapping within the group.

Metasedimentary Rocks in the Lee Peak Window

The Lee Peak window contains metasedimentary rocks that are lithologically and metamorphically distinct from other units in the central East Range. It is surrounded by rocks of the Valmy Formation and intruded by the Lee Peak pluton and various stocks (Fig. 1.10 and Plate 1). The contact with the Valmy Formation is an outward-dipping, dome-shaped fault, the Lee Peak fault, which is described in a later section. The Lee Peak pluton is responsible for contact metamorphism and disruption of original structures within the metasedimentary rocks.

Two units have long been distinguished in the window (Ferguson et al., 1951; Whitebread, 1978), a crystalline limestone (marble) unit and a unit dominated by phyllite and slate. Ferguson et al. (1951) originally described the carbonate unit as overlying the phyllite unit, but Whitebread's (1978) mapping indicated that the opposite is true. In this study, the carbonate unit is named the Marble unit, and the phyllite unit is named the Phyllite unit. Only minimum thickness can be estimated for either unit since the base of the marble unit is not exposed and the top of the phyllite unit is cut out by the Lee Peak fault. Disruption by the Lee Peak pluton also obscures the thickness of the two units. Best estimates for minimum unit thickness, based on cross-sections through the window (Plate 2), is >1,000m for the marble unit and approximately 1,000m for the phyllite unit.

Marble Unit

The Marble unit consists entirely of light grey to white marble, and is easily visible from a distance (Fig. 2.20) and on aerial photographs. Most exposures of the marble unit are in the center of the window, but other small bodies of the unit occur to the east (Fig. 1.10 and Plate 1). Bedding measurements in the marble unit and map relations indicate that it underlies the phyllite unit along a gently dipping contact (Plate 2).

The Marble unit consists entirely of white to grey, fine to coarse-grained crystalline marble. Centimeter scale bedding is defined by dark graphitic layers and lighter layers (Fig. 2.21). Large 1cm long crystals of tremolite are visible in some hand samples.

Phyllite Unit

The Phyllite unit surrounds exposures of the Marble unit and is found mostly around the edge of the Lee Peak window (Fig. 2.20). It consists primarily of phyllite and slate, with minor marble and fine-grained quartzite, and metavolcanics. Marble beds are most abundant near the contact with the underlying marble unit and are identical in appearance to those in the underlying unit. The contact between the two units is thus interpreted to be depositional and gradational.

Overall, the Phyllite unit appears to consist of about 90% phyllite and slate, with 10% interbedded quartzite and marble. Due to the abundance of fine-grained strata, the phyllite unit has poor exposure and only rarely outcrops except when strata are hornfelsed (Fig. 2.22), or where marble and quartzite beds are present. Where outcropping is poor, the Phyllite unit can be recognized by an abundance of phyllitic

rocks found in the float. Where outcrops of the siliciclastic rocks are found, the phyllite and slate form thinly interbedded light and dark layers, and the quartzite forms 10-20 cm thick beds that are not laterally continuous. Marbles are white to light grey and form laterally discontinuous beds up to 1m thick.

Metamorphosed fine-grained sandstone collected near the Lee Peak pluton for microscopic examination suggested a protolith of very fine-grained, sub-rounded, well-sorted quartz wacke (Fig. 2.23 A). The composition is 60% quartz grains with an average grain size of 0.02mm, 30% biotite and muscovite, and10% cordierite ranging in size from 0.25-0.75mm. An abundance of metamorphic cordierite, biotite, and muscovite indicates that the protolith had significant clay content.

A sample of quartzite from the Phyllite unit collected near the Wadley Mine stocks (Fig. 1.10 and Plate 1) for microscopic examination indicates that the protolith is a coarse-grained, sub-rounded to rounded quartz arenite (Fig. 2.23 B). Framework grains make up 95% of the rock, and ranged in size from 0.25-1.25mm. They consist almost entirely of quartz, with about 3% unknown (possibly feldspar) altered grains. The matrix represents 2% of the rock and consists of muscovite, chlorite and oxides.

Phyllite collected from one of the scarce outcrops of this rock type in the Phyllite unit appears to have been derived from a silty mudstone. Composition is 15% quartz with an average grain size of 0.001-0.005mm, 80% muscovite and biotite, and 5% oxides. Faint spots are found locally and reflect incipient cordierite growth (Fig. 2.24). This sample was collected by the top of Yellowstone Canyon, an area near the Lee Pluton and surrounded by the Rawhide metagabbro (Fig. 1.10 and Plate 1).

The metasedimentary rocks within the Lee Peak window are clearly of a higher metamorphic grade than the other formations in the central East Range. A significant amount of this metamorphism within the Lee Peak window can be attributed to contact with the Lee Peak pluton and the surrounding stocks.

Comparison with Prior Studies and Biostratigraphic Age Relations

The Marble and Phyllite units, as defined here, correspond respectively to units OCsl and OCsu of Whitebread (1978). Detailed mapping of these units in the area around the Lee Peak pluton shows that the distribution of the Marble unit is very similar to that shown by Whitebread (1978), but that the Phyllite unit has a significantly different distribution on the northeast side of the pluton in the drainage basins of Rawhide and Yellowstone Creeks (Fig. 1.10 and Plate 1). Whitebread (1978) shows most of this area as underlain by the Phyllite unit (his OCsl), all the way east to the valley at the mouths of Rawhide and Yellowstone Creeks. Mapping for this study, however, indicates that most of this area is actually underlain by the Argillite member of the Valmy Formation, and that phyllite and marble occur only in a restricted area that forms a subordinate window east of the main window (Fig. 1.10 and Plate 1).

The Phyllite unit of the window and the Argillite member of the Valmy Formation appear to be similar in composition and appearance, leading to ambiguous map relations. The Phyllite unit rarely outcrops and distinguishing the two is a problem in areas where the Argillite member is poorly exposed, such as characterizes the Rawhide-Yellowstone drainage. Nonetheless, there are distinct differences between the two units and it is possible to map them in poorly exposed areas. The Valmy Argillite member is

characterized by dark siliceous argillite and dark grey to black chert. These rock types are not present in the Phyllite unit which instead is dominated by phyllitic rocks. In the field, the presence or absence of dark argillite and chert versus phyllite can thus be used to distinguish the two units. In addition, carbonates in the Phyllite unit are white to light grey marble, whereas carbonates in the Argillite member are darker grey (dirty) and less metamorphosed. Finally, quartzites in the Phyllite unit have a distinctive dark pink or off-white color and are very fine grained and thinly bedded, in contrast with the darker color, coarser grain size and thicker bedding of quartzites in the Argillite member. Characteristics of interbedded carbonate and quartzite can therefore also be used to distinguish the units. The area of the Rawhide-Yellowstone drainages was remapped using these criteria, yielding the new boundaries for the Valmy Formation and window units shown in figure 1.10. Of particular importance is the area along the mouth of Rawhide Creek, where Ordovician fossils were found (see below). This area is very poorly exposed, but float characteristics and rare outcrops are clearly consistent with the Argillite member and are not what is expected for the Phyllite unit (Fig. 2.25).

These new map relations have strong implications for interpretation of the age and stratigraphic affinity of the window units, and for structural relations in the area. Only one fossil collection has ever been obtained from rocks considered to be part of the window units. These fossils are Early Ordovician conodonts from a limestone exposed along the mouth of Rawhide Canyon (Whitebread, 1978). Based on these fossil ages and Whitebread's (1978) mapping, the window units were interpreted to be in part of Early Ordovician age and potentially correlative with the Cambrian to Ordovician Preble Formation (Ketner, 2000, 2008). However, mapping now indicates that the Ordovician

fossils are located within the Ordovician Valmy Formation, leaving the window units undated and open for interpretation.

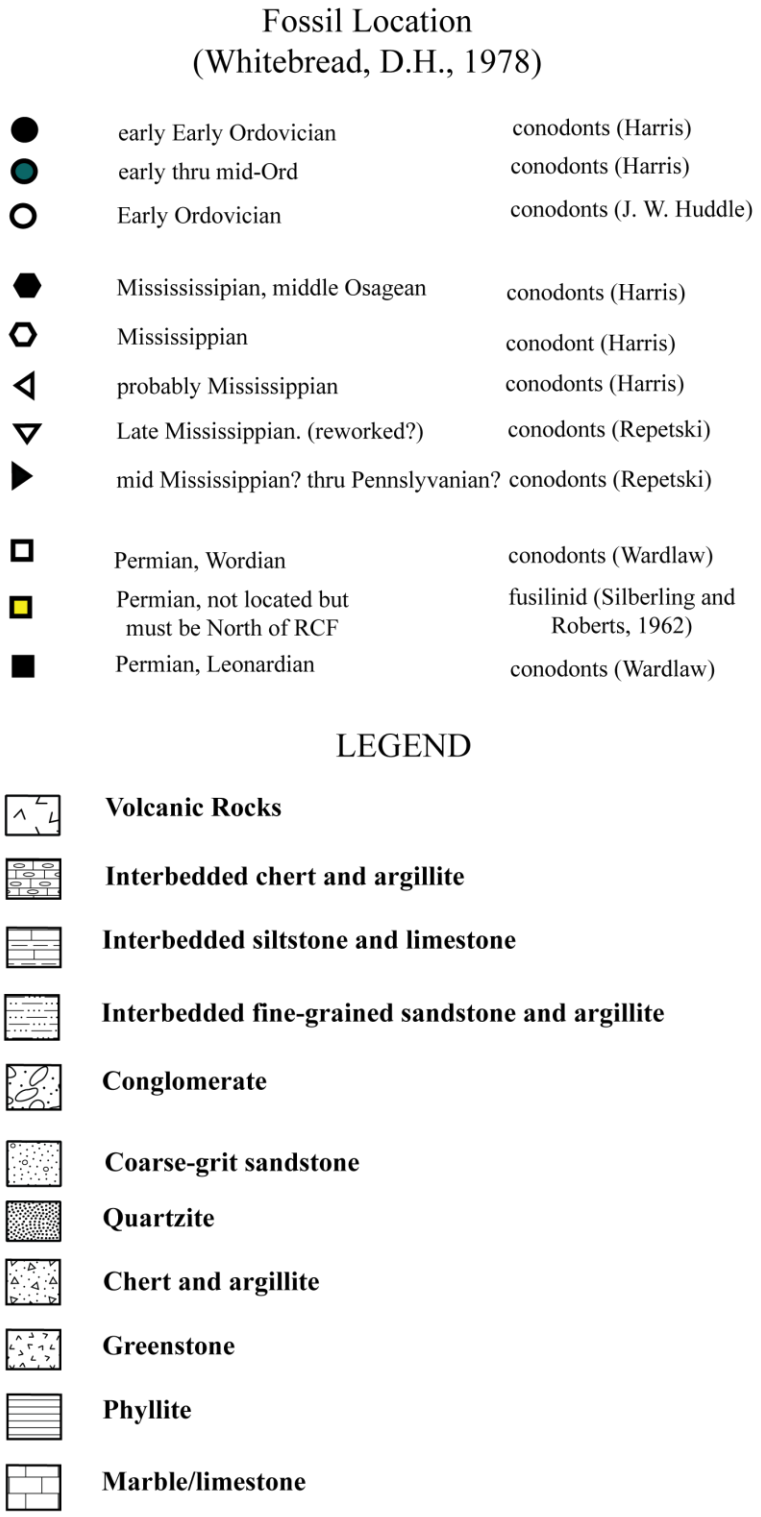

Fig. 2.1. Stratigraphic column of the central East Range showing true thickness, lithologic variation, and fossil locations (see Fig. 2.6).

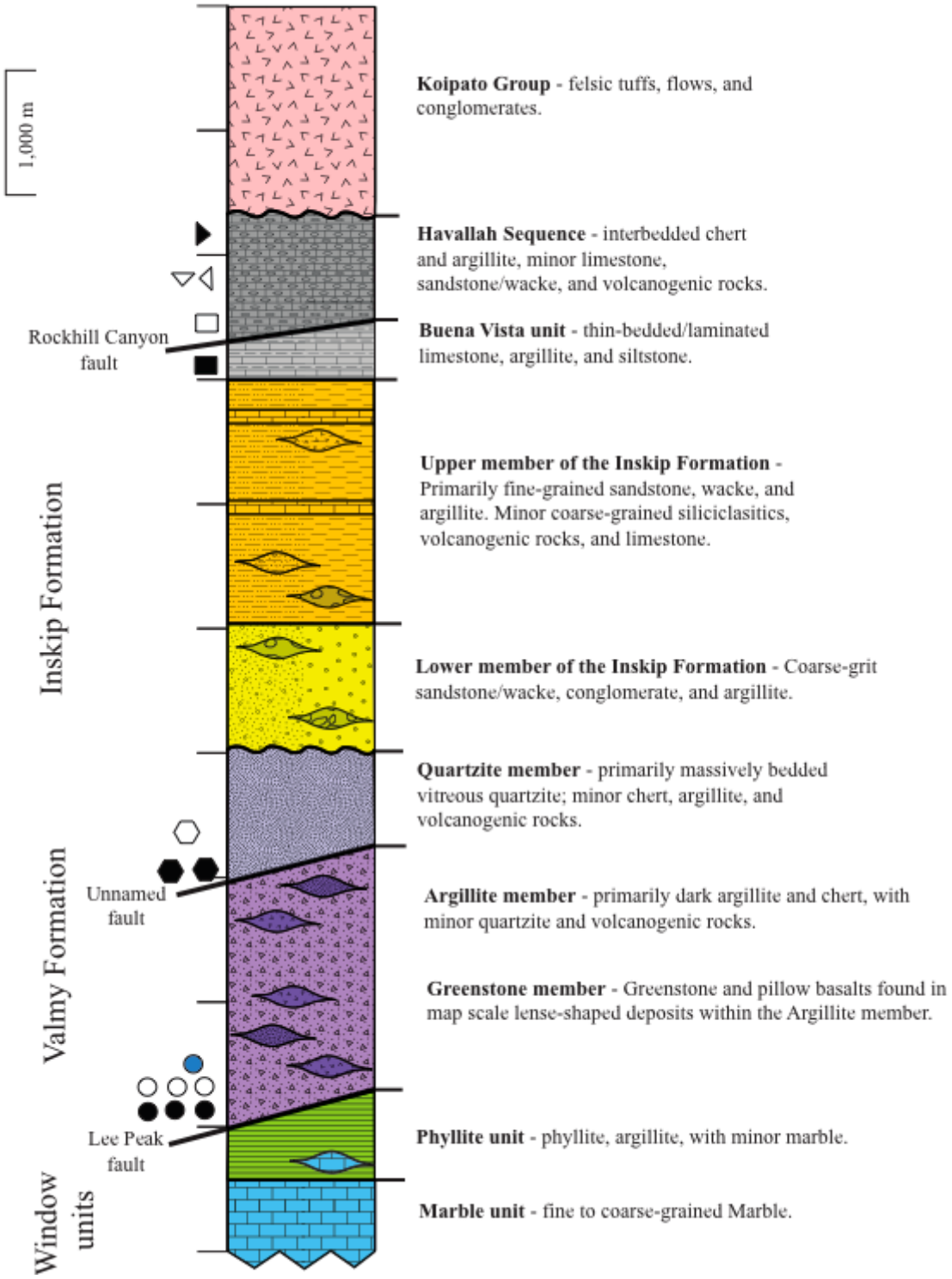
1,000 m
Koipato Group - felsic tuffs, flows, and conglomerates.
Havallah Sequence - interbedded chert and argillite, minor limestone, sandstone/wacke, and volcanogenic rocks.
Rockhill Canyon fault
Buena Vista unit - thin-bedded/laminated limestone, argillite, and siltstone.
Inskip Formation
Upper member of the Inskip Formation - Primarily fine-grained sandstone, wacke, and argillite. Minor coarse-grained siliciclasitics, volcanogenic rocks, and limestone.
Lower member of the Inskip Formation - Coarse-grit sandstone/wacke, conglomerate, and argillite.
Quartzite member - primarily massively bedded vitreous quartzite; minor chert, argillite, and volcanogenic rocks.
Valmy Formation
Unnamed fault
Argillite member - primarily dark argillite and chert, with minor quartzite and volcanogenic rocks.
Greenstone member - Greenstone and pillow basalts found in map scale lense-shaped deposits within the Argillite member.
Lee Peak fault
Phyllite unit - phyllite, argillite, with minor marble.
Window units
Marble unit - fine to coarse-grained Marble.

Fig. 2.2. Photographs of the Valmy Formation. (Top) Picture of Valmy Quartzite member. Quartzite interbedded with lesser amounts of chert and argillite. Hammer for scale. (Bottom) Different view of the same outcrop. Note: the interbedded chert and argillite in the bottom of the picture is identical to that found in the Argillite member. Note channelization structures and hammer for scale.

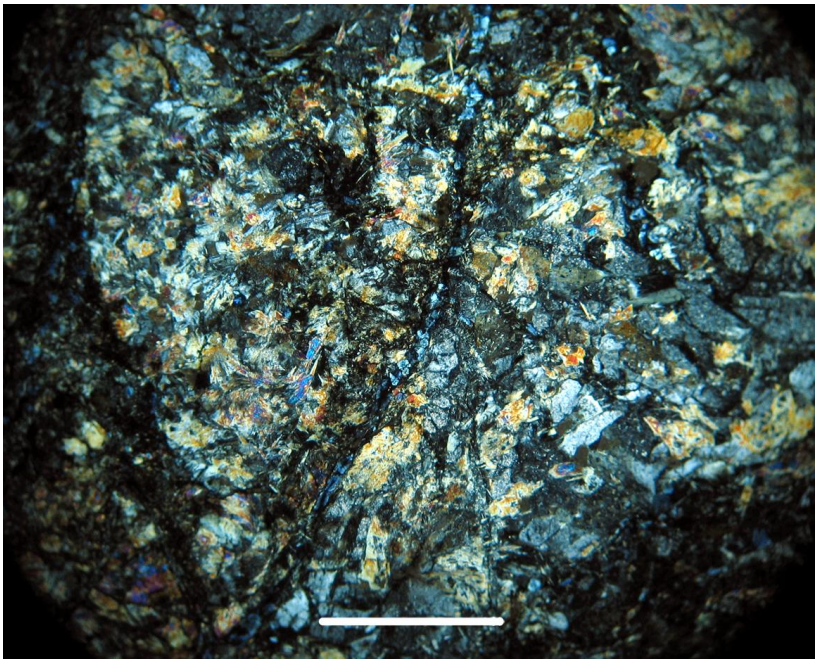

Fig. 2.3. Photomicrograph showing greenstone from the Argillite member. The greenstone has a brecciated texture, with „clasts" containing actinolite (replacing clinopyroxene), chlorite, oxides, and veins filled with clinozoisite, chlorite, quartz and calcite. Note Photomicrograph (XP) is at 4x magnification, and white line is 1mm.

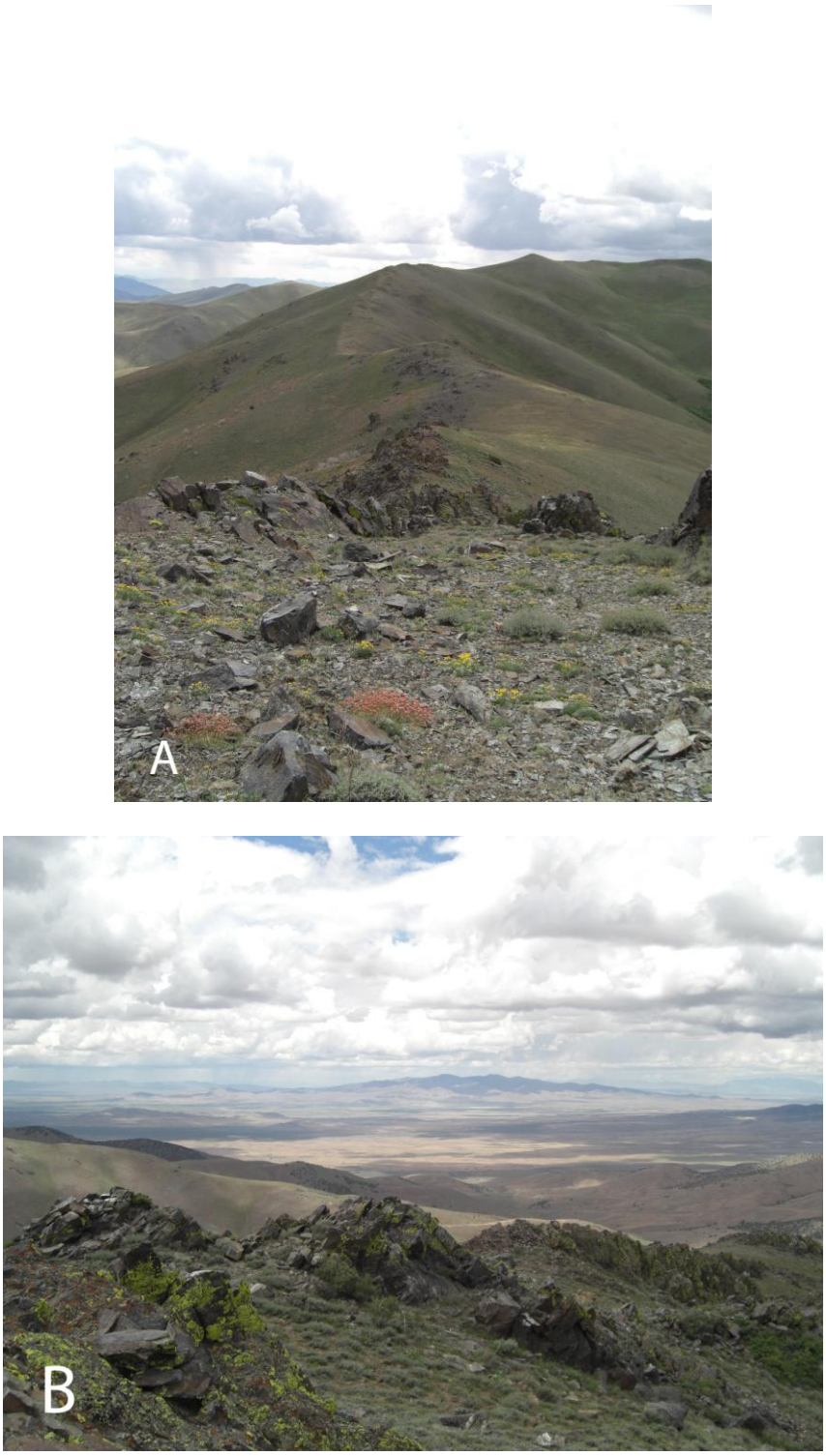

Fig. 2.4. Photographs of the Quartzite member. (A) View to the south of quartzite from the Quartzite member capping the ridge. (B) View to the east of quartzite from the Quartzite member capping the ridge in the foreground.

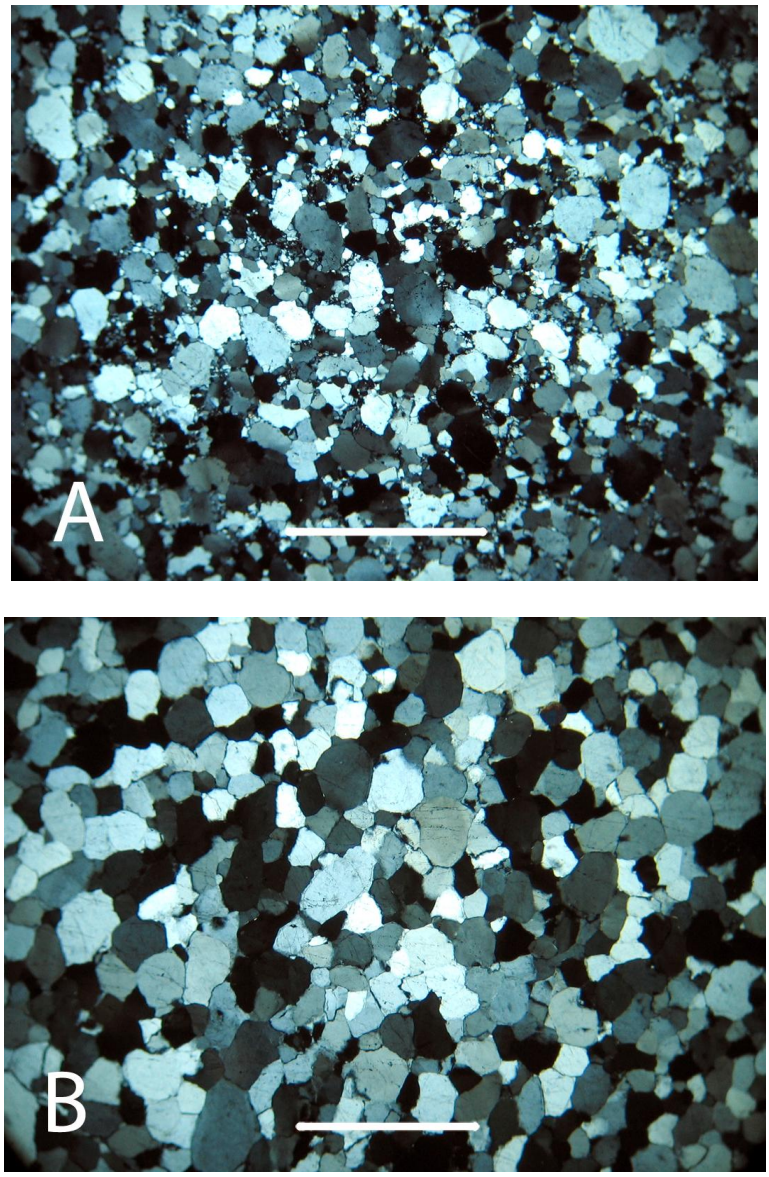

Fig. 2.5. Photomicrographs showing quartzite from the Quartzite member. (A) Photomicrograph (XP) at 4x magnification of quartzite from the Valmy Quartzite member with possible subgrain formation and no foliation. (B) Photomicrograph (XP) at 4x magnification of undeformed quartzite from the Valmy Quartzite member. White line represents 1mm for scale.

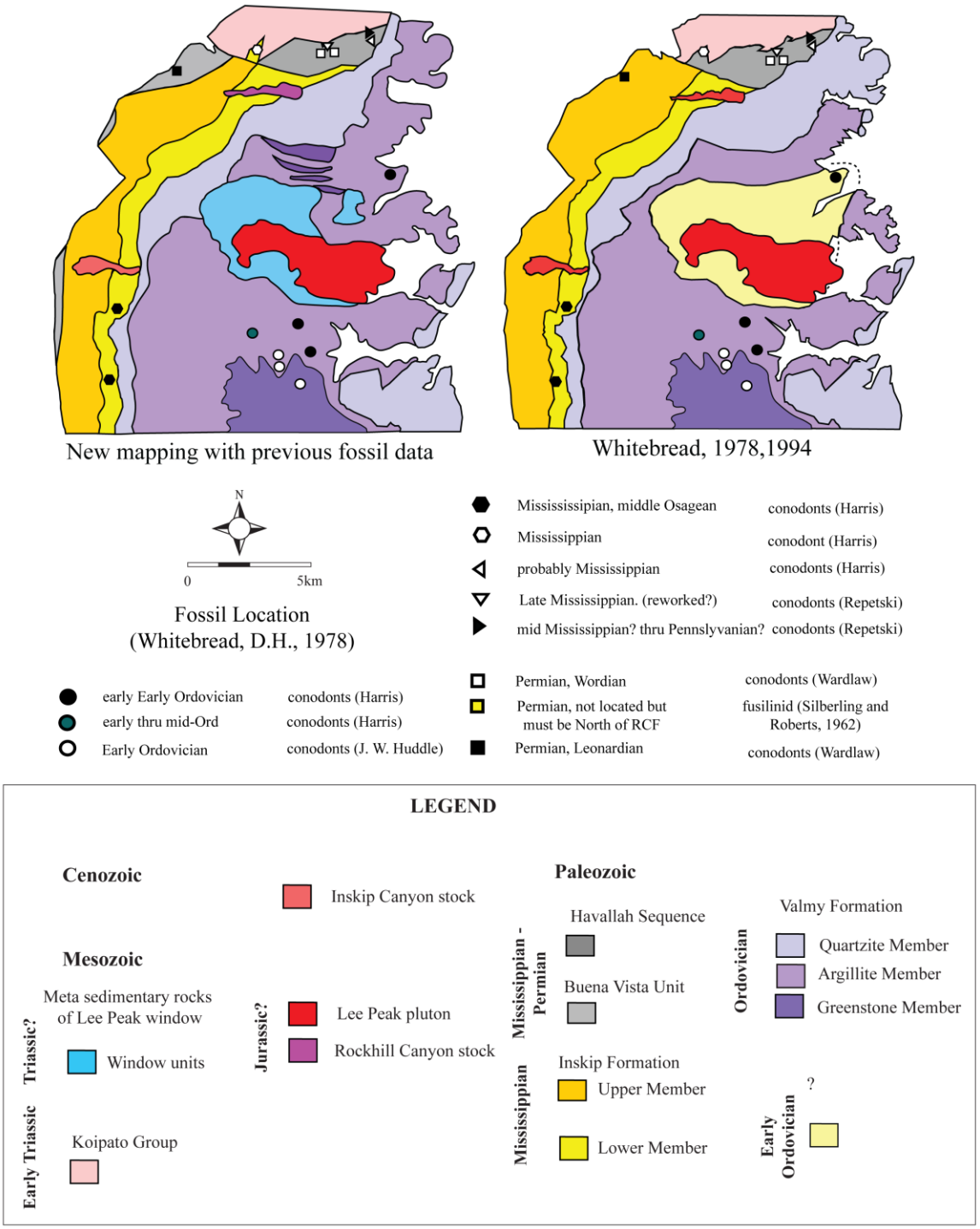

Fig. 2.6. Simplified geologic map showing fossil age and location from Whitebread (1978). Shown on the left is mapping from this study overlain with fossil locations from Whitebread (1978). Shown on the right is mapping and fossil data from Whitebread (1978).

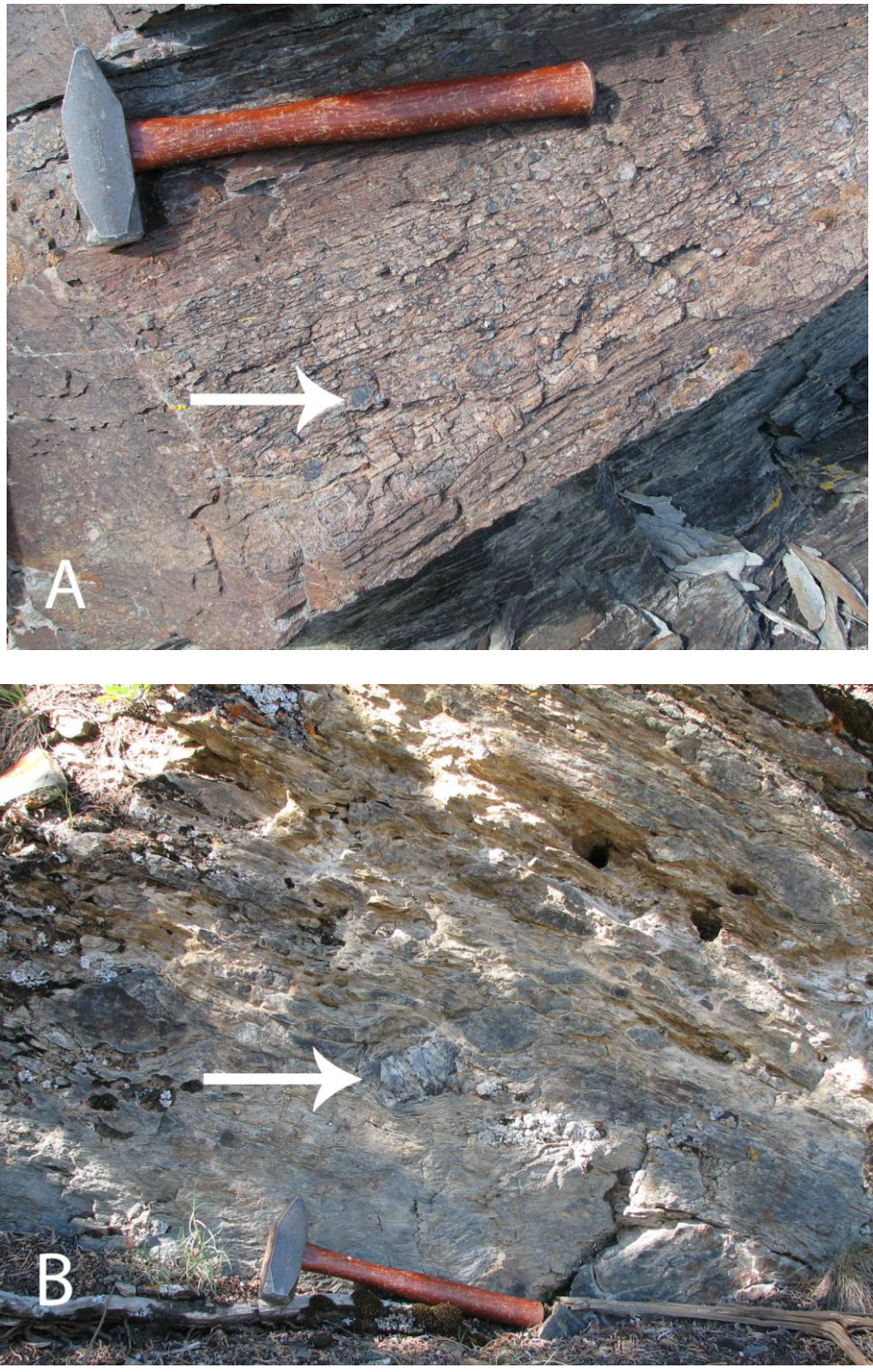

Fig. 2.7. Photographs showing the lower member of the Inskip Formation. (A) Coarse grit wacke from the lower member of the Inskip Formation. Granules (1-3mm) consisting of quartzite and chert. Quartzite granules closely resemble quartzite from the Valmy Formation. White arrow points to quartzite granule, hammer for scale. (B) Mylonitic conglomerate from the Inskip Formation. Large clasts are quartzite (described in text). Note deformed clast in center of photograph (white arrow), and hammer for scale.

Fig. 2.8. Photographs of the Inskip Formation. (A) View to the north coarse-grained horizons from the lower member of the Inskip Formation with meter scale bedding. (B) A View to the south.

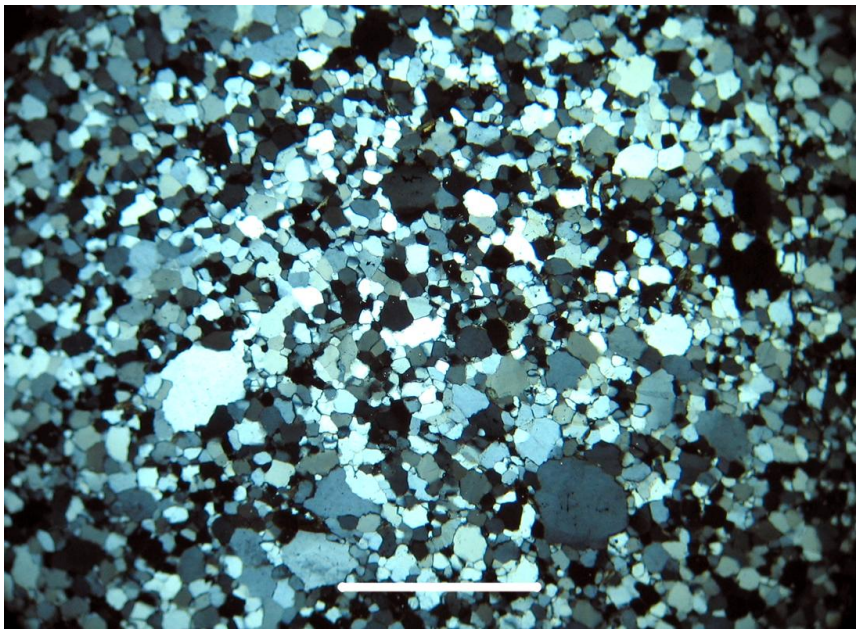

Fig. 2.9. Photomicrograph of a quartzite cobble. Cobble was collected from conglomerate (see Fig. 1.10 and Plate 1) in the lower member of the Inskip Formation. The quartzite is fine/medium-grained, moderately sorted, sub-rounded, and possibly derived from the Valmy Formation (see Fig. 2.5). Note photomicrograph is in (XP) at 4x magnification, white line represents 1mm for scale.

Fig. 2.10. Photomicrographs of quartz wacke from lower member of the Inskip Formation. (A) Medium-grained, sub-angular, poorly sorted, feldspathic wacke. Large grains consist of quartz with lesser amounts of feldspar. Matrix is silt-sized quartz, feldspar, and oxides. Note large grain with pressure shadow. Foliation is defined by elongate grains and residual layers of mica and oxides. (B) medium/coarse-grained, sub-angular, poorly sorted quartz wacke. Note poly- and mono-crystalline quartz grains (C) Coarse grit, poorly sorted quartz rich mudstone from the western wedge of Inskip Formation north of Rockhill Canyon. Large grains are quartz and matrix is composed of equal amounts of mica and silt-sized quartz, feldspar, and oxides. Foliation is defined by elongate grains and residual layers of mica and oxides. Note photomicrographs (XP) at 4x magnification White lines represent 1mm for scale.

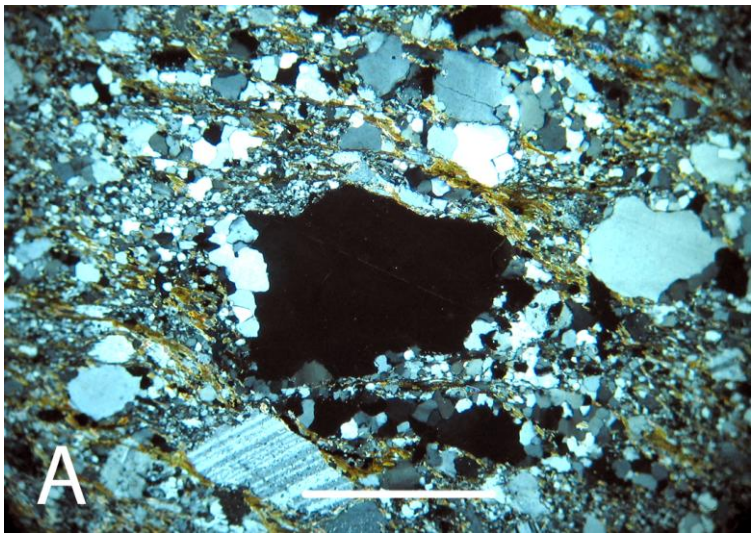
A

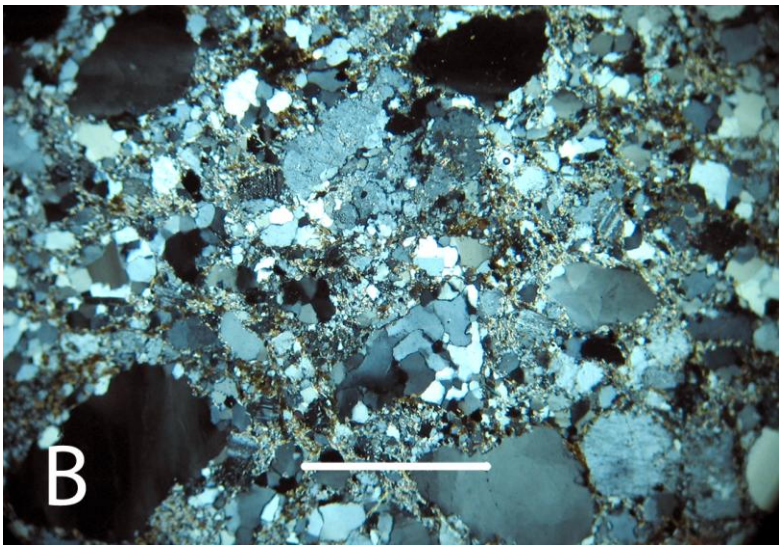
B

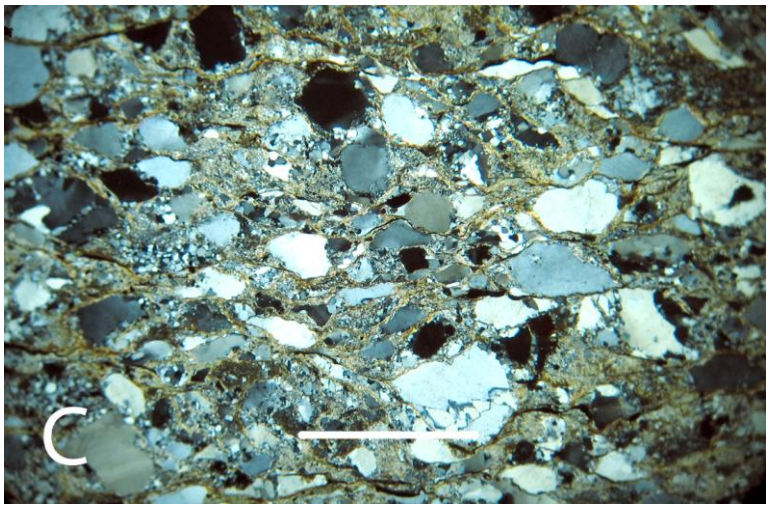
C

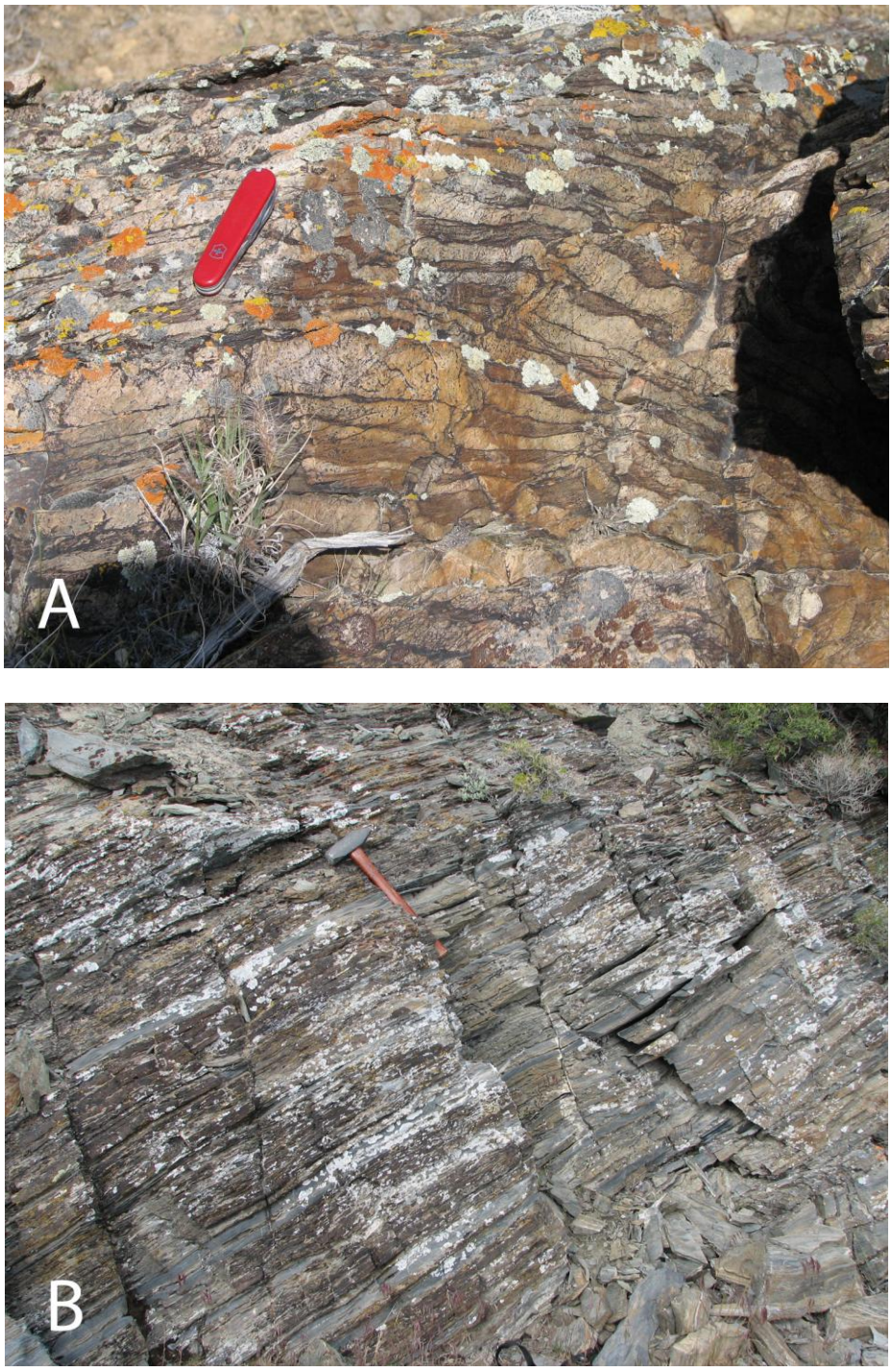

Fig. 2.11. Photographs from the upper member of the Inskip Formation. (A) Typical bedding in the upper member of the Inskip Formation between argillite (dark) and fine-grained sandstone (light), pocket knife for scale. (B) cm scale bedding between silty argillite and limestone, note hammer for scale.

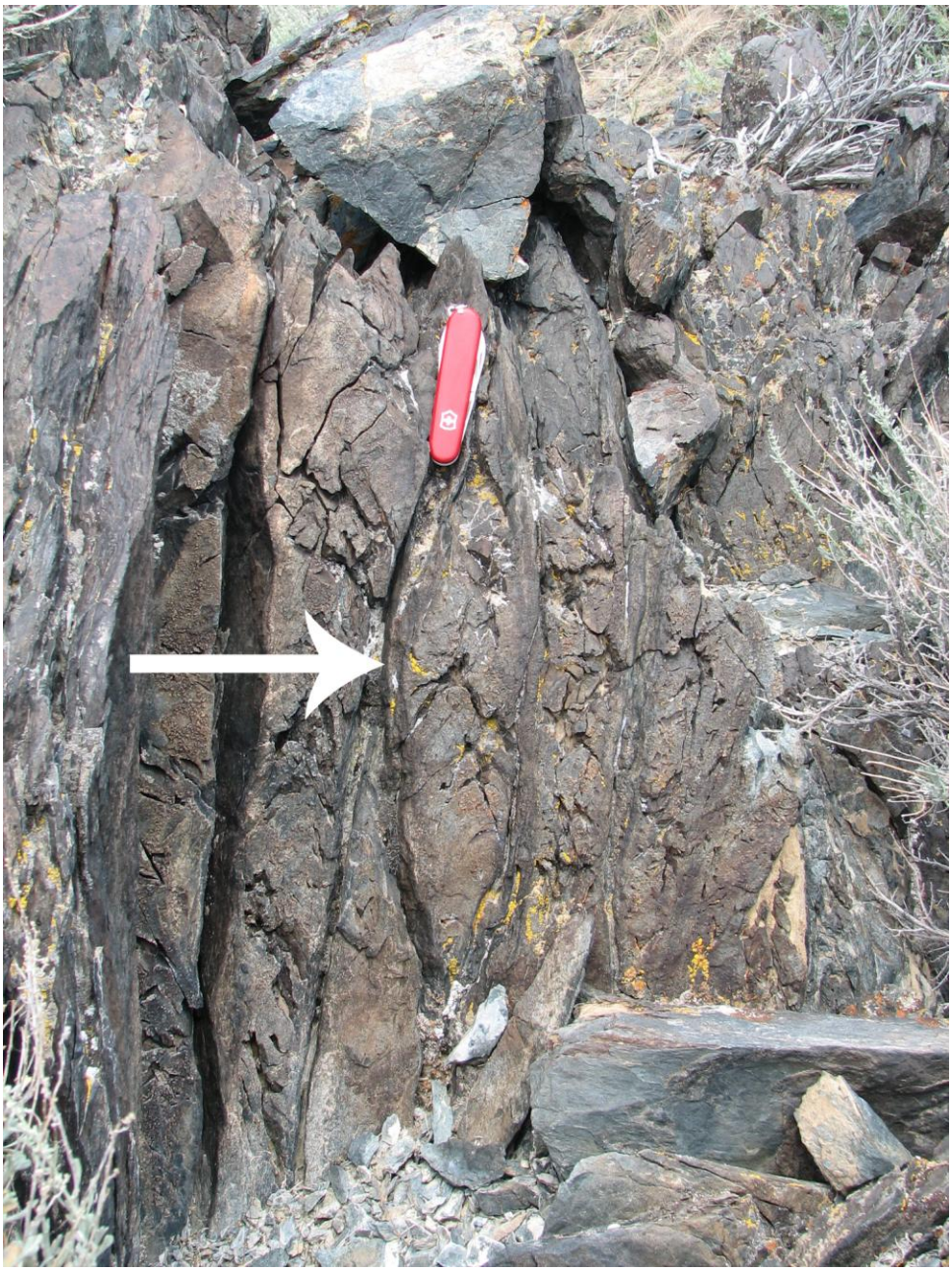

Fig. 2.12. Photograph of pillow lava from the upper member of the Inskip Formation. White arrow points to pillow, calcite forms white residue in between pillows. Note pocket knife for scale.

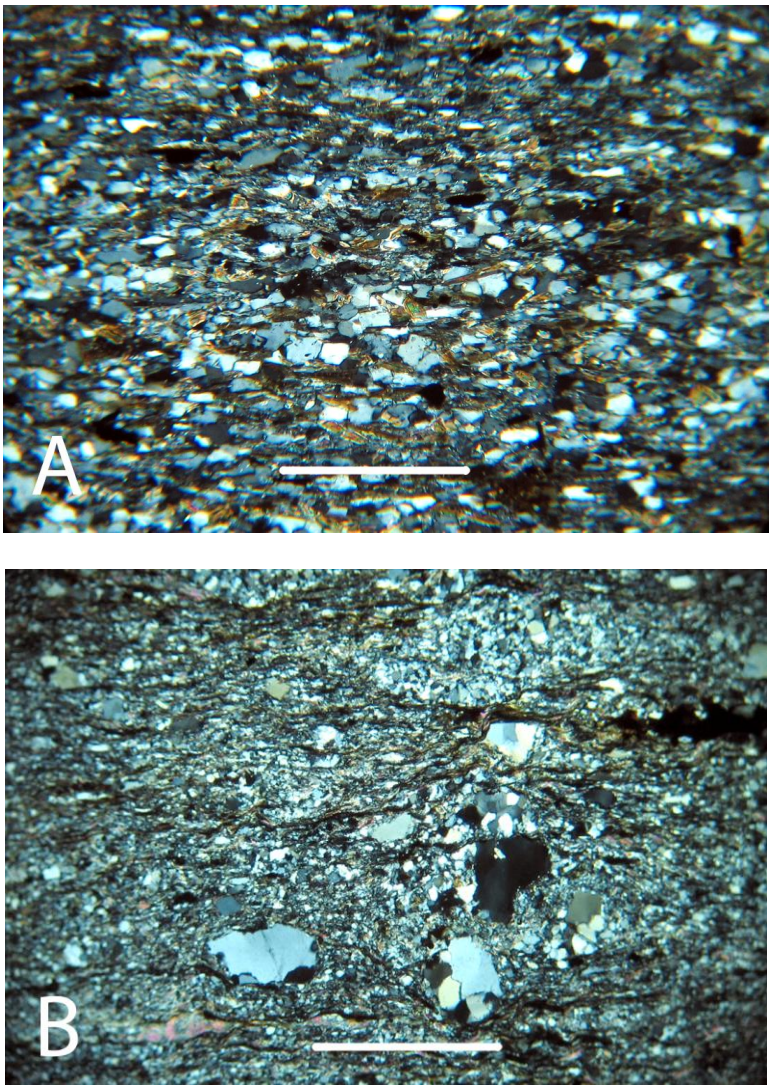

Fig. 2.13. Photomicrographs of siliciclastics from the upper member of the Inskip Formation. (A) (XP) at 4x magnification of silty well-sorted quartz wacke from the upper member of the Inskip Formation. Grains consist entirely of quartz and matrix is composed of biotite, chlorite, and muscovite. Foliation is defined by elongate grains and preferred orientation of micas. (B) (XP) at 4x magnification of medium-grained, sub-rounded, poorly sorted gritty quartz wacke from the upper member of the Inskip Formation. Large grains consist of poly- and mono-crystalline quartz up to 1.5mm. Matrix is composed of quartz, oxides, and micas. Foliation is defined by elongate grains most evident in poly-crystalline quartz and preferred orientation of micas. White lines represent 1mm.

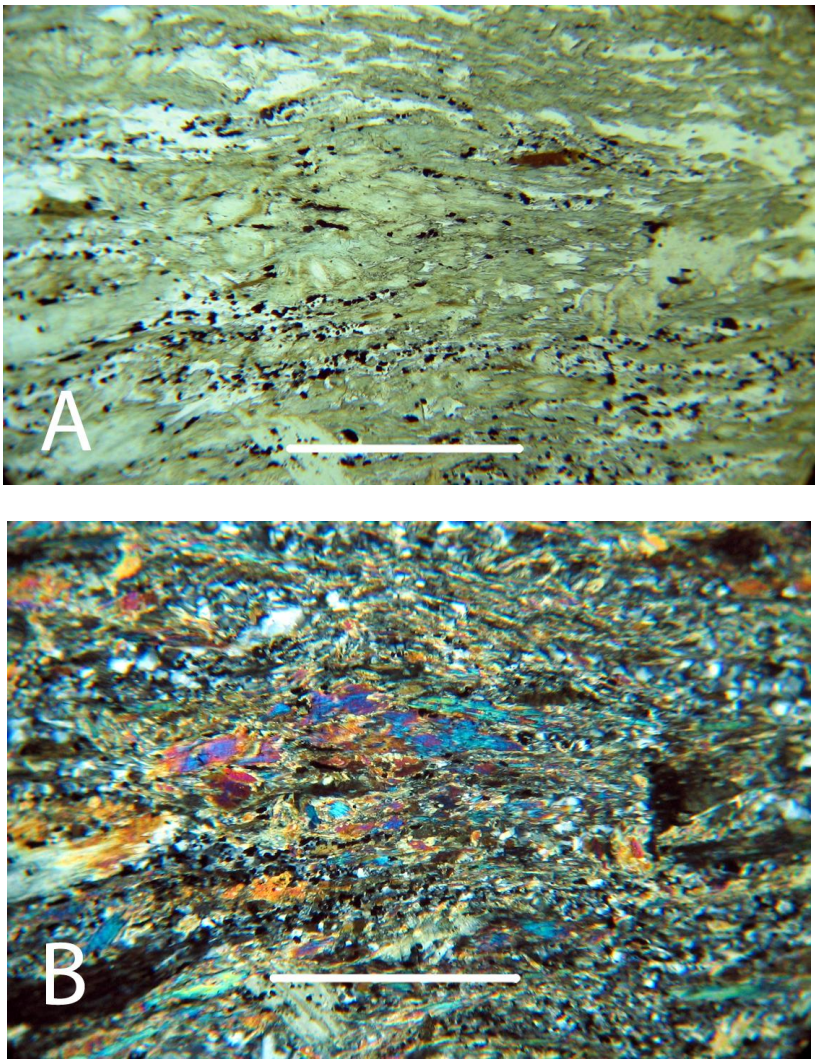

Fig. 2.14. Photomicrographs of greenstone from the upper member of the Inskip Formation. (A) View in PPL. Note the abundance of green metamorphic minerals (actinolite, epidote, and chlorite) (B) View in XP. Note acicular actinolite (high first order), chlorite, biotite (brown), fine-grained plagioclase, and oxides. 10x magnification, white line represents 0.5mm for scale.

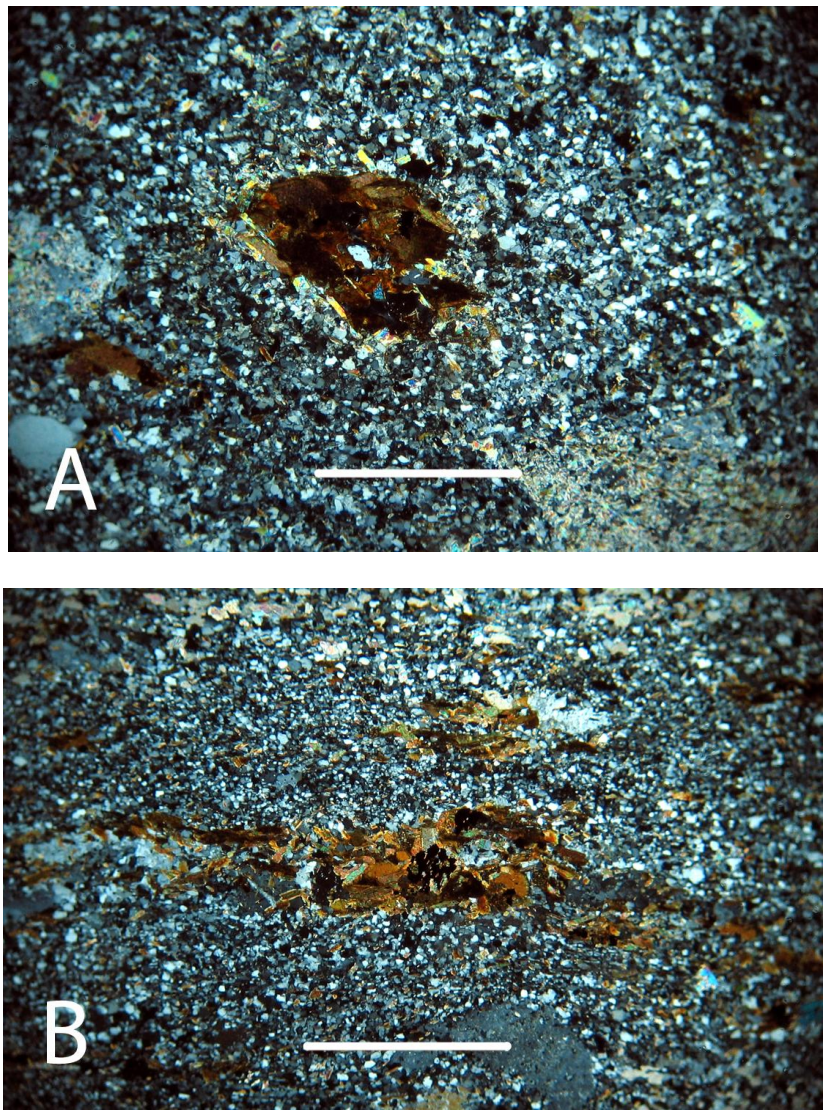

Fig. 2.15. Photomicrographs of felsic volcanic rocks. Cumulophyric, fine-grained biotite-rich felsic volcanic rocks are common throughout the Inskip Formation. (A) Weak foliation. (B) Strong foliation. Note biotite clusters in the center of each photomicrograph. Note photomicrographs (XP) are at 4x magnification, and white line represents 1mm.

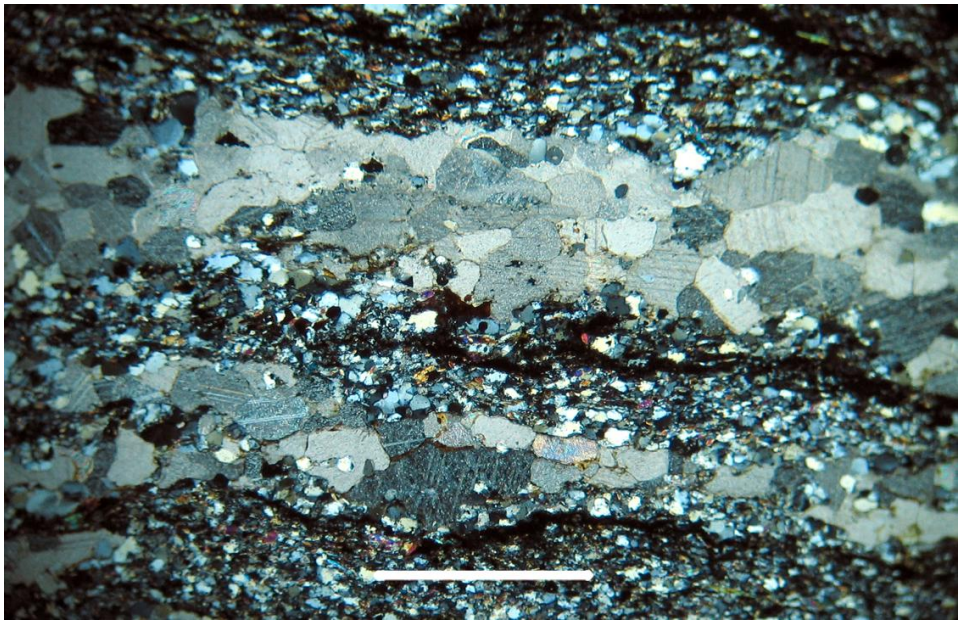

Fig. 2.16. Photomicrograph showing calcareous siltstone from the Buena Vista unit. Bedding up to 5mm thick containing recrystallized limestone interbedded with quartz siltstone. Limestone is slightly silty, and siltstone contains calcite, tremolite, and oxides. Note (XP) at 4x magnification, white line represents 1mm.

Fig. 2.17. Photograph of a typical outcrop within the Havallah Sequence. Contains cm scale bedding between chert and argillite. Note hammer for scale.

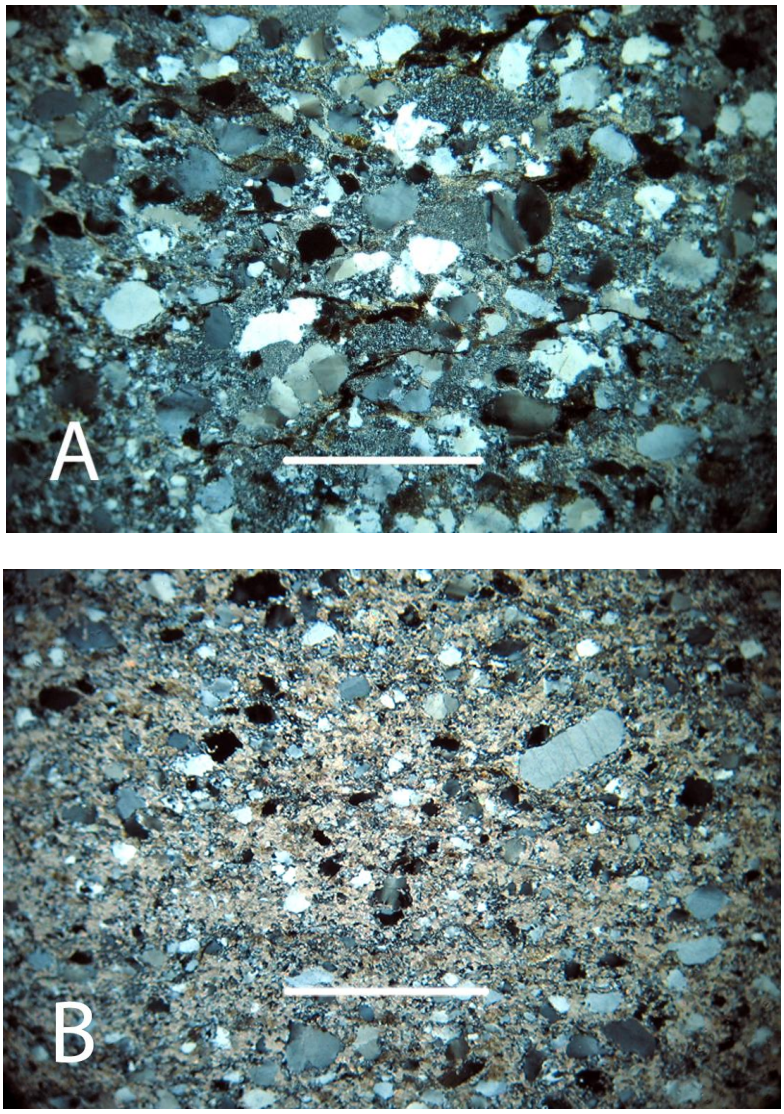

Fig. 2.18. Photomicrographs of wackes from the Havallah Sequence. A) Medium-grained, sub-angular, moderately sorted quartz wacke. Large grains consist of equal amounts of poly-crystalline quartz and mono-crystalline quartz up to 1mm. The matrix is composed of silt-sized quartz, oxides, and muscovite. Weak foliation is defined by elongate grains most noticeable in poly-crystalline grains. B) Fine-grained, sub-rounded, poorly sorted calcitic mudstone. Large grains are mono-crystalline quartz up to 0.5mm, and the matrix consists of calcite and lesser amounts of silt-sized quartz grains, oxides and micas. Note photomicrographs (XP) are at 4x magnification, and white lines represent 1mm.

Fig. 2.19. A view of the Koipato Group and underlying Inskip Formation and Havallah Sequence taken from position south of Rockhill Canyon looking north.

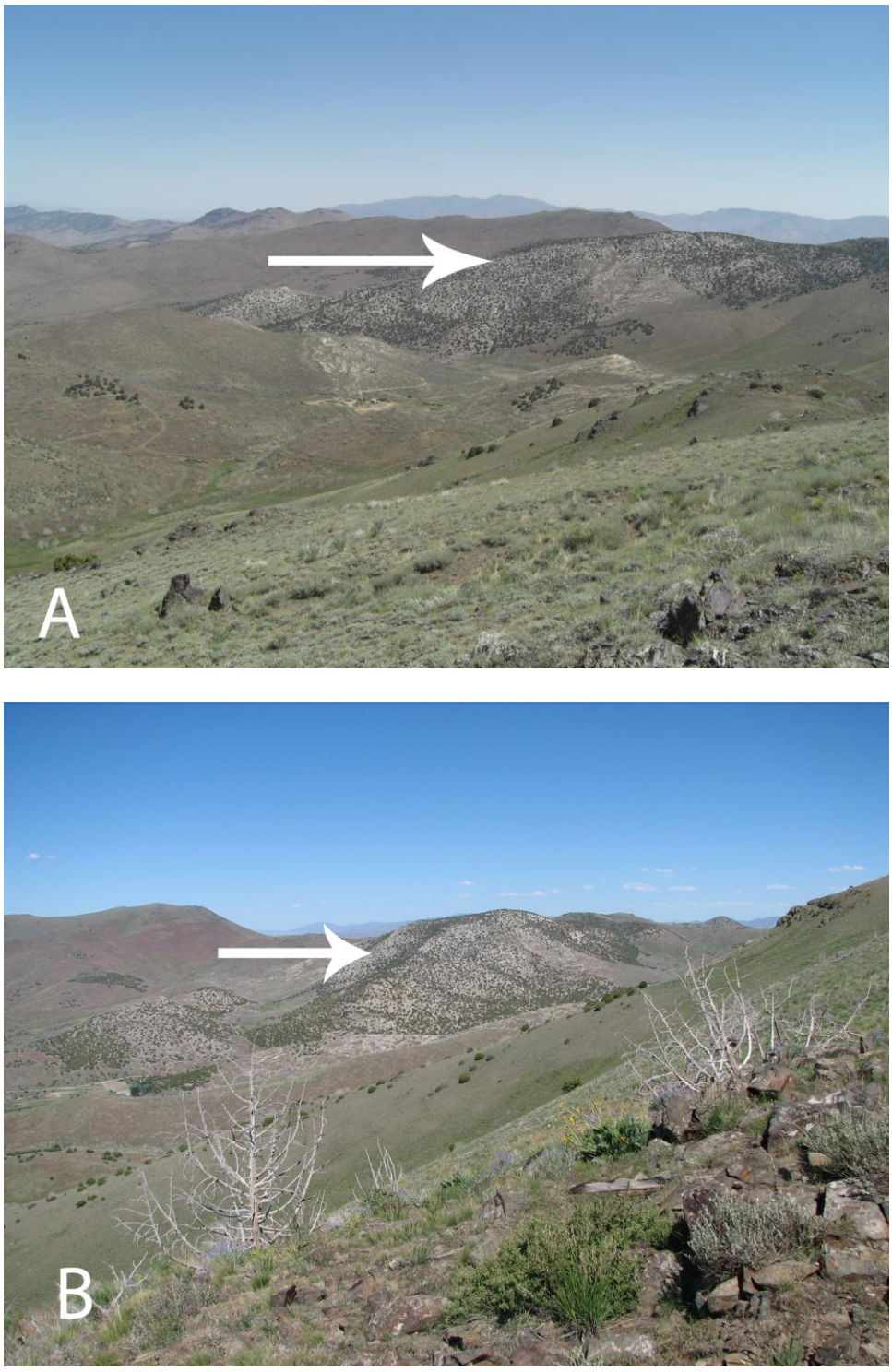

Fig. 2.20. Two views of the Lee Peak window. (A) From SW of the window facing NE. (B) From west of the window facing east. The Marble unit forms large outcrops visible from a distance and is overlain by the Phyllite unit that does not outcrop. White arrows point to the Marble unit within the Lee Peak window.

Fig. 2.21. Photographs showing bedding within the Marble unit. Defined by compositional layering of light and dark marble. Pocket knife for scale in bottom photograph.

Fig. 2.22. Photographs taken along the contact between the Lee Peak pluton and Phyllite unit. (A) Phyllite is partially melted with zenoliths identified by white arrow. (B) Phyllite is hornfelsed, forming more resistant outcrops along the contact with the Lee Peak pluton. Note pencils for scale.

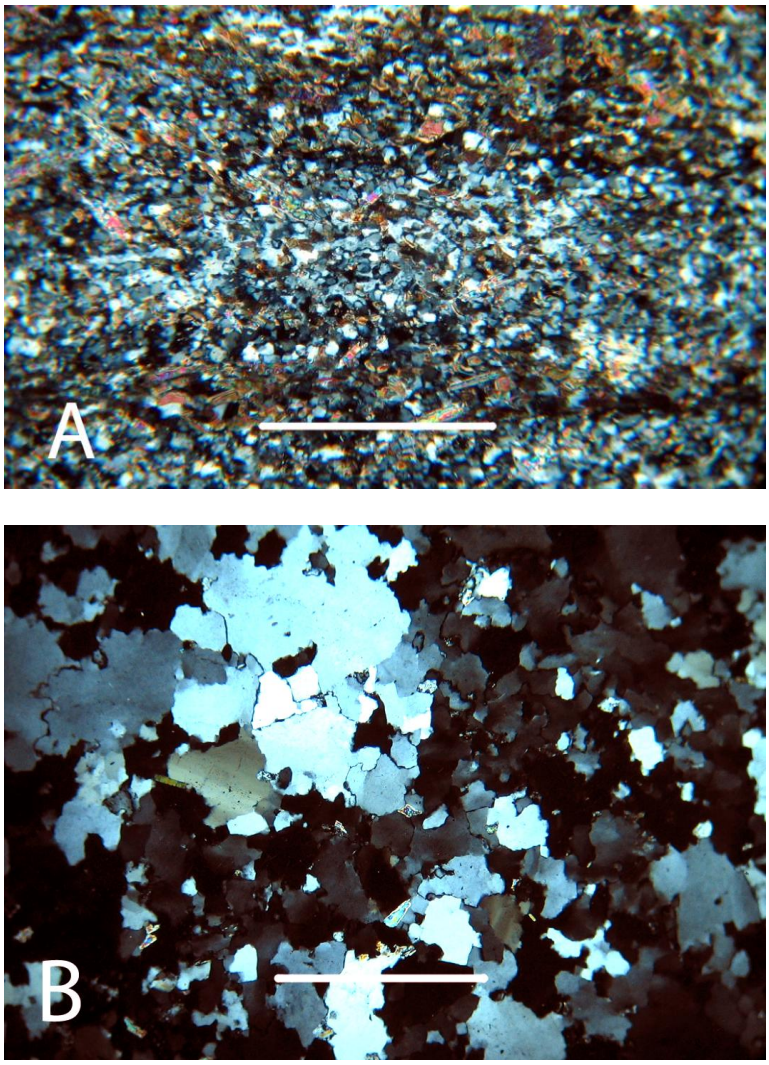

Fig. 2.23. Photomicrographs showing siliciclastics from the Phyllite unit. (A) Photomicrograph (XP) at 10x magnification of metamorphosed foliated siltstone. Grains consist mostly of quartz with subordinate amounts of cordierite and micas. Foliation is defined by orientation of biotite and muscovite, and is overprinted by contact metamorphism indicated by cordierite, muscovite, and biotite cross-cutting foliation. White line represents .5mm. (B) Photomicrograph (XP) at 4x magnification of coarse-grained, sub-rounded quartzite arenite. Grains display subgrain boundary formation and grain boundary migration, but no foliation. White line represents 1mm.

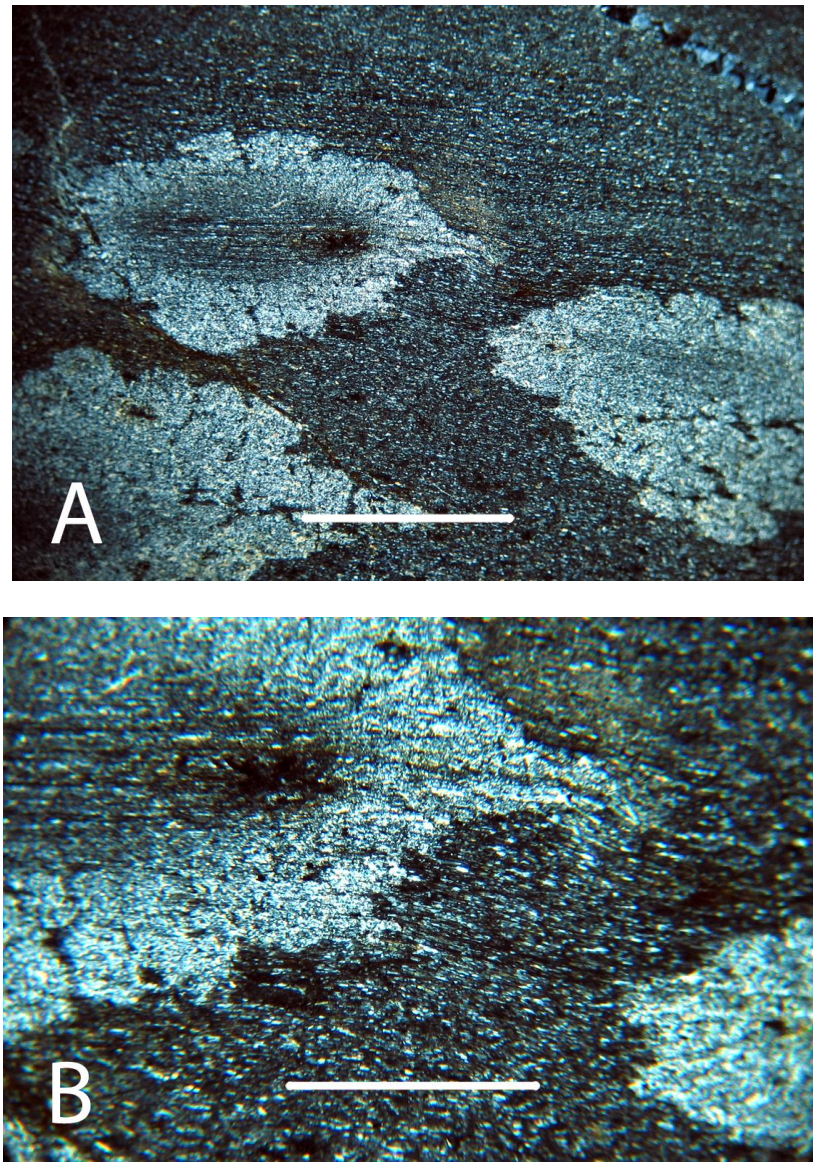

Fig. 2.24. Photomicrographs showing contact metamorphosed phyllite from the Phyllite unit. (A) Photomicrograph (XP) at 4x magnification of phyllite with contact metamorphism. Light colored areas represent incipient cordierite forming in response to contact metamorphism. Composition of non-cordierite areas 80% silt-sized micas and 15% quartz. White line represents 1mm. (B) 10x magnification of shows that cordierite rich zones are overprinting foliation, but are also elongate and aligned with the foliation. White line represents .5mm.

Fig. 2.25. Photographs comparing the Valmy with the disputed window area. (A) Typical chert and argillite found within the Valmy Formation. (B) Chert and argillite found at the disputed fossil location on the eastern side of the East Range (see Fig. 2.6), previously interpreted to be the Phyllite unit. Note hammer for scale.

CHAPTER 3: INTRUSIVE ROCKS

The distribution of intrusive rocks in the central East Range was mapped in the same detail by Whitebread (1978), but described only briefly in the map legend. In this study all intrusive bodies were remapped objectively. Samples were collected for thin section petrography. Based on the new mapping, six distinct sets of intrusive rocks were identified: the Wadley Mine stocks (WMS), Rawhide metagabbro (RMG), Lee Peak pluton (LPP); Rockhill Canyon stock (RCS); Inskip Canyon stock (ICS); and Cenozoic dikes (Fig. 1.10 and Plate 1). The WMS, RMG, LPP, and RCS are all inferred to be Jurassic.

Lee Peak Pluton

The Lee Peak pluton (Fig. 1.10 and Plate 1) is a large granitic body that intrudes the metasedimentary units of the Lee Peak window and in places cuts the Lee Peak fault. Mapping of the pluton has changed little from when it was first recognized by Ferguson et al., (1951). New mapping in this study is consistent with previous work. The age of the Lee Peak pluton in discussed in the following section.

The Lee Peak pluton shows slight variability in composition from granodiorite to granite (Fig. 3.2). In the vicinity of Lee Peak the pluton is a medium grained granite that contains 20% mafic minerals and forms prominent outcrops. Towards the south and west

the composition changes to granodiorite, with a slightly larger mafic content (25-30%). In these locations, the pluton is commonly not well exposed. The Lee Peak pluton is in contact with the two window units and the Argillite member of the Valmy Formation (Fig. 1.10 and Plate 1). Rocks along this boundary are commonly hornfelsed or show evidence of contact metamorphism (Fig. 2.22 A). Although altered in areas, rocks of the Lee Peak pluton are not metamorphosed.

Two samples from the Lee Peak pluton were examined by thin section petrography: one sample was taken by Lee Peak, and the other was from the southern portion of the pluton along Spaulding Canyon. The sample from Lee Peak is subhedral, medium-grained, hornblende biotite granite (Fig. 3.1 A). The composition is 20% quartz, 30% plagioclase, 30% potassium feldspar, 10% biotite, 10% hornblende, and trace amounts of epidote, sphene, chlorite, clinozoisite, and muscovite. Quartz grains are interstitial, and are 0.25-0.5mm. Feldspars are subhedral to tabular, are 1-2mm, and are partially replaced by clinozoisite and muscovite. Plagioclase frequently displays zoning. Biotite is interstitial with 1.5mm grains: it is fresh in some areas and replaced by chlorite in others. Hornblende is green and forms grains 0.5-2mm in size. Some hornblende is range fresh but some is partially replaced by chlorite and epidote.

The sample collected from the southern portion of Lee Peak pluton is a subhedral to porphyritic, fine-grained, hornblende biotite granodiorite (Fig. 3.1 B). The composition is 25% quartz, 30% plagioclase, 10% potassium feldspar, 20% biotite, 10% epidote, 5% chlorite, and trace amounts of muscovite. Quartz is subhedral, 0.25mm in diameter. Feldspars consist of subhedral grains that are 0.25-0.5mm in size and have moderate zoning and sericitic alteration. However, some phenocrysts of feldspar are 1.75mm long

and also display zoning and mild sericitic alteration biotite is light to dark brown and shows varying degrees of birefringence caused by alteration to chlorite. These grains are 0.75mm and have a ragged, interstitial texture.

Rockhill Canyon Stock

The Rockhill Canyon stock intrudes the Inskip and Valmy Formations south of Rockhill Canyon (Fig. 1.10 and Plate 1). New mapping of the stock is consistent with previous work by Whitebread (1978). The contact aureole of the Rockhill Canyon stock is narrow (~500m) and is characterized by mild alteration and hornfelsed rock. This is especially evident on the western side of the stock where it intrudes the upper member of the Inskip Formation.

Two samples of the Rockhill Canyon stock were examined by thin section petrography are analyzed. Both samples are from the western side of the stock. The first sample is a subhedral granular, medium-grained hornblende granodiorite (Fig. 3.2). The composition is 30% quartz, 30% plagioclase, 20% actinolite, 5% potassium feldspar, 5% muscovite, 5% epidote, 5% calcite, and trace amounts of clinozoisite, sphene, and oxides (Fig. 3.3A). The quartz is interstitial and up to 0.5mm. Actinolite replaces hornblende and forms 1.25mm tabular grains. Feldspars average 1mm in size and are moderately altered into muscovite and oxides.

The second sample from the Rockhill Canyon stock is a subhedral, medium-grained hornblende granodiorite (Fig. 3.2). The sample is composed of 30% quartz, 40% plagioclase, 10% K-spar, 10% actinolite, and 10% chlorite, with trace amounts of calcite, epidote, clinozoisite, biotite, muscovite, and sphene (Fig 3.3B). Quartz is interstitial with

up to 0.3mm grains. Feldspars form 1.25mm laths that are extensively altered to muscovite. Actinolite, replaces hornblende. Minor uralitization of pyroxene is responsible for the formation of all the actinolite. Chlorite is up to 0.5mm.

Wadley Mine Stocks

The Wadley Mine stocks are a group of hornblende granodiorite (Fig. 3.2) stocks surrounding the Wadley Mine on the western side of the Lee Peak window (Fig. 1.10 and Plate 1). Four stocks were identified, two of which cut the unnamed metasedimentary rocks within the Lee Peak window and two of which cut the Argillite member of the Valmy Formation outside the Lee Peak window. The Wadley Mine stocks thus straddle the Lee Peak fault (Fig. 1.10 and Plate 1). These intrusions lack large outcrops and consist of heavily weathered pieces of float, making the map extent of the stocks somewhat ambiguous.

Two samples from the Wadley Mine stocks were examined for thin section petrography. One sample was from a stock within the window and the other was from a stock outside the window. The sample collected within the Lee Peak window is a subhedral granular medium-grained hornblende granodiorite (Fig. 3.4A). This rock consists of 25% quartz, 25% plagioclase, 15% potassium feldspar, 20% hornblende and actinolite, 5% chlorite, 5% clinozoisite, and 5% muscovite. Quartz is interstitial with grains up to 0.75mm. Feldspars consisted of 2mm grains that have extensive sericitic alteration. Hornblende is partially replaced by actinolite, forming laths of actinolite 2mm long. Chlorite within this sample is up to 0.5mm.

The sample collected from outside the Lee Peak window is a subhedral to porphyritic, medium-grained, hornblende granodiorite (Fig. 3.4B). Minerals within this sample consists of 25% quartz, 30% plagioclase, 5% potassium feldspar, 25% actinolite, 10% chlorite, and 5% clinozoisite, with trace amounts of epidote and sphene. Quartz forms 1.5mm interstitial and subhedral grains. Feldspars form 1.5mm subhedral grains that show extensive sericitic alteration. Actinolite grains are tabular to euhedral and up to 2.5mm and completely replace hornblende. Plagioclase and hornblende form large phenocrysts in a relatively finer grained matrix containing the same suite of minerals, plus quartz.

Rawhide Metagabbro

The Rawhide metagabbro is in a cluster of small stocks within the NE portion of the Lee Peak window at the top of Rawhide Canyon (Fig. 1.10 and Plate 1).

Samples collected from these intrusions indicate a range of textures including: subhedral, poikilitic, and felty. These rocks are classified as fine to medium-grained pyroxene hornblende gabbro (Fig. 3.2). Minerals assemblages include 45% plagioclase, 25% actinolite, 15% epidote, up to 15% pyroxene, with trace amounts of clinozoisite, quartz, calcite, biotite, chlorite, muscovite, sphene, and oxides. Plagioclase forms 1-5mm laths that are moderately altered. Actinolite replaces hornblende, which originally formed phenocrysts up to 5mm and smaller (0.2mm) actinolite grains are also formed within the groundmass. Widespread uralitization is visible in one sample, and manifested rims of actinolite around a core of pyroxene (Fig. 3.5B).

Inskip Canyon Stock

The Inskip Canyon stock is located on the western side of the East Range and intrudes the both members of the Inskip Formation (Fig. 1.10 and Plate 1). New mapping agrees with previous work by Whitebread (1978). This stock is more mafic than the other large intrusive bodies of the central East Range as evident by the greater density and higher color index in hand samples. In the field, the Inskip Canyon stock is characterized by large, meter scale outcrops that display spheroidal weathering.

One sample collected for thin section petrography is an ophitic medium-grained hornblende pyroxene quartz monzo-diorite (Fig. 3.2). This sample collected from the western side of the stock, contains 60% plagioclase, 20% pyroxene, 10% potassium feldspar, 10% oxides, and trace amounts of quartz (Fig. 3.6). Plagioclase forms of 2.5mm laths that show little to no alteration, and also forms smaller interstitial grains. Myrmekitic textures are present in some plagioclase crystals. Pyroxene crystals are up to 0.5mm and are colorless to pinkish. Minor uralitization is visible in a few pyroxene grains.

Cenozoic Dikes

In the central East Range these dikes and stocks inferred to be Cenozoic consist of diabase and felsic porphyritic rocks. They are found throughout the Inskip Formation, the northern portion of the Lee Peak window, and in the subordinate portion of the Lee Peak window (Plate 1).

Two samples collected are from the Inskip Formation in Willow Creek Canyon and slightly north of Inskip Canyon. These samples are fine to medium-grained

porphyritic diabase (Fig. 3.7). These samples contain 35% plagioclase, 45% actinolite that is replacing hornblende, up to 15% chlorite, 5% quartz, biotite, and oxides. Phenocrysts consists of actinolite were hornblende (up to 4mm).

One sample collected of a felsic porphyryitic dike is identified as a coarse-grained biotite, quartz, feldspar porphyry. Phenocrysts consist of 10% euhedral quartz up to 1.5mm, 10% plagioclase up to 5mm that is heavily altered to muscovite, 10% potassium feldspar and 10% ragged biotite up to 1.25mm. The groundmass consists of 30% quartz (0.25mm) and 30% muscovite, possibly derived from altered feldspar.

Geochronology

Throughout the East Range, igneous rocks were collected for U-Pb geochronology (see Plate 1 for sample locations). Igneous samples collected include: the Lee Peak pluton, Rockhill Canyon stock, Inskip Canyon stock, Rose Creek Pluton (located by Rose Creek Canyon in the northeastern East Range, not shown in figures).

Previous work on the ages of these intrusions is discussed by Elison (1990). Rb/Sr age dating yields ages of 93.4 ± 2.8Ma for the Rose Creek pluton, 168.8 ± 25 and 196Ma for the Rockhill Canyon stock, and 567.2 ± 95.8Ma for the Lee Peak pluton (Elison, 1990). K/Ar on biotite yields ages of 153 ± 3Ma, and 134 ± 3Ma for the Lee Peak pluton (Silberling and McKee, 1971).

The Lee Peak pluton, Rose Creek pluton, and the Rockhill Canyon and Inskip Canyon stocks are significant features in the central East Range, and precise dating of these plutons is needed to fully understand the geologic history of the East Range. However, after processing the samples, only the Lee Peak and Rose Creek plutons

yielded usable zircons. The Lee Peak pluton and Rose Creek pluton were the only samples dated at the Arizona Laserchron Center and the University of Arizona using the Laser-Ablation Multicollector ICP Mass Spectrometer. U-Pb geochronology offers a more accurate age than K-Ar hornblende previously used for the Lee Peak pluton. However, due to extremely high uranium content, a reliable age for the Lee Peak pluton was not found. Zircons within the Rose Creek pluton have an age of 162 ± 1.1 Ma.

Based on the age data for the Rose Creek pluton (162 ± 1.1 Ma and 93.4 ± 2.8Ma), and data on other intrusions from previous studies, a Jurassic age for all intrusions in the central East Range is inferred. This has significant implications for the timing of deformation in the central East Range, because these intrusions are not deformed and cut major structures such as the Buena Vista shear zone and the Lee Peak fault.

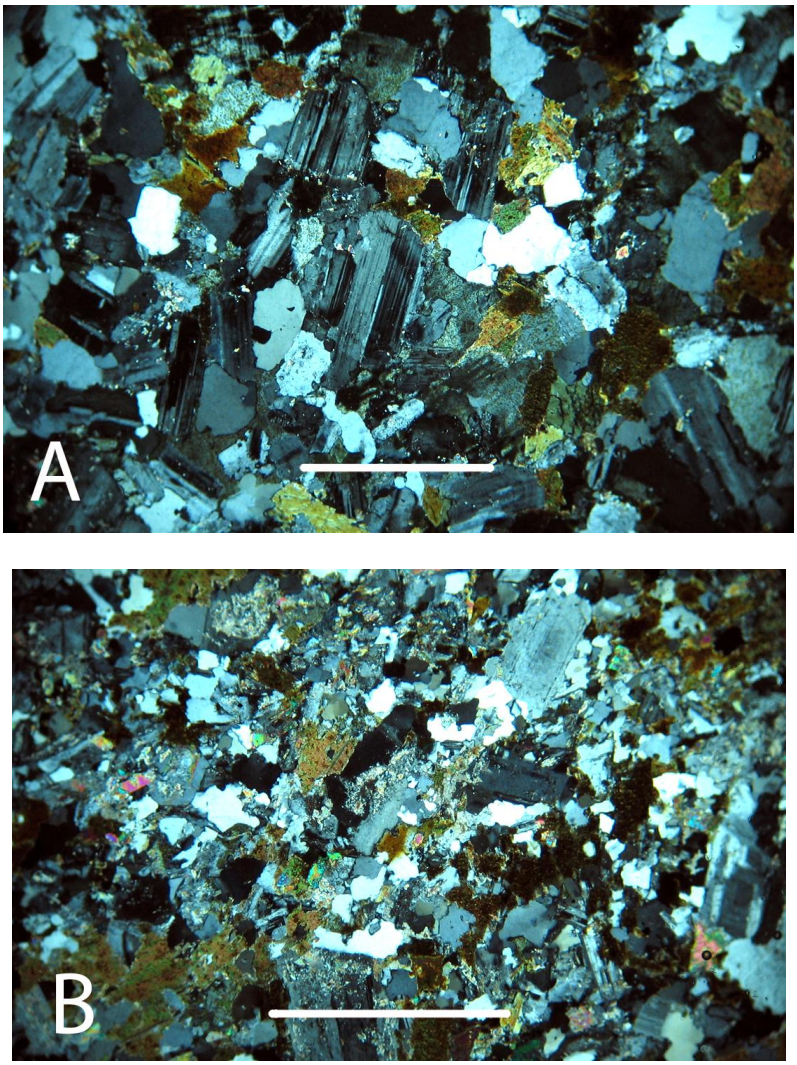

Fig. 3.1. Photomicrographs of the Lee Peak pluton. A) A medium-grained unfoliated, subhedral granular hornblende biotite granite collected from the northeastern portion of the pluton near Lee Peak. B) A fine-grained, unfoliated biotite granodiorite collected from the southern portion of the pluton in Spaulding Canyon. Note photomicrographs (XP) are at 4x magnification, and white lines represent 1mm.

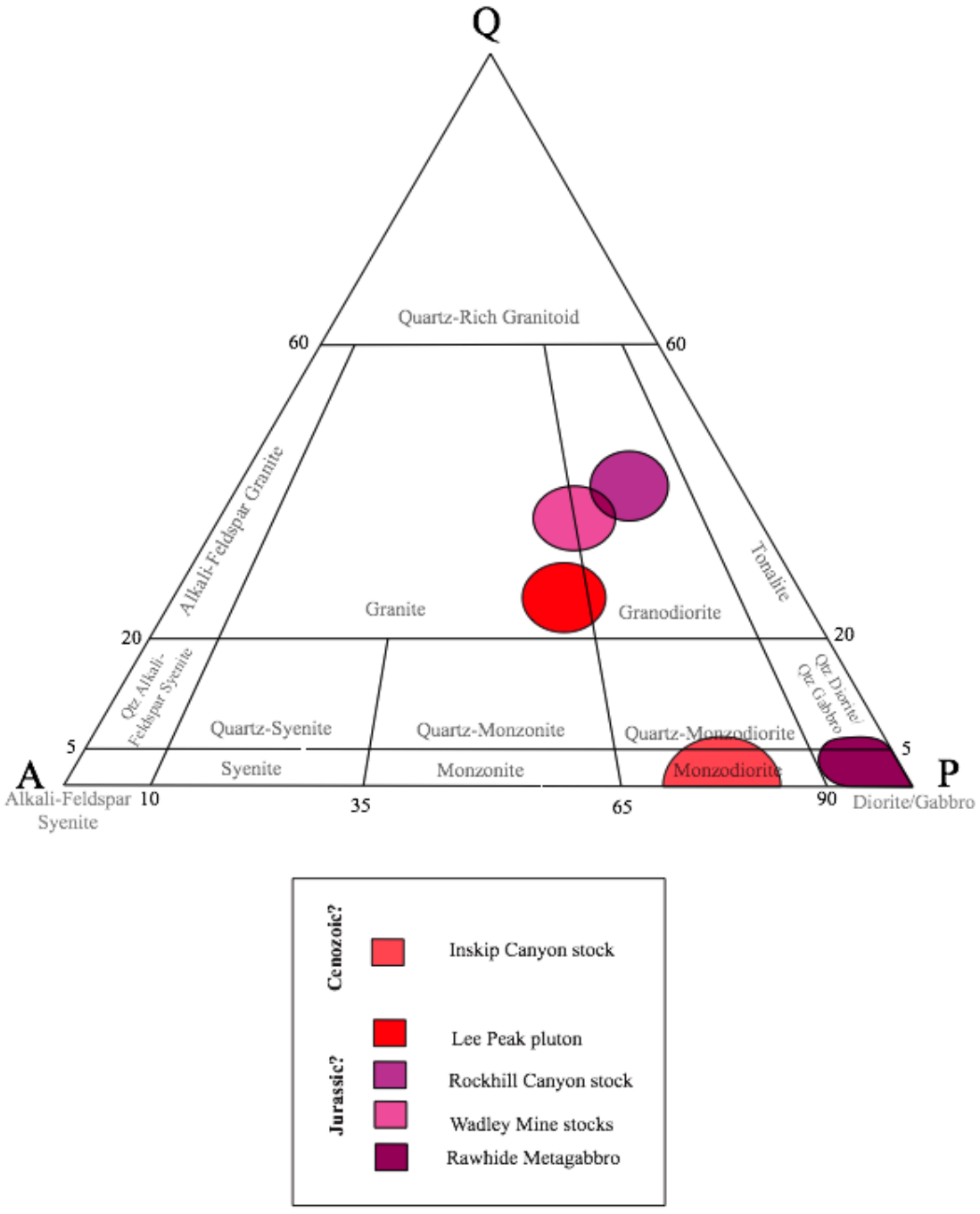

Fig. 3.2. QAP diagram that shows the composition of intrusive bodies in the central East Range.

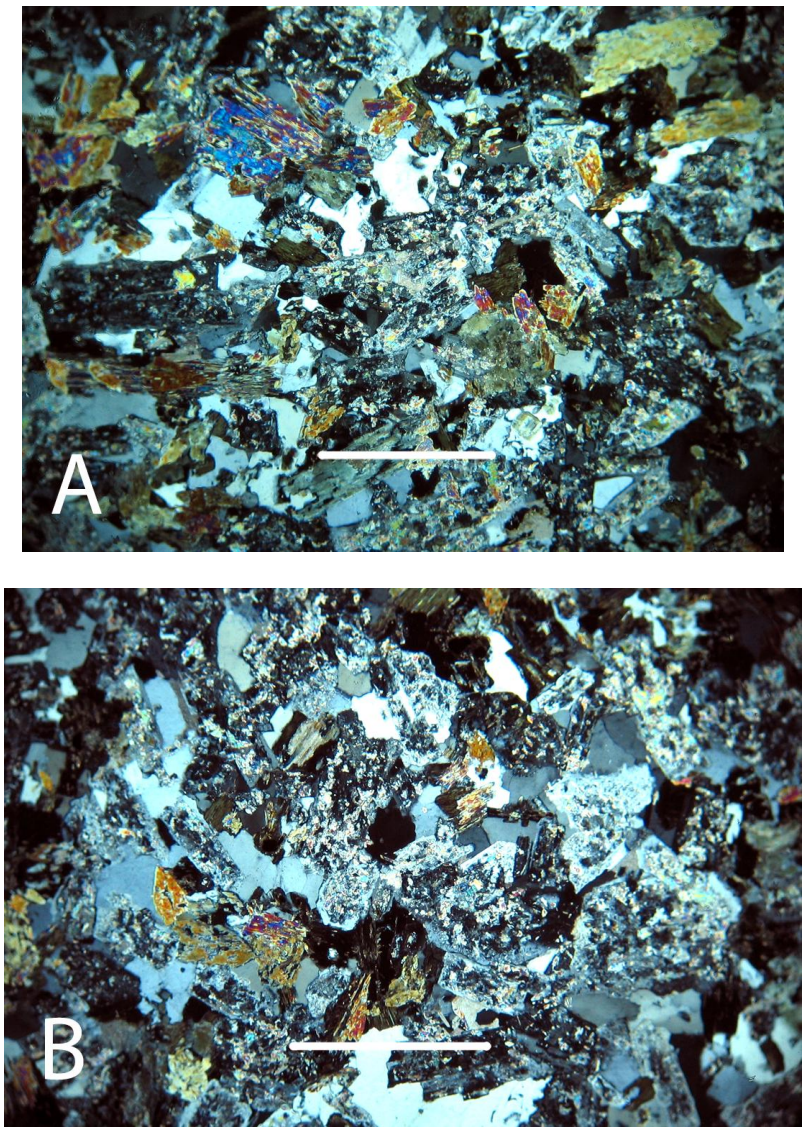

Fig. 3.3. Photomicrographs of the Rockhill Canyon stock. Medium-grained, subhedral granular hornblende granodiorite. Feldspars have extensive sericitic alteration. Both photographs show interstitial quartz, actinolite, plagioclase (altered to muscovite), and epidote. Note photomicrographs (XP) are at 4x magnification, and white lines represent 1mm.

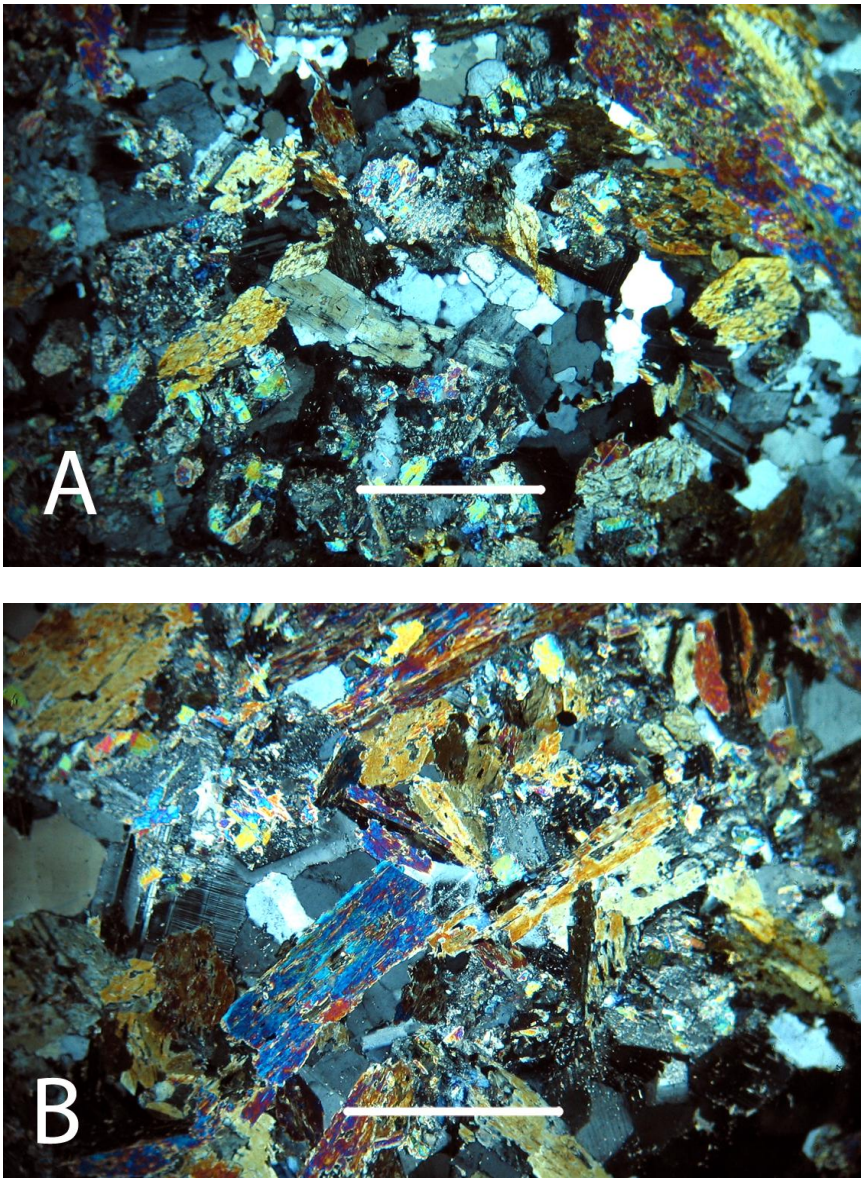

Fig. 3.4. Photomicrographs of the Wadley Mine stocks. (A) Medium-grained hornblende granodiorite collected within the Lee Peak window. Photograph shows plagioclase (altered to muscovite), quartz, and actinolite (partially replacing hornblende). (B) Medium-grained hornblende granodiorite collected from outside the Lee Peak window. Photograph shows actinolite (partially replacing hornblende), plagioclase (altered to muscovite), and quartz. Note photomicrographs (XP) are at 4x magnification, and white lines represent 1mm.

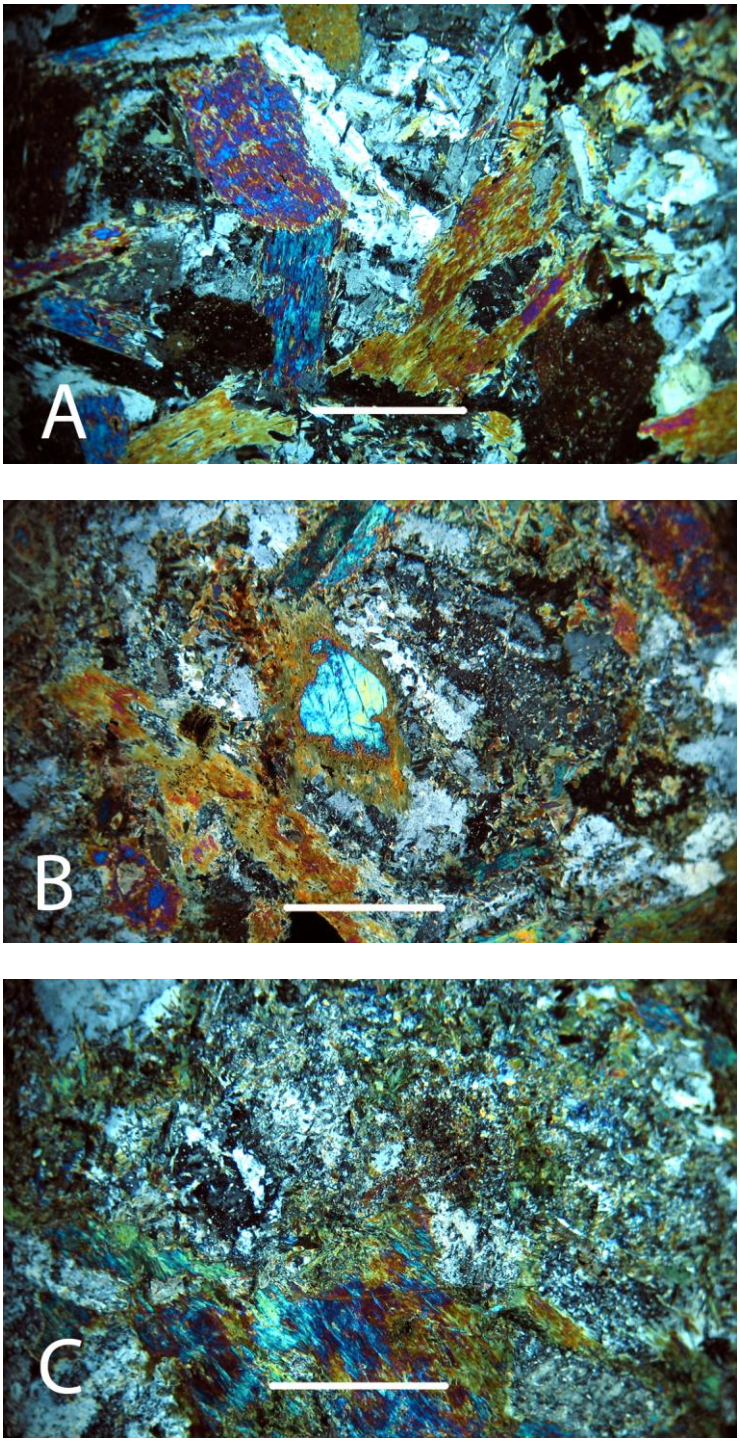

Fig. 3.5. Photomicrographs of the Rawhide Metagabbro. (A) Medium-grained pyroxene, hornblende gabbro. Photograph shows subhedral granular texture with laths of actinolite and plagioclase. (B) Medium-grained, pyroxene, hornblende gabbro. Photograph shows pyroxene being replaced by actinolite (center), plagioclase, and epidote. (C) Medium-grained pyroxene, hornblende gabbro. Note felty texture with actinolite, plagioclase, and chlorite. Note photomicrographs (XP) are at 4x magnification, and white lines represent 1mm.

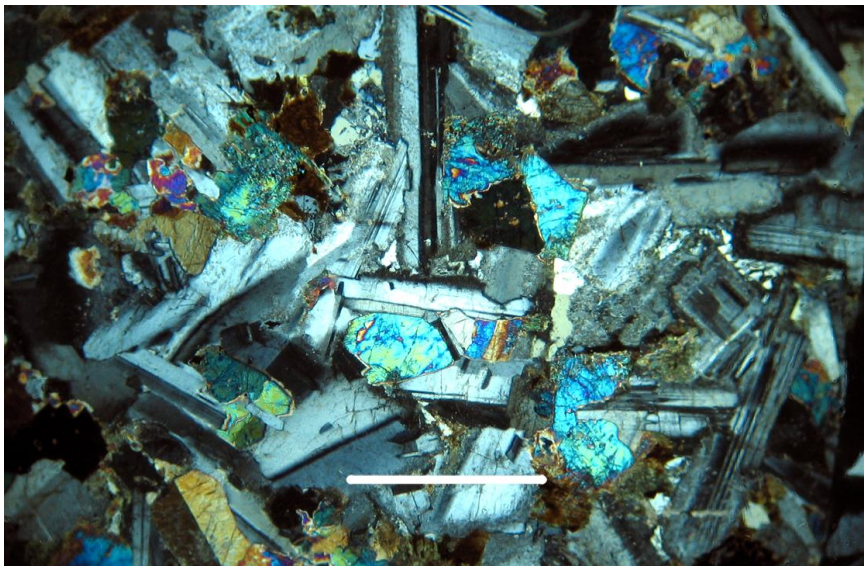

Fig. 3.6. Photomicrograph of the Inskip Canyon stock. Nesophitic medium-grained pyroxene quartz monzo-gabbro. Photograph shows plagioclase with laths up to 2.5mm, pyroxene, oxides, and trace amounts of quartz. Note photomicrographs (XP) are at 4x magnification, and white line represents 1mm.

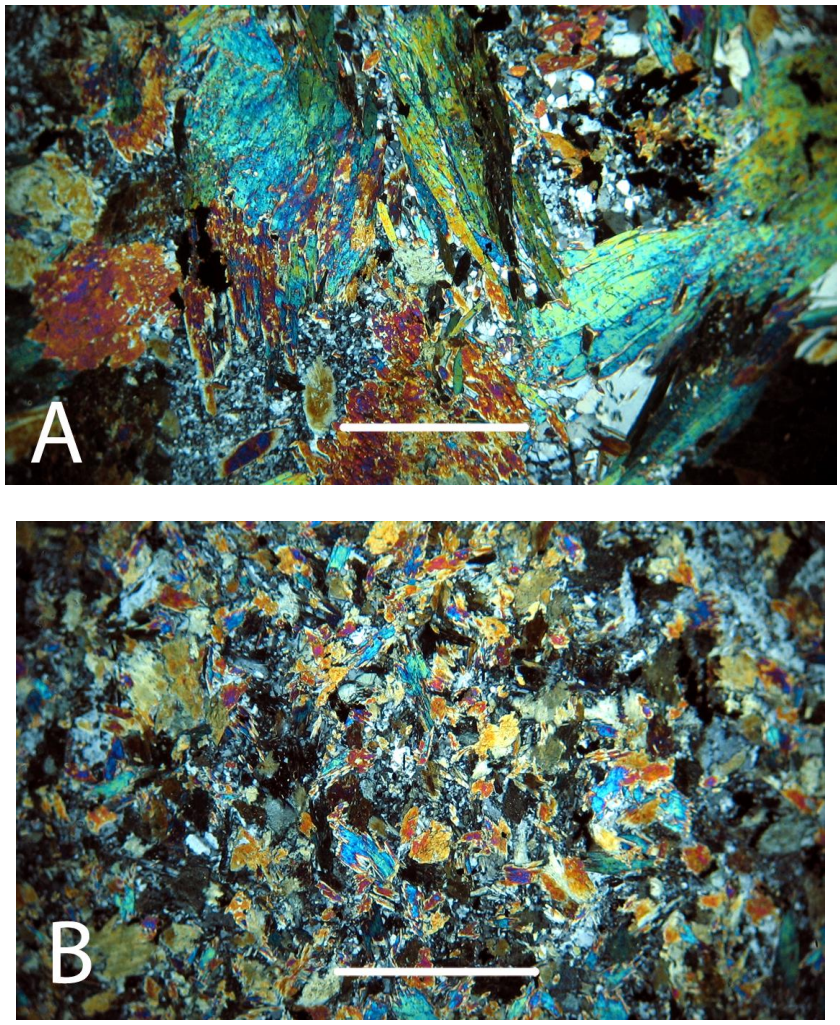

Fig. 3.7. Photomicrographs of the Cenozoic diabase. (A) A medium-grained, porphyritic diabase. Photograph shows phenocrysts of actinolite with a groundmass of plagioclase. (B) A porphyritic to subhedral granular fine-grained diabase. Photograph shows plagioclase, actinolite, and epidote. Note photomicrographs (XP) are at 4x magnification, and white line represents 1mm.

CHAPTER 4: DEFORMATION AND METAMORPHISM

Structural relations and metamorphism have never been the focus of prior studies in the central East Range (Ferguson et al., 1951; Silberling and Roberts, 1962; Whitebread, 1971; Elison, 1987; Ketner, 2008), and these aspects of the geology of the area were thus previously only defined in a very limited sense. Several faults were recognized, including the Rockhill Canyon and Lee Peak Faults, as well as faults parallel to some unit boundaries and other miscellaneous faults, but no analysis of structural or timing relations along these faults was ever done, and most of them have a controversial history (see Ch. 1, and figure 1.7). Structural features at the outcrop scale, such as folds and foliation, have received even less attention, as has metamorphism. Apparent doming of strata and structures around the Lee Peak pluton has long been recognized, but never actually documented or analyzed. Presence of a ductile shear zone on the west side of the range appears to have been completely unrecognized, although Ketner (2008) did describe these rocks as "mylonized" and note that they were more deformed than rocks elsewhere.

Despite these limitations, structural models for the area have been discussed by numerous authors. Probably the most widely discussed interpretation is that deformation in the central East Range reflects west-vergent deformation (Silberling and Roberts, 1962) associated with the Late Jurassic WDB (Elison, 1987; Stahl, 1989; Speed et al., 1988), although Ketner (2008) has argued against elements of this model and has placed

more emphasis on doming related to the Lee Peak pluton. New mapping and structural analysis for this study demonstrates that all prior models have fundamental flaws and fail to account for the full spectrum of structural relations in the central East Range. This is documented in the sections below, which examine structural features and metamorphic relations in the central East Range based on the new detailed analyses done in this study.

Overview of Principal Structures and Structural Domains

All of the stratigraphic units in the central East Range are deformed and metamorphosed, some more so than others. The principal structural features in these units are a space to penetrative foliation, formed under greenschist facies metamorphic conditions, and mesoscopic folds which appear to have formed synchronous with foliation development. These are referred to as D1 structures (S1 refers to foliation, F1 refers to folds of bedding), although fabrics in different units may not all be correlative, as discussed below. Foliation is much more prominent in all areas than is folding.

Megascopic folds are also evident locally, including the domal features around the Lee Peak pluton, an eastward deflection of strata south of the Rockhill Canyon fault, and a NE-trending fold north of this fault. The megascopic folds deform the regional foliation and are therefore referred to as D2 folds, although they likely did not all form at the same time.

On the west side of the range, the rocks bear a much stronger foliation that reflects deformation in the Buena Vista shear zone, which records top to the east sense of offset. This shear zone is confined to the Inskip Formation (Fig.1.10, Plate 1). A stronger

foliation is also evident in strata of the Lee Peak window, except close to the Lee Peak pluton where contact metamorphism overprints and obscures older structures.

The contact between the Valmy and Inskip Formations is identified as an unconformity and a fault (Fig. 1.10 and Plate 1). This fault is folded on a scale that is not seen elsewhere in the central East Range, having variable dip and orientation throughout its trace. The Rockhill Canyon fault is a high angle dextral strike-slip fault. This fault trends E-W, and curves to the north on the western side of the East Range (Fig. 1.10 and Plate 1). Faulting around the Lee Peak window is identified as the Lee Peak fault (Fig. 1.10 and Plate 1). The Lee Peak fault dips gently away from the window, forming a dome around the window (Fig.4.1). Faulting in the NE portion of the central East Range trend to the NE and are high angle brittle faults (Fig. 4.2). Directly north of the Rockhill Canyon fault there is a fault bound wedge of the lower member of the Inskip Formation. The faults surrounding this wedge also appear to be high angle.

In order to analyze structural features of the central East Range more quantitatively, the field area is broken into four structural domains (Fig. 4.3) that highlight folding and foliation in different units, areas and fault blocks. The domains are divided in ways that isolate the effect of certain features such as the Buena Vista shear zone and doming of the Lee Peak pluton. Structural analysis of these domains is used in conjunction with field observations and thin section petrography in the sections below which focus on describing and interpreting structural relations in the central East Range.

Foliation, Metamorphism, and Mesoscopic Folds

Window Units

The two units within the Lee Peak window have a higher metamorphic grade than other rocks found in the central East Range. The Phyllite unit is commonly hornfelsed and partially melted at the contact with the pluton (Fig. 2.22). When examined in thin section the Phyllite unit shows strong evidence for high temperature metamorphism (Figs. 2.23 and 2.24). Phyllite samples show metamorphic minerals that are not aligned with the foliation, which indicates a separate phase of contact metamorphism (Fig. 2.23A). Quartzites display no foliation but have pervasive grain boundary migration indicative a high temperature (500°- 700°C, Passchier and Trouw) and a low strain rate (Fig. 2.23B). Another sample of phyllite from the window shows the growth of incipient cordierite that is similarly overprinting the foliation, also indicative of a separate phase of contact metamorphism (Fig. 2.24). This is partially explained by contact metamorphism from the Lee Peak pluton. Cordierite is most commonly associated with high temperatures ranging from 300°- 800° C (Passchier and Trouw) and low pressure indicative of contact metamorphism

Valmy Formation

Foliation within the Valmy Formation is dominantly a spaced cleavage that is most evident in chert and argillite. Quartzite in the Valmy Formation commonly shows abundant fractures and quartz veins, but foliation is conspicuously absent. Folding of bedding in the Valmy Formation is tight to open, parallel, and have rounded hinges.

These folds have wavelengths and amplitudes up to a few meters. In thin section greenstones found in both the Greenstone and Argillite members display a fractured texture (Fig. 2.3). The texture is interpreted to be both pre- and post-tectonic based on fractures filled with metamorphic minerals, and others with non-metamorphic minerals. The Valmy Formation is characterized by greenschist facies metamorphism for two reasons. First, pyroxenes within the greenstones are completely replaced by actinolite. Second, quartzites contain small amounts of metamorphic muscovite, biotite, and chlorite. Quartz grains within quartzite commonly display undulatory extinction, the formation of subgrains, and lesser amounts of grain boundary migration (Fig. 2.5). This is indicative of low-grade conditions at 300°- 400°C (Passchier and Trouw, 2005).

Inskip Formation

Foliation within the Inskip Formation along the western margin of the central East Range is controlled by the Buena Vista shear zone. Within the shear zone, foliation is penetrative and parallel to bedding (Fig. 4.4), but is also found at a low angle to bedding (Fig. 4.5A). Small-scale D1 folding is commonly associated with the foliation (Fig. 4.5B). The Buena Vista shear zone is here interpreted to represent east-vergent deformation possibly associated with the Fencemaker thrust. Folding within the Inskip Formation occurs within the Buena Vista shear zone, and consists of tight to open, parallel, D2 folds with rounded to sub-rounded hinges (Figs. 4.6). Ductile deformation is common throughout the Inskip, and in the field this deformation is most obvious in coarser-grained rocks (Fig. 4.11). In thin section these rocks have deformation consistent with the greenschist facies, evident by metamorphic minerals such as muscovite, chlorite,

and biotite found in sandstones and wackes (Fig. 2.12). Quartz grains in these sample show undulatory extinction, frequent subgrain formation, and occasionally dynamic recrystallization and pressure shadows. Outside of the Buena Vista shear zone the level of deformation is considerably less.

Havallah Sequence

Deformation in the Havallah Sequence of the East Range is characterized by a single foliation that is folded. Wackes collected from the Havallah (Fig. 2.18) show a foliation that is defined by elongate grains, most noticeable in poly- and crypto-crystalline quartz. Deformation in Quartz grains is limited mostly to undulatory extinction, with lesser amounts of subgrain boundaries forming around the edges of quartz grains (Fig. 2.18). Metamorphic mineral consist of muscovite, biotite, and chlorite. These micas form in residual layers along with oxides that also define the foliation.

Domain 1

Domain 1 (Fig. 4.7) consists of Paleozoic and Triassic rocks within the field area north of the Rockhill Canyon fault. It is in this area that major NW overturned folding is interpreted (Silberling and Roberts, 1962; Wallace and Roberts, 1964; Whitebread, 1978; Elison 1987). Domain 1 is divided into 3 subdomains. Subdomain 1a is the Havallah Sequence, 1b is the Koipato Group, and 1c is the western wedge of lower member of the Inskip Formation.

Figure 4.7 shows that there is a fold north of the Rockhill Canyon fault. The fold is a D2 fold, folding foliation and trending NE and plunging (57, 34). Note that

subdomains 1a and 1c are located on either side of the range, and do not show complete folding, but instead only display limbs of the fold. Subdomain 1b extends the entire width of the East Range in the area, showing a complete fold. This is to be expected due to their relative positions to one another.

Domain 2

Domain 2 (Fig. 4.8) consists of the Valmy Formation and a portion of the lower member of the Inskip Formation. This domain shows effects of doming caused by the Lee Peak pluton. As well as major folding south of Rockhill canyon (Fig. 1.8), specifically in the NE portion of the Valmy Formation. To address these issues domain 2 is divided into five subdomains. Subdomain 2a represents the Valmy north of the Lee Peak window, 2b is the lower member north of the window, and 2c-e represent the Valmy W, SW, and S of the window respectively.

Figure 4.8 indicates that subdomain 2a is the only domain where evidence exists for doming related to emplacement of the Lee Peak pluton. Bedding and foliation in subdomain 2a dip to the NW indicating that this strata is possibly influenced by strike-slip faulting along the Rockhill Canyon fault. Subdomain 2a does not show evidence of major folding such as that found in domain 1. Subdomain 2b is oriented similarly to 2a. However, the dip in 2b is significantly steeper, indicating that the bedding and foliation in this subdomain is controlled by the Rockhill Canyon fault rather than doming. The orientation of bedding and foliation in subdomains c-e does not show any clear trends and are most likely unrelated to doming of the Lee Peak pluton. This foliation most likely

represents deformation from the emplacement of the RMA, and predates Mesozoic deformation.

Domain 3

Domain 3 (Fig. 4.9) represents the Inskip Formation except for the NE part of the formation that is included in Domain 2. Domain 3 is divided into four subdomains. 3a and 3b encompass the Buena Vista shear zone. Because the shear zone curves slightly to the east, it is divided into two domains, north and south of Willow Creek Canyon. Subdomain 3c is the area west of the Rockhill Canyon pluton that is not a part of the Buena Vista shear zone. Subdomain 3d represents a small area north of Inskip Canyon where bedding is overturned due to back-thrusting. This domain is important because it will emphasize features of the Buena Vista shear zone, and clarify any relationship to the LFTB. The Inskip Formation clearly curves eastward and structural data from this domain helps illustrate whether this is caused by doming or strike-slip faulting.

In figure 4.9 subdomains 3a and 3b show that bedding and foliation within the Buena Vista shear zone is dipping approximately 60° to the west. Lineations in 2a and 2b demonstrate that the sense of shear is in an E or W direction. However, it is evident that domains 3b and 3c are dipping more to the NW showing that the original orientation of the Buena Vista shear zone and the Inskip formation is altered. This could be a result of doming, although, the Inskip Formation is not deflected south of the Lee Peak window. Another possibility is that strike-slip faulting along the Rockhill Canyon fault is responsible for the deflection of this formation. Bedding and foliation found in subdomain 3c is similar to that found in subdomain 2b, dipping steeply to the NW. The

angle of bedding and foliation here is caused by the Rockhill Canyon fault dragging the Inskip Formation to the east. Subdomain 3d isolates the effect of back-thrusting discussed in previous sections. The overturned bedding and foliation associated with this back-thrusting is not found anywhere else along the contact, suggesting minor displacement.

Domain 4

Domain 4 (Fig. 4.10) represents the Marble and Phyllite units of the Lee Peak window. This domain is important for two reasons. First, it will show if the bedding and foliation within the Lee Peak window units is related to that found in the Valmy Formation. Secondly, this domain may show signs of doming even though none were present in domain 2.

Data in figure 4.10 shows that domain the window units are not in stratigraphic succession with the Valmy Formation. The window units display bedding and foliation that is distinct from the Valmy Formation. The bedding and foliations within domain 4 are conspicuously flat lying. This also suggests that these rocks are uplifted and domed by the Lee Peak pluton. This shows that a minimal amount of doming did occur, and it is most evident within the Lee Peak window.

Large-Scale Deformation

In addition to small-scale deformation, the central East Range contains many large-scale geologic structures such as map-scale folds, the Rockhill Canyon fault, the Lee Peak fault, the Buena Vista shear zone, doming (?), and a variety of subordinate faulting. Many of these structures have been identified (Ferguson et al., 1951; Silberling

and Roberts, 1962; Whitebread, 1978) and interpreted to be the result of west-vergent deformation. New mapping and new data has led to the reinterpretation of previously identified features and the identification other features that must be incorporated into a new structural model of the East Range.

The Rockhill Canyon fault (Fig. 1.10 and Plate 1) is here interpreted to be a vertical dextral strike-slip fault. The trace of the Rockhill Canyon fault is identified by disconcordant bedding and foliation, truncation of the Inskip and Valmy Formations, and fault breccia in the Valmy Formation. Structure contouring indicates that this faulting is at a high angle because the trace of the fault is unaffected by topography (Fig. 4.12 and Plate 2). The trace of the fault is difficult to distinguish on the western side of the East Range, because of the absence of fault breccia. However, a low-angle stretching lineation (281, 8) is found in a foliated conglomerate of the Havallah Sequence along the E-W portion of the fault in Rockhill Canyon supports strike-slip motion. The eastern extent of the fault curves to the north when it comes in contact with the Valmy Formation. This portion of the fault is characterized by brittle deformation, as evidenced by prominent outcrops of fault breccia (Fig. 4.13). This deflection is caused by the Quartzite member that is rheologically stronger that the Havallah and Inskip. This curve in the Rockhill Canyon fault results in compression, forming the major NE trending syncline north of the Rockhill Canyon fault (Fig. 4.7) discussed in previous sections. Although this data supports a major fold north of Rockhill Canyon, it does not show evidence of the fold being overturned, or resulting from west-directed deformation. Folding north of Rockhill Canyon can now be explained without the need of west-vergent deformation. However, structural analysis (Fig. 4.8) of the central East Range does not support the previous

interpretation of a large NW overturned anticline within the Paleozoic rocks south of the Rockhill Canyon fault (Fig. 1.8).

Although the amount of displacement along the Rockhill Canyon fault is unknown, it is inferred that it is relatively small (10s of kms) and possibly oblique. This is suggested, for two reasons by rocks within the small outcrop from the lower member of the Inskip Formation north of the Rockhill Canyon fault. First, this exposed piece of the lower member is most likely not far traveled. The lower member of the Inskip Formation is relatively thin and only found in the East Range. Second, if the fault is to be considered a dextral strike-slip fault then this piece from the lower member must have come from the down-dip direction of the Inskip Formation south of the fault. Because the Inskip is dipping approximately 60°W, the wedge of Inskip must have come from that section of the formation. However, there are most likely more complicated processes at work to create this relationship, possibly involving normal faulting. Dextral motion is also evidence of dragging along the fault. Figure 1.10, and structural data (Figs. 4.8 and 4.9) in the previous section shows how the Inskip Formation appears to be pulled along the southern side of the fault. This not only demonstrates the motion of the fault, but also that the fault effects structures in this area of the East Range.

Brittle faulting in Rockhill Canyon is juxtaposed against the ductile deformation of the Buena Vista shear zone. Considerable vertical offset is required for this relationship to be possible. Rocks within the shear zone indicate that they must have formed below 4km, where ductile deformation can occur. The extent of the shear zone is determined by presence of the characteristic foliation found only in the Inskip Formation (Fig. 4.4). This deformation is restricted to the Inskip Formation for the same reason that

the Rockhill Canyon fault is deflected. The underlying Quartzite member is rheologically stronger than the Inskip Formation and confined the deformation within the Inskip Formation.

Ductile deformation and mylonitization within the Inskip Formation is mentioned by Ketner (2008). However, it has not been described in detail or analyzed for shear sense indicators (SSI). The Buena Vista shear zone is described in this study as a zone of bedding-parallel shear resulting in penetrative mylonitic foliation. To the north, the Buena Vista shear zone dissipates between Willow Creek and Rockhill Canyon (Fig. 1.10 and Plate 1). To the south, the Buena Vista shear zone continues south, out of the field area, but possibly for the entire length of the Inskip Formation. Multiple samples collected from the Buena Vista shear zone were analyzed for SSI. However, only one sample contains definitive SSI (Fig. 4.14). This SSI shows top to the east sense of shear in a mylonitic quartz wacke. This supports the idea that the deformation in the Buena Vista shear zone is not a result of the WDB.

In this study, the Lee Peak fault is interpreted to be a west-vergent thrust fault, separating the Marble and Phyllite units from the Valmy Formation. The Lee Peak fault is recognized by fault breccia (Fig. 4.115), disconcordant bedding, truncation the Valmy Quartzite on the western side of the window, and truncation of greenstone lenses to the north (Fig. 1.10 and Plate 1). Structure contouring of the fault (Fig. 4.1) indicates a low angle fault, forming a dome around the metasedimentary units (Fig. 4.16). Like the Rockhill Canyon fault the Lee Peak fault is a brittle fault that is juxtaposed to the Buena Vista shear zone. This relationship suggests that the Lee Peak fault is younger than the

Buena Vista shear zone and may have been responsible for bringing this zone of deformation from depth to the surface.

Map relations suggest that doming caused by the intrusion of the Lee Peak pluton has occurred. The existence of the Lee Peak pluton within the Lee Peak window may be coincidental, but most likely suggests that at least a small amount of doming has occurred, or topographic relief was present before faulting occurred. The Inskip Formation could also be affected by doming, subsequently altering the orientation of the Buena Vista shear zone. The Inskip and Valmy Formations noticeably curve to the east (Fig. 1.10 and Plate 1), north of the Lee Peak pluton. This also could be a result of doming, however, to the south of the Lee Peak pluton this potential doming is not present. This is most likely a product of strike-slip faulting along the Rockhill Canyon fault. Structural data (Fig. 4.8) presented in the previous section shows that bedding and foliation outside of the Lee Peak window does not definitively support significant doming.

The contact between the Inskip and Valmy Formations is found to be partially faulted (Fig. 1.10 and Plate 1). The section of the contact north of Inskip Canyon is a reverse fault placing the Quartzite member over the Inskip Formation (Fig. 4.17). This faulting is characterized by localized overturned bedding within the Inskip Formation, and fault breccia. Faulting is only identified within a 2km section of the contact. Either faulting is not laterally continuous or extends into the Inskip formation and is unidentified. This fault is interpreted to represent minor west directed displacement (Fig. 4.18).

Multiple high angle faults have been identified in the NE section of the field area (Fig. 1.10 and Plate 1). Previously undocumented, these faults are highly brecciated linear features (Fig. 4.2). These faults are parallel and appear to splay off the Rockhill Canyon fault. However, displacement along these faults is unknown and their association with the regional structures is uncertain. Similar faulting is present along the Havallah/Koipato contact and farther north in the Triassic shelf terrane (Plate 1). These faults are interpreted to be related to later events, possibly Basin and Range extension.

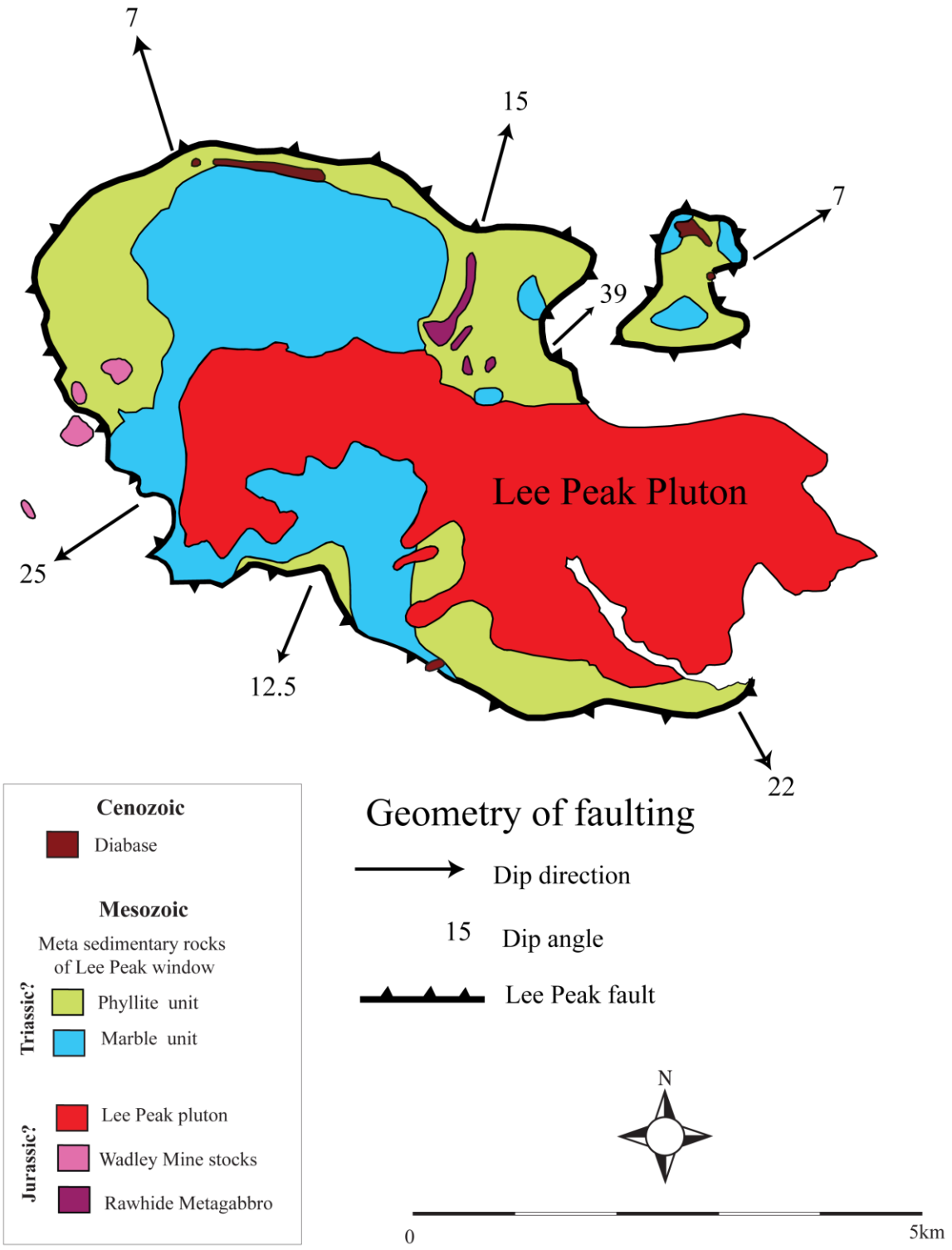

Fig. 4.1. Diagram showing the orientation of the Lee Peak fault plane. The Lee Peak fault forms a dome around the Lee Peak window.

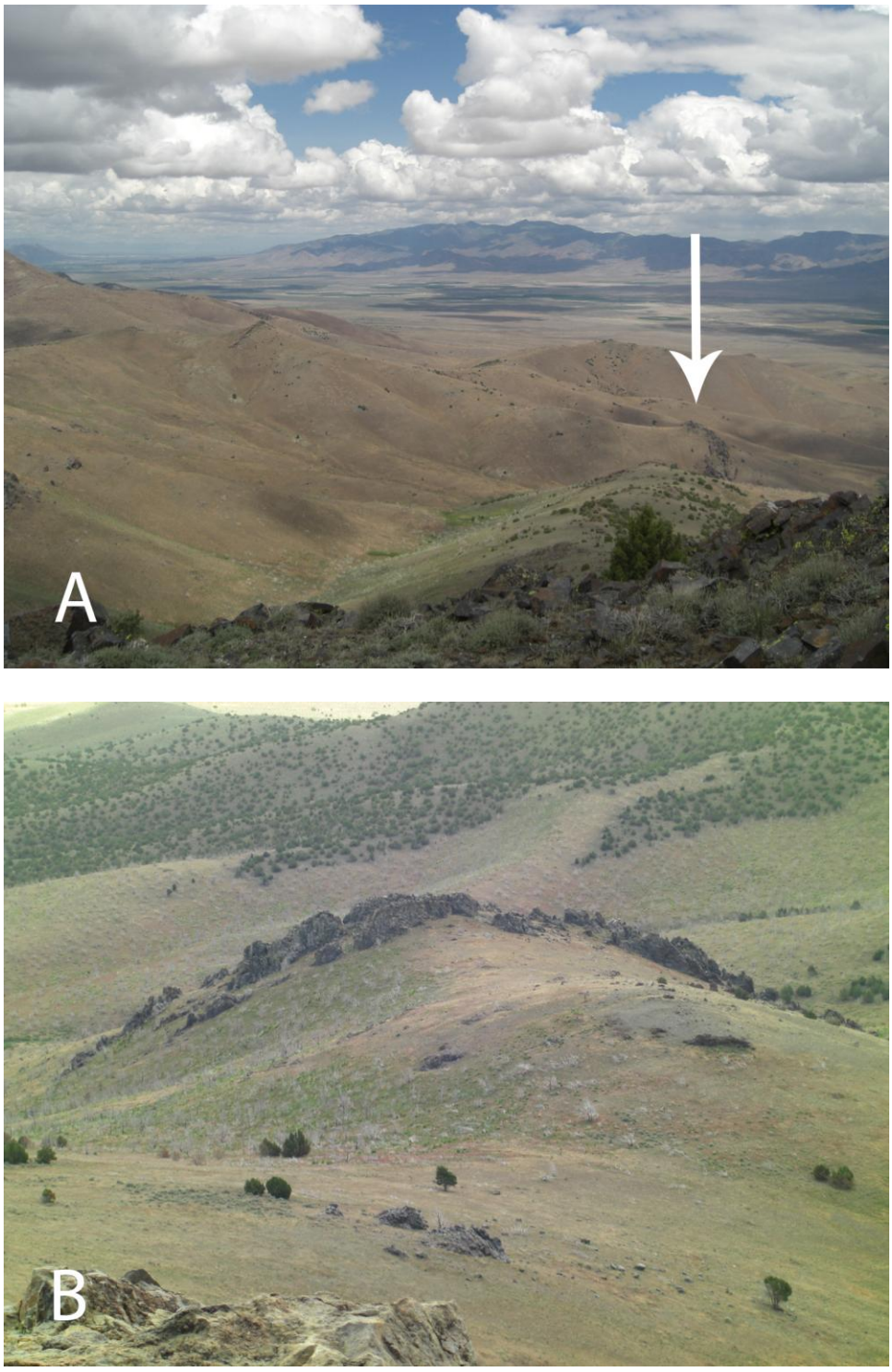

Fig. 4.2. Photographs of high angle NE trending faults. NE trending brittle faults a characterized by fault breccia forming prominent outcrops. (A) View from the south to the northeast showing the fault breccia from a distance (white arrow). (B) View from the west to the southeast, perpendicular to linear outcrops of fault breccia shown in (A). Note outcrops are not affected by topography, indicating a vertical fault.

Fig. 4.3. Map of the central East Range divided into four structural domains. Dotted lines indicated domain boundaries. Domain1represents the rocks within the field area north of the Rockhill Canyon fault, Domain 2 represents rocks surrounding the Lee Peak window consisting of the Valmy Formation and some of the Inskip Formation, Domain 3 represents the majority of the Inskip Formation and the Buena Vista unit, and Domain 4 represents the rocks within the Lee Peak window.

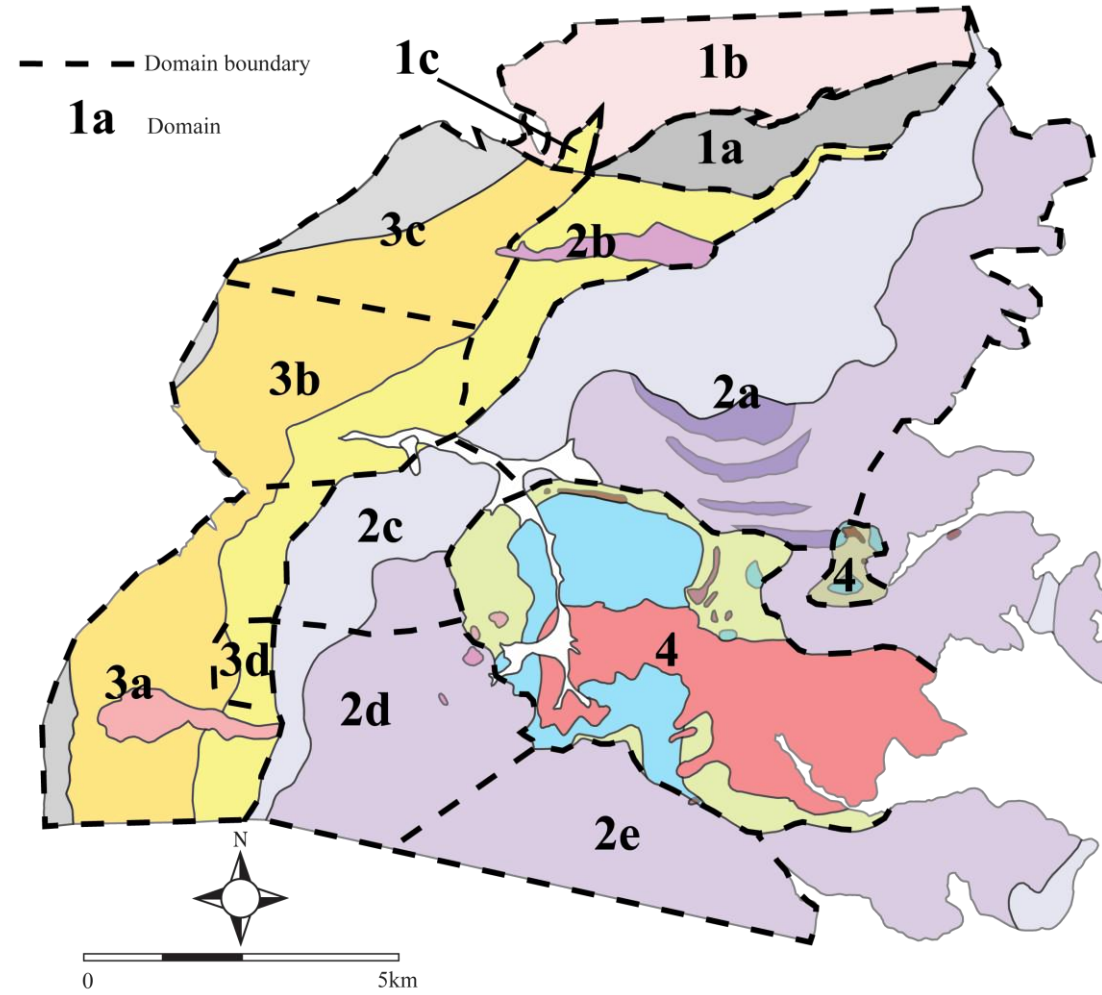

LEGEND

Cenozoic

Qal

Diabase

Inskip Canyon stock

Mesozoic

Meta sedimentary rocks of Lee Peak window

Triassic?

Phyllite unit

Marble unit

Early Triassic

Koipato Group

Jurassic?

Lee Peak pluton

Rockhill Canyon stock

Wadley Mine stocks

Rawhide Metagabbro

Paleozoic

Mississippian - Permian

Havallah Sequence

Buena Vista Formation

Mississippian

Inskip Formation

Upper Member

Lower Member

Ordovician

Valmy Formation

Quartzite Member

Argillite Member

Greenstone Member

Fig. 4.4. Photograph of foliation in the Buena Vista shear zone. View to the north of foliated Inskip sandstone within the Buena Vista shear zone. Note stretched clasts of quartzite indicated by white arrow. Pocket knife for scale.

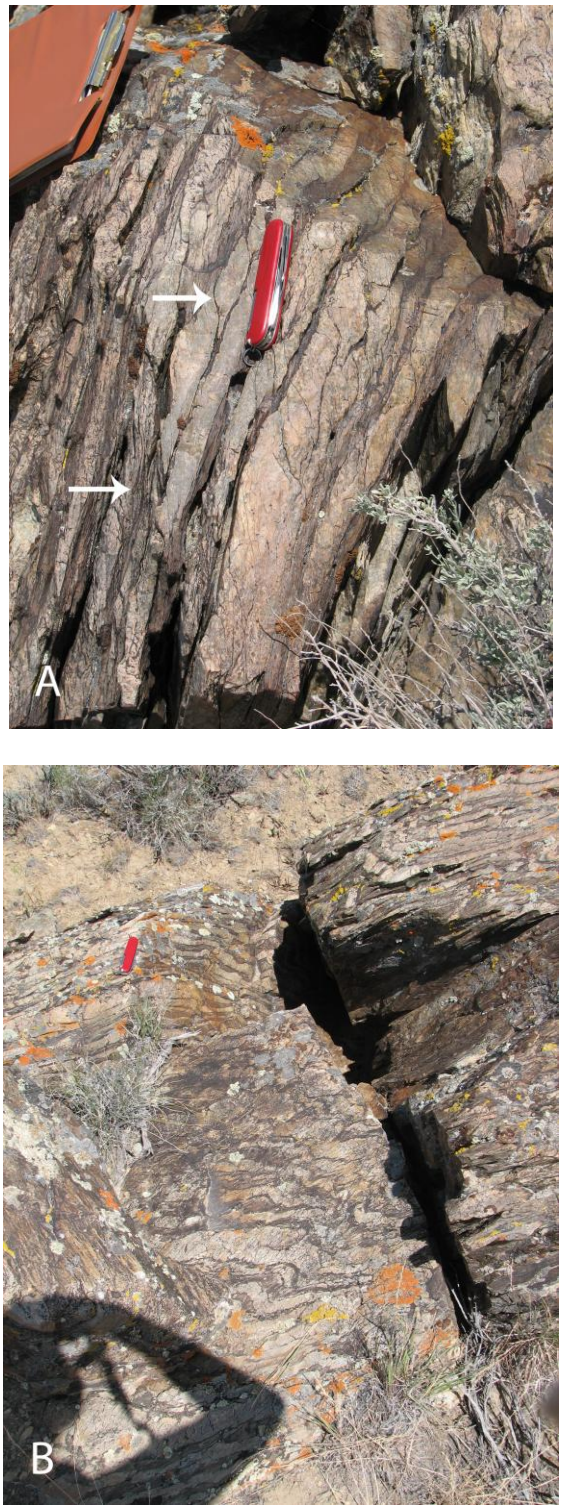

Fig. 4.5. Photographs showing deformation in the upper member of the Inskip Formation. (A) foliation at an angle to bedding indicated by white arrows. The angle between bedding is higher in fine sandstone layers (light) compared to argillite layers (dark). (B) small scale D1 folds with fine-grained sandstone (light) and argillite (dark). Note pocket knife for scale.

Fig. 4.6. Photograph of folding in the Inskip Formation. View to the north, of open, sub-rounded, parallel D2 fold in fine-grained sandstone from lower member of the Inskip Formation within the Buena Vista shear zone. Note hammer for scale.

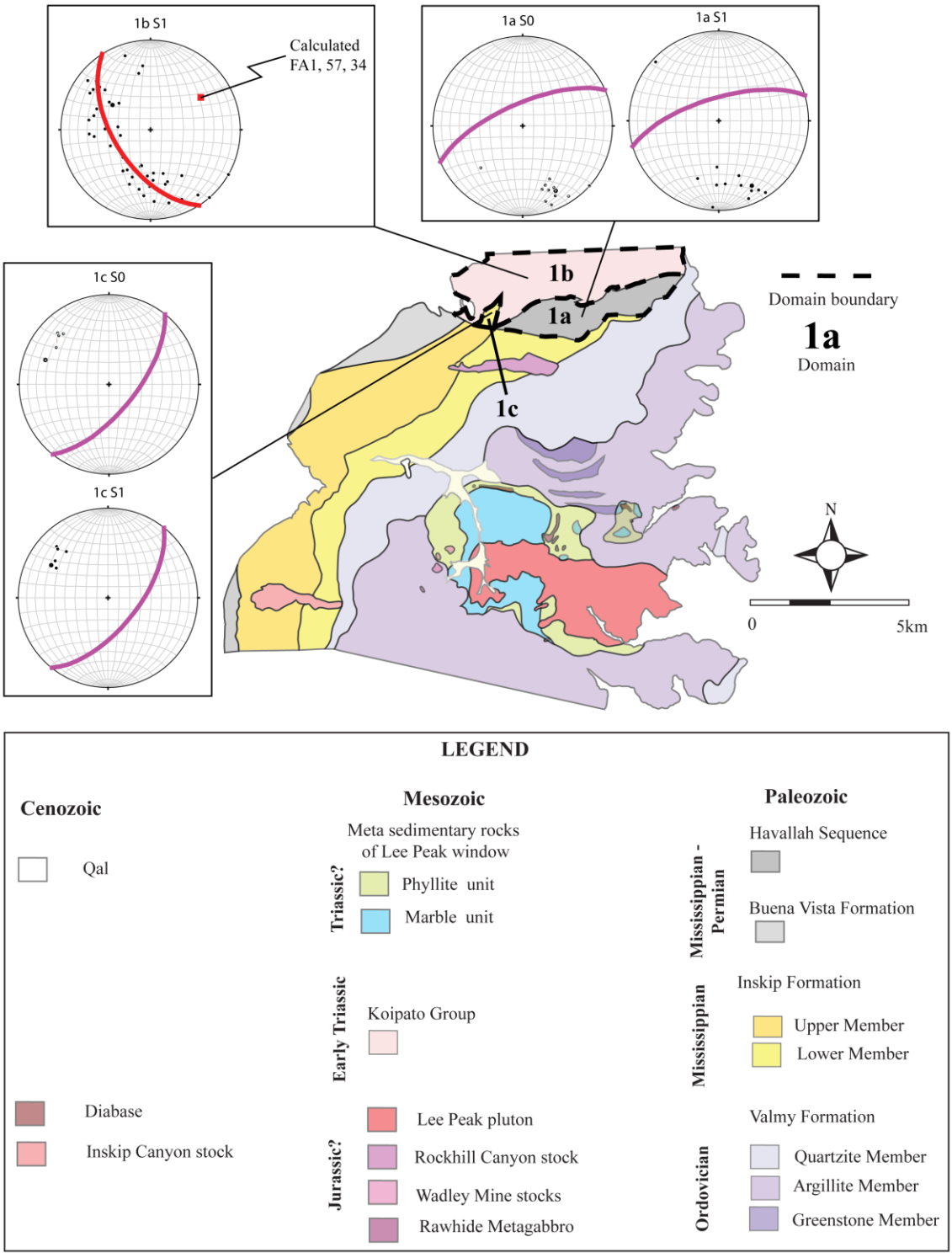

Fig. 4.7. Domain 1. Subdomains are 1a (Havallah), 1b (Koipato), 1c (western wedge of Inskip). Open circles are poles to bedding planes, solid dots are poles to S1 foliation, magenta line indicates the average planes, and red squares are calculated fold axis.

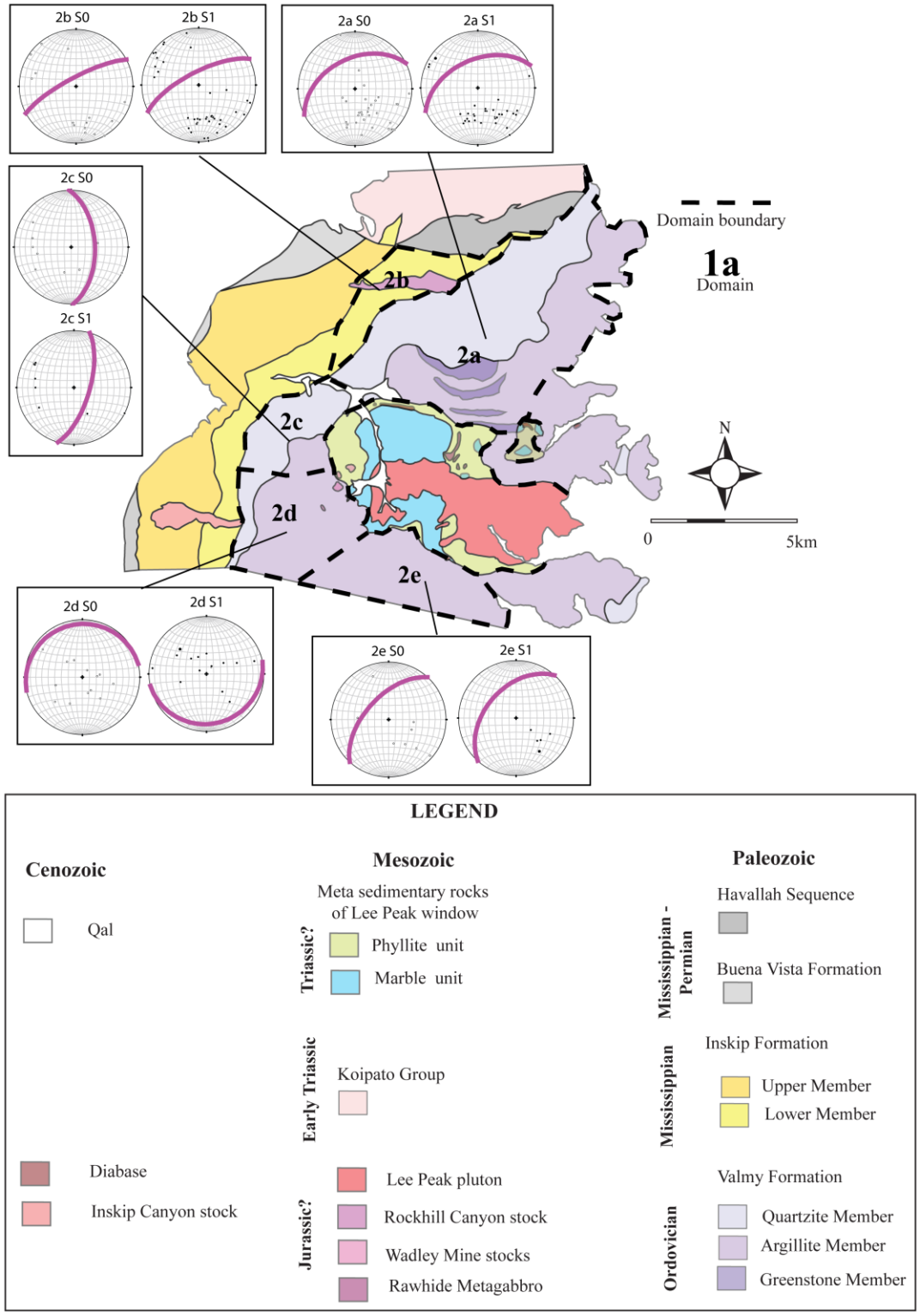

Fig. 4.8. Domain 2. Subdomains are 2a (north Valmy), 2b (north Inskip), 2c (west Valmy), 2d (southwest Valmy), 2e (south Valmy). Circles represent poles to bedding, dots represent poles to S1 foliation, and magenta line indicates the average planes. Note the absence of obvious doming around the Lee Peak pluton within the Valmy Formation.

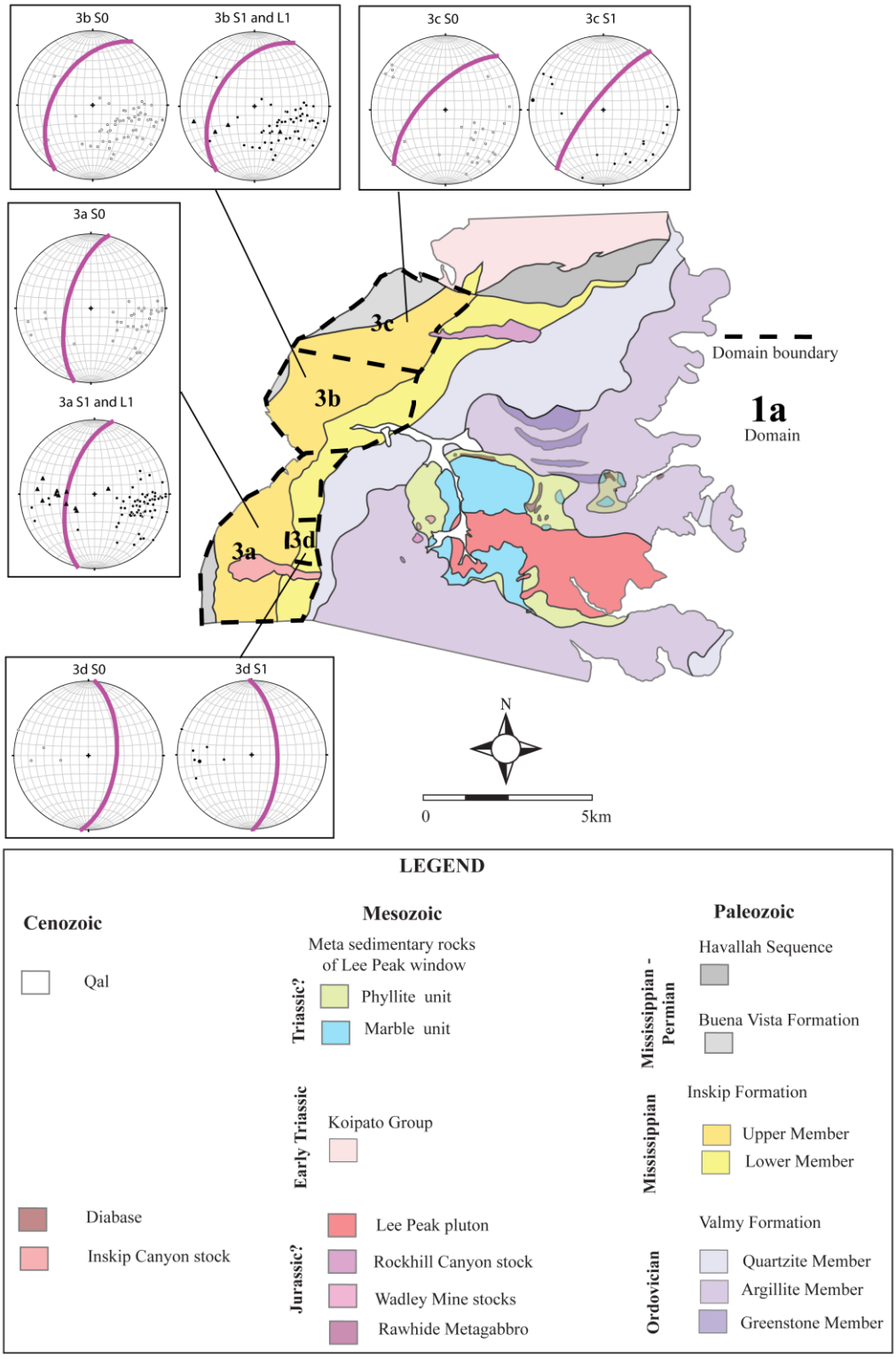

Fig. 4.9. Domain 3. Subdomains are 3a (south Buena Vista shear zone), 3b (north Buena Vista shear zone), 3c (NW Inskip Formation), 3d (overturned Inskip). Circles represent poles to bedding, dots represent poles to S1 foliation, triangles represent lineations, and magenta lines indicate average planes.

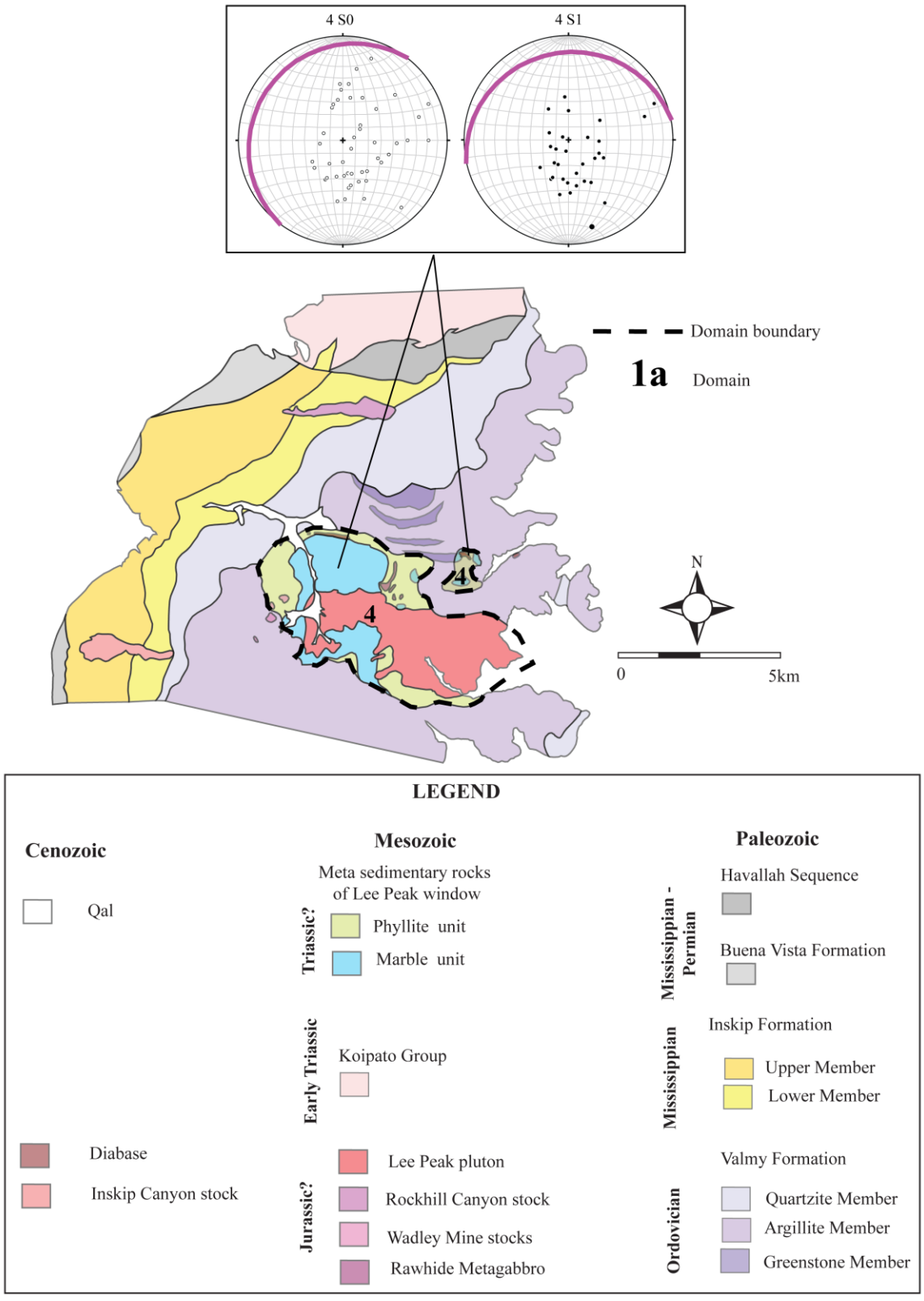

Fig. 4.10. Domain 4. Circles represent poles to bedding, dots represent poles to S1 foliation, and magenta lines indicate average planes.

Fig. 4.11. Photographs of ductile deformation in the Inskip Formation. (A) Conglomerate from outside the Buena Vista shear zone. Note sigma-shapes and cataclastic fractures in chert clasts (white arrow points to two deformed chert clasts, large sigma shaped quarzite clast indicated by white arrow (hammer for scale).

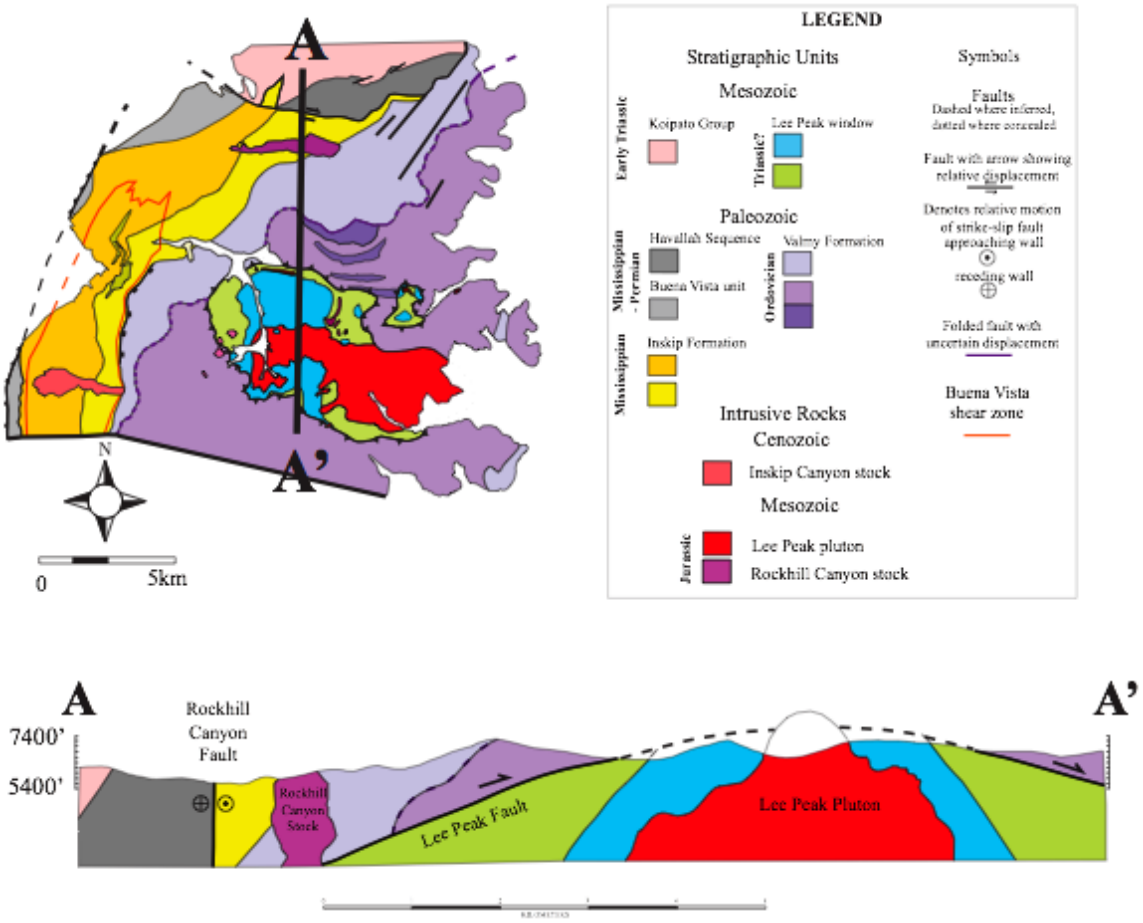

Fig. 4.12. Cross section along A-A‟. See Plates 1 and 2.

Fig. 4.13. Photographs of fault breccia along the Rockhill Canyon fault within the Quartzite member. Fault breccia consists of brecciated quartzite with quartz cement. Note brecciated rocks are easily identifiable within the Valmy Formation because of the abundance of quartzite clasts.

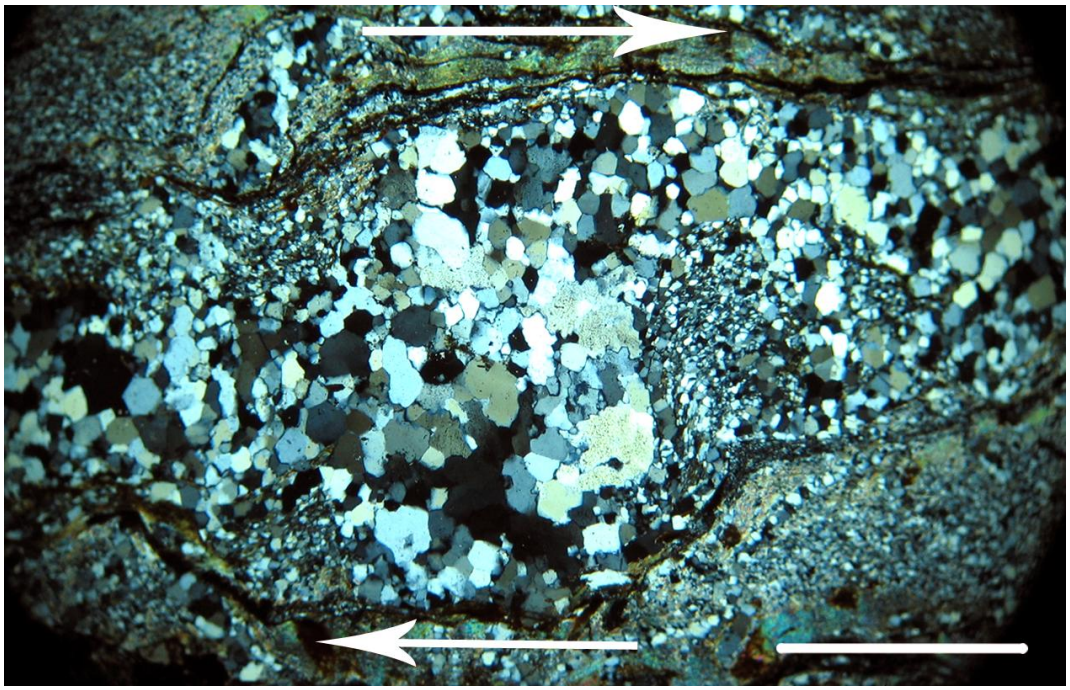

Fig. 4.14. Photomicrograph of a SSI found in the upper member of the Inskip Formation. SSI in the quartz wacke indicates a top to the east sense of shear. Note white arrows indicate sense of shear, and white line represents 1mm.

Fig. 4.15. Photograph of fault breccia from the Lee Peak fault. Fault breccia consists of brecciated quartzite with quartz cement from the Lee Peak fault. Note pocket knife for scale.

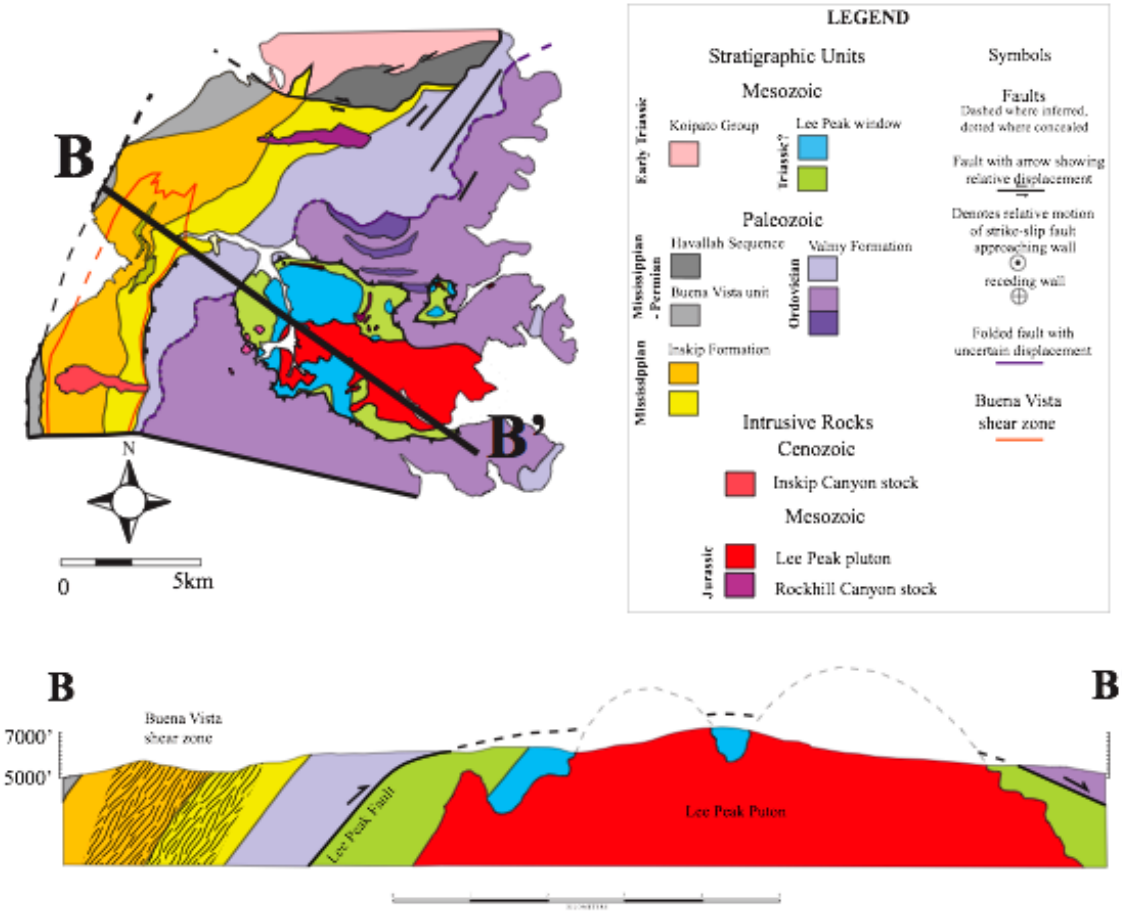

Fig. 4.16. Cross section along B-B'. See Plates 1 and 2.

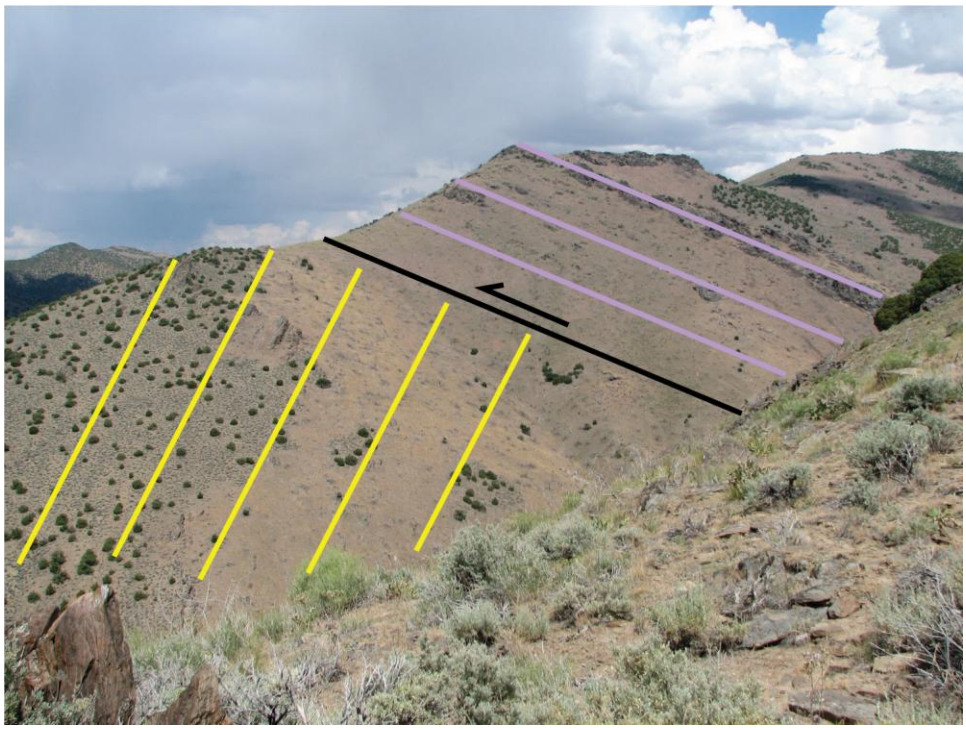

Fig. 4.17. Photograph showing back-thrusting along the Inskip/Valmy contact. View to the NE of back-thrusting along the Inskip/Valmy contact north of Inskip Canyon. The Quartzite member (lavender) is thrust over the lower member of the Inskip Formation (yellow). The black line represents the localized fault. Bedding in the lower Inskip is locally overturned at the fault contact.

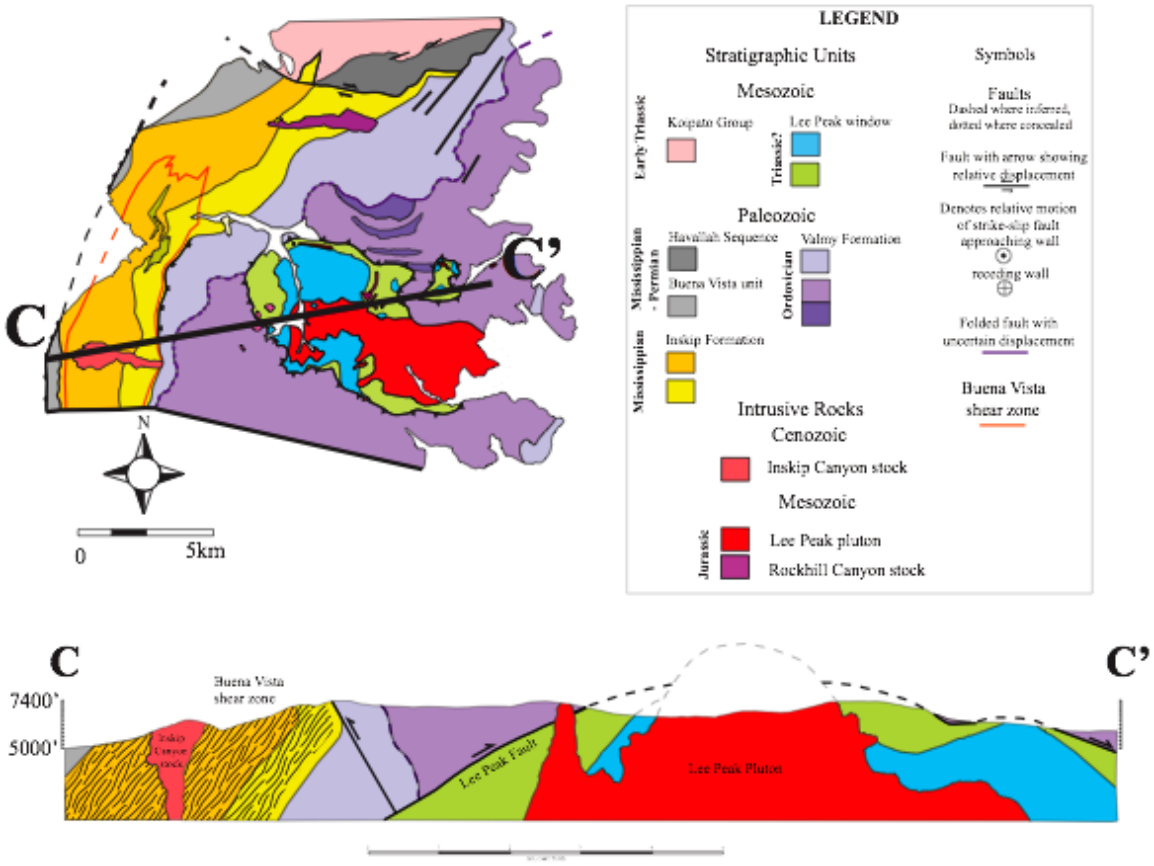

Fig. 4.18. Cross section along C-C'. See Plates 1 and 2.

CHAPTER 5: STRATIGRAPHIC AND STRUCTURAL ANALYSIS, AND COMPARISON WITH PRIOR STUDIES

Correlation of Units within the Lee Peak Window

As previously described, the metasedimentary rocks within the Lee Peak window have been interpreted in many ways. New mapping (Fig. 1.10 and Plate 1) shows that the Early Ordovician fossil found in Rawhide Canyon cannot be used to date the window units, because it is now located within the Valmy Formation. This study has also confirmed faulting around the Lee Peak window units. This proves that the window units are not in depositional contact with the overlying Valmy Formation as previously suggested by Ketner (2008). With no evidence to support an Early Ordovician age for the window units, they are here reinterpreted to be part of the Triassic shelf terrane as originally documented by Ferguson et al. (1951).

The Triassic shelf terrane contains abundant carbonates and siliciclastics (Fig. 1.6) that may represent the protoliths of the metasedimentary rocks of the window units. However, it is unclear as to which of these formations the window units correlate to. The Prida Formation (Fig. 5.1) shows many similarities to the window Marble, such as bedding and composition, making this formation a possible candidate. However, there is no overlying siliciclastic unit that would correlate with the Phyllite unit. The Upper Canes Spring Formation is described (Elison, 1987) as thick bedded (10-100cm) platform carbonate strata, and is overlain by the Grass Valley group. The Grass Valley group

consists of mostly fine-grained siliciclastics that are similar in composition to the Phyllite unit. The Upper Canes Spring Formation and the overlying Grass Valley Group correlate best with the Marble and Phyllite units and will tentatively be considered equivalent.

Comparison between the Inskip Formation and Havallah Sequence

As discussed above, the distinction between the Inskip Formation and Havallah Sequence has been unclear. Previous interpretations of the relationship between the two formations relied upon map relations, lithologies, and fossil age data. Information presented in the previous section is objectively compared and possible relationships between the two formations are addressed.

Various interpretations of faulting occurring in Rockhill Canyon have contributed to the confusion between the Inskip and Havallah. The initial mapping of the East Range (Ferguson et al. 1951) indicates no continuous faulting; therefore there is no need to distinguish separate formations. Continued work on the area led to the interpretation of the WCT and the subsequent identification of the Havallah Sequence (Silberling and Roberts, 1962; Whitebread, 1978; Elison, 1987; Speed et al., 1988). Most recently Ketner (2008) interprets no major faulting in Rockhill Canyon, ultimately leading to the consolidation of the Inskip and Havallah. In this study, data suggests that the Rockhill Canyon fault is a dextral strike-slip fault. The evidence of such faulting supports the possibility that the Inskip and Havallah are separate formations.

The comparison of the lithologies of the Inskip Formation and Havallah Sequence has previously been used to justify consolidation or separation of the two formations. In this study field observations and thin section petrography indicates that there are

significant lithologic differences between the Inskip and Havallah. The Inskip Formation is dominated by coarse grit wacke (lower member), fine-grained sandstone/wacke and argillite (upper member), conglomerate, and minor amounts of limestone and volcanic strata. In contrast the Havallah Sequence is characterized by interbedded chert and argillite, and lesser amounts of sandstone/wacke, limestone, and volcanic strata. The Havallah Sequence is differentiated from the Inskip by its relatively finer-grained strata, and the presence of bedded chert. Thin section petrography from the Havallah Sequence (Fig. 2.18) indicates that wackes are fine-grained (up to 1mm framework grains), have poor to moderate sorting, and grains are sub-angular. Framework grains compose up to 50% of the sample, and consist mostly of mono-crystalline quartz, with lesser amounts of poly-crystalline quartz, and little to no feldspar. Thin section petrography from the Inskip Formation (Fig. 2.10) shows wackes are medium/coarse-grained (1-3mm framework grains), are poorly sorted, and have sub-angular grains. Framework grains compose up to 60% of the sample, and consist of equal parts of mono- and poly-crystalline quartz, and up to 15% feldspar grains. Although the high amount of poly-crystalline quartz in the Inskip Formation could be a result of subgrain boundary formation due to a higher level of deformation, it most likely suggests a different sediment source than that of the Havallah Sequence.

As discussed above, previous mapping and fossil data (Whitebread, 1978) show that the Inskip Formation and Havallah Sequence span the Mississippian through Permian (Fig. 2.6). However, new data in this study shows that the Inskip Formation only contains Mississippian aged fossils and the Havallah Sequence contains possibly

Mississippian, but definitively Permian aged fossils. This new interpretation of fossil data indicates that the Inskip and Havallah are distinct formations.

Previous data used to support the interpretation of Paleozoic rocks north of Rockhill Canyon as the Inskip Formation are suspect. In this study the Inskip Formation is distinguished from the rocks identified as the Havallah Sequence.

New Structural Model

The structures of the central East Range that are discussed above are incorporated into a new structural model of the East Range. This new model explains deformation and map relations in the central East Range without the need of west-vergent deformation. In the vicinity of the Humbolt and East Range, the Fencemaker thrust bulges out to the west in response to a protuberance of the shelf terrane (Fig. 5.2). The East Range is located in the center of this bulge. Within this bulge, it is interpreted that imbricate thrusting within the footwall of the Fencemaker thrust has occurred causing the eastward propagation of stress resulting in the geology in the central East Range (Fig. 5.3).

The new model (Fig. 5.3) depicts the structural evolution of the East Range, showing how structures and map relations are explained without the WDB. Figure 5.3A-B) depicts the evolution of the Fencemaker thrust. The basinal terrane is thrust over the shelf terrane along the Fencemaker thrust (Elison and Speed, 1989). Figure 5.3C) shows bedding parallel thrusts initiating in the shelf terrane (Elison and Speed, 1989). After continued propagation along the bedding parallel thrust of the Fencemaker thrust, displacement along the Buena Vista fault occurs (Fig. 5.3). This fault is not exposed but its existence is inferred. The Buena Vista fault represents the propagation of east-vergent

deformation into the footwall of the Fencemaker thrust. This fault is necessary to explain the Buena Vista shear zone. While displacement is occurring along the Buena Vista fault, the Inskip Formation is buried at depth. The top to the east sense of shear results in the bedding parallel mylonitic foliation found in the shear zone. It is at this time that dextral tear faulting of the Rockhill Canyon initiates to compensate for displacement in the footwall. Figure 5.3E depicts the formation of the Lee Peak fault. This fault is responsible for bringing Paleozoic basement rocks, including the Buena Vista shear zone to the surface. This explains how the brittle faulting of the Rockhill and Lee Peak faults can be juxtaposed against the Buena Vista shear zone. Figure 5.3F shows the emplacement of the Lee Peak pluton during the Jurassic (note that the effect of doming is exaggerated). Figure 5.3G shows the current structural setting

Conclusions

1) There is no evidence to support the WDB or significant west-vergent deformation in the East Range. Rather, structural data indicates that the central East Range is characterized by east-vergent deformation. The Rockhill Canyon fault is a dextral strike-slip fault, and the large fold directly north of Rockhill Canyon is a result of the strike-slip motion. The Lee Peak fault represents progressive east-vergent thrusting into the footwall of the Fencemaker thrust, and is not directly related to the Rockhill Canyon fault as previously thought. The Lee Peak fault is responsible for bringing Paleozoic basement rocks to the surface, exposing the RMA.

2) New mapping of the central East Range yields new boundaries for the Marble and Phyllite units of the Lee Peak Window. These units were previously interpreted to be

Early Ordovician based on a fossil data from the NE corner of the Lee Peak window. However, new mapping shows that this fossil is within the Valmy Formation and is consistent with other fossils from this formation. These rocks are now interpreted to be equivalent to the Triassic shelf terrane found in the northern East Range, possibly the Prida or upper Canes Spring Formation.

3) The Buena Vista shear zone is identified as a zone of bedding parallel shear resulting in a mylonitic foliation. The shear zone formed when displacement along the inferred Buena Vista fault occurred at depth. SSI shows that the sense of shear is top to the east.

4) The Buena Vista unit is identified. This unit is lithologically distinct from the upper member of the Inskip Formation. Fossil data indicates a Permian age for this unit supporting its distinction form the Mississippian Inskip Formation.

5) Doming caused by the Lee Peak pluton is present, but minimal, and only noticeable in the window units. Motion along the Rockhill Canyon fault is proven to be a more significant factor in shaping the center East Range.

6) The extent of the Inskip Formation is modified from previous mapping. To the north, a wedge of the lower member is identified north of the Rockhill Canyon fault. The western extent of the Inskip is altered by the addition of the Buena Vista Formation along the Range front. This has implications for the age of the Inskip Formation and Havallah Sequence.

7) The Inskip Formation and Havallah Sequence in the East Range are found to be distinct formations based on lithology, fossil age data, and map relations.

8) Data discussed in previous sections is incorporated into a new structural model of the central East Range. This new model shows that the eastward propagation of stress has led to progressive thrusting into the footwall of the Fencemaker thrust, and subsequent tear faulting in Rockhill Canyon. This model can explain all of the previously controversial features of the central East Range by eliminating west-vergent deformation of the WDB.

Fig. 5.1. Photographs comparing the Marble unit to the Prida Formation. (A) Typical outcrop from the Marble unit, hammer for scale. (B) Outcrop of the Prida Formation in the northern East Range, hammer for scale. The Prida Formation is potentially correlative to the Marble unit in the central East Range. Note hammers for scale.

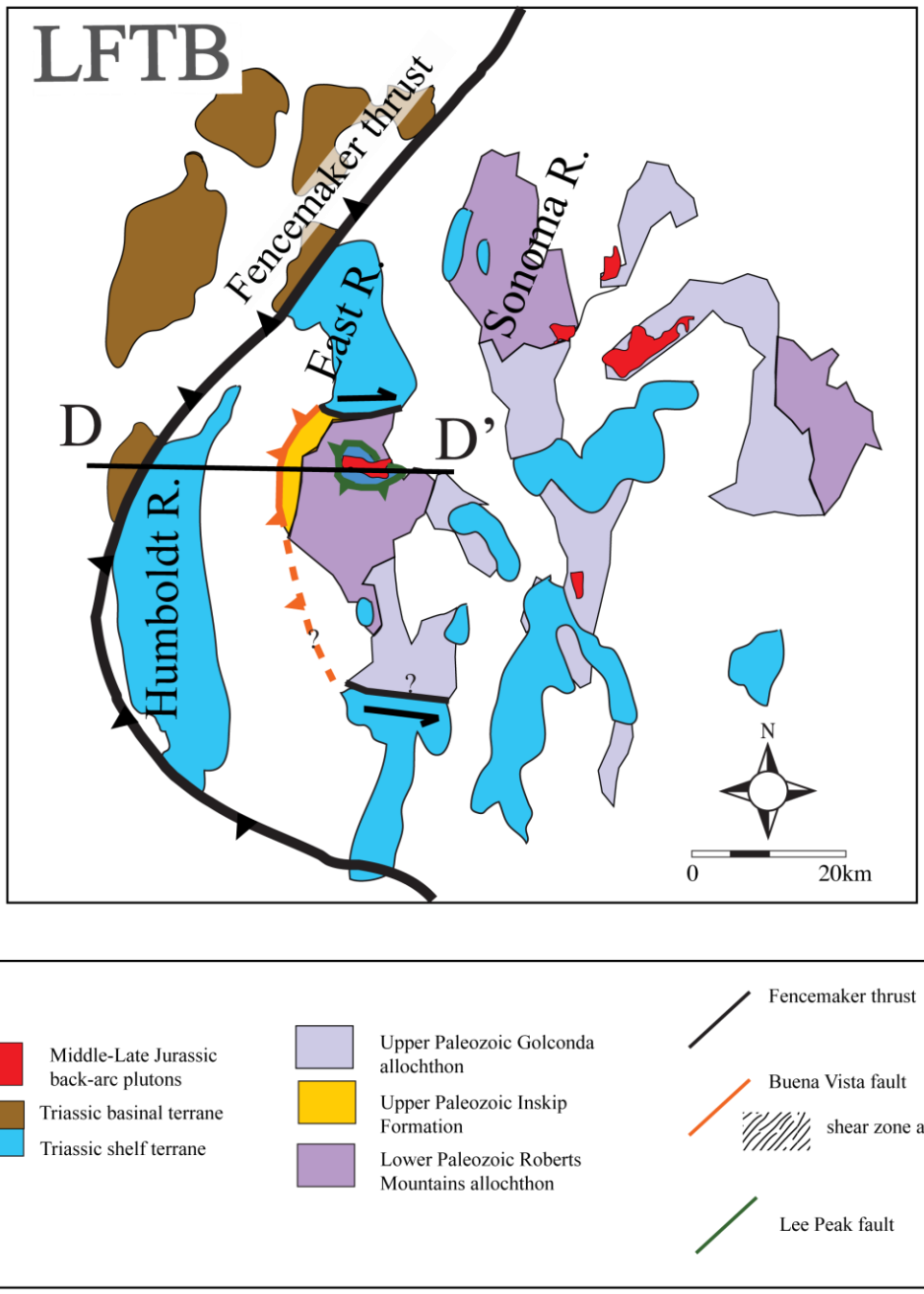

Fig. 5.2. New structural model: map view (see Fig. 5.3 for cross section).

Fig. 5.3. New structural model: cross section view. D-D‟ schematic cartoon depicting the structural evolution of the East Range in cross sectional view. A-C) Progressive emplacement of the basinal terrane over the shelf terrane along the Fencemaker thrust. Note the location for the future Buena Vista fault. D) Displacement occurs along the Buena Vista fault placing shelf terrane over shelf terrane. Note the formation of the Buena Vista shear zone buried at depth and the location of the future Lee Peak fault. E) Displacement occurs along the Lee Peak fault, carrying the shear zone to the surface and placing Paleozoic basement over shelf terrane. F and G) The intrusion of the Lee Peak pluton at (date) doming Paleozoic and Triassic rock, and erosion.

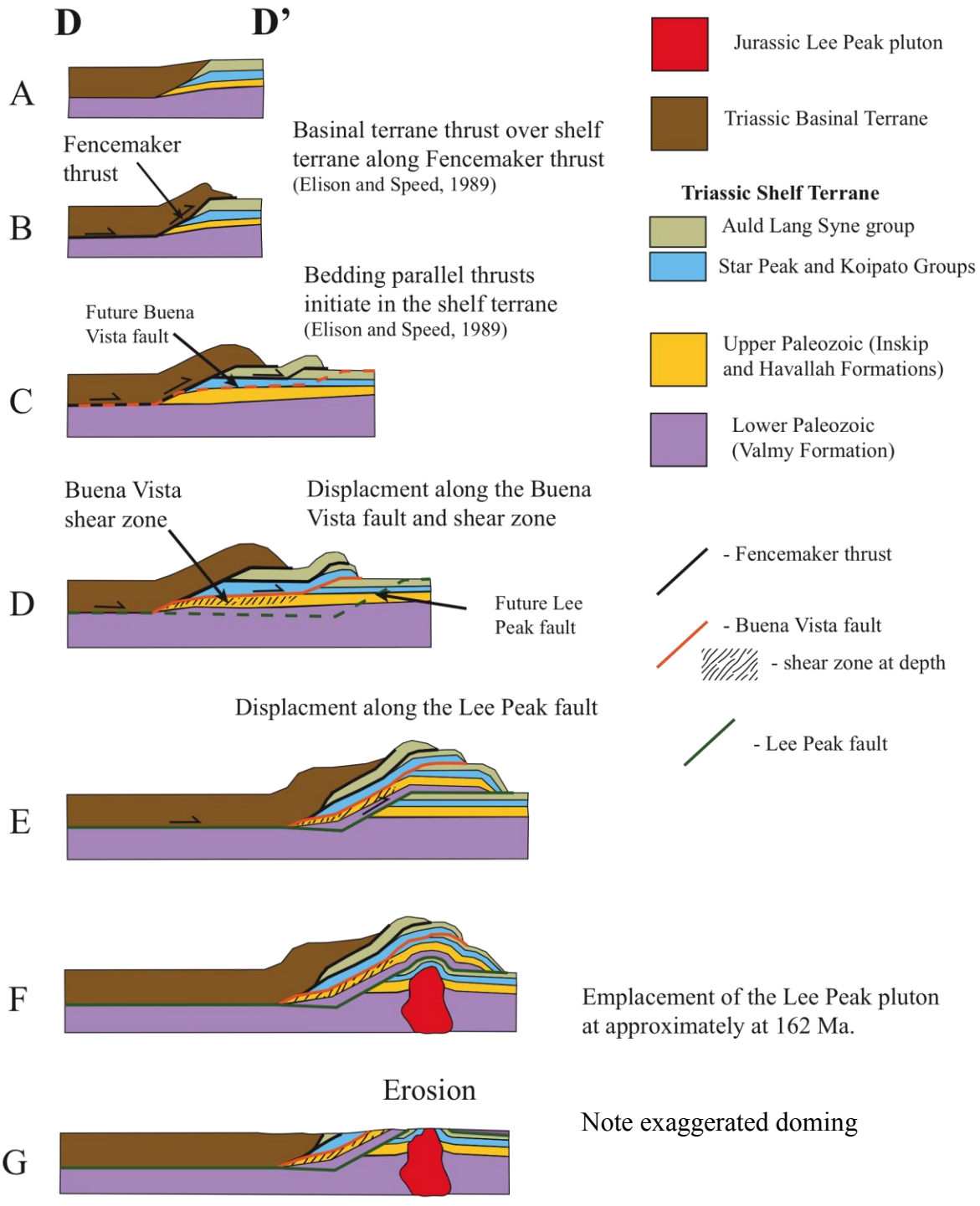
D
D'
A
Basinal terrane thrust over shelf terrane along Fencemaker thrust (Elison and Speed, 1989)
Fencemaker thrust
B
Bedding parallel thrusts initiate in the shelf terrane (Elison and Speed, 1989)
Future Buena Vista fault
C
Buena Vista shear zone
Displacment along the Buena Vista fault and shear zone
D
Future Lee Peak fault
Displacment along the Lee Peak fault
E
F
Emplacement of the Lee Peak pluton at approximately at 162 Ma.
Erosion
G
Note exaggerated doming
Jurassic Lee Peak pluton
Triassic Basinal Terrane
Triassic Shelf Terrane
Auld Lang Syne group
Star Peak and Koipato Groups
Upper Paleozoic (Inskip and Havallah Formations)
Lower Paleozoic (Valmy Formation)
- Fencemaker thrust
- Buena Vista fault
- shear zone at depth
- Lee Peak fault

REFERENCES

Burchfiel, B.C., Cowan, D.S., and Davis, G. A., 1992, Tectonic overview of the Cordilleran orogen in the western United States, in Burchfiel, B. C., Lipman, P. W., and Zoback, M. L., editors., The Cordilleran Orogen: Conterminous U. S. Geological Society of America, The Geology of North America, v. G-3, p. 407–480.

DeCelles, P.G., 2004, Late Jurassic to Eocene evolution of the Cordilleran thrust belt and foreland basin system, western U.S.A.: American Journal of Science, v. 304, p. 105-168.

DeCelles, P.G., and Coogan, J.C., 2006, Regional structure and kinematic history of the Sevier fold-and-thrust belt, central Utah.: Geological Society of America Bulletin, Vol. 118, Issue 7-8, pp. 841-864.

Elison, M.W., 1987, Structural geology and tectonic implications of the East Range, Nevada [Ph.D. thesis]: Evanston, Illinois, Northwestern University, 308 p.

Elison, M.W., and Speed, R.C., 1989, Structural development during flysch basin collapse: the Fencemaker allochthon, East Range, Nevada: Journal of Structural Geology, v. 11, p. 523-538.

Elison, M.W., Speed, R.C., and Kistler, R.W., 1990, Geologic and isotopic constraints on the crustal structure of the northern Great Basin: Geological Society of America Bulletin v. 102, p. 1077 – 1092.

Ferguson, H.G., Muller, S.W., and Roberts, R.J., 1951, Geology of the Winnemucca Quadrangle, Nevada: U. S. Geological Survey Map GQ-11.

Gehrels, E.G., Dickinson, W.R., Riley, B.C.D., Finney, S.C., 2000, Detrital zircon geochronology of the Roberts Mountains allochthon, Nevada, *in* Soreghan, M.J. and Gehrels, G.E., eds., Paleozoic and Triassic paleogeography and tectonics of western Nevada and northern California: Boulder, Colorado, Geological Society of America Special Paper347, p. 19-42.

Gradstein, F.M., Ogg, J. G., and 17 others, 2004, Geologic Timescale 2004: Cambridge, Cambridge University Press, 500p.

Heck, F.R., and Speed, R.C., 1987, Triassic olistostrome and shelf-basin transition in the western Great Basin: Paleogeographic implications: Geological Society of America Bulletin, v. 99, p. 539-551.

Johnson, M.G., 1977, Geology and mineral deposits of Pershing County, Nevada: Nevada Bureau of Mines Bulletin 89, 115p.

Ketner, K.B., Wardlaw, B.R., Harris, A.G., and Repetski, J.E., 2000, The East Range, northwestern Nevada - A neglected key to the tectonic history of the region, *In* Cluer, J.K., Price, J.G., Stuhsacker, E.M., Hardyman, R.F., and Moris, C.L., eds., Geology and ore deposits 2000 - The Great Basin and beyond: Geological Society of Nevada Symposium Proceedings, May 15-18, p. 389-396.

Ketner, K.B., 2008, The Inskip Formation, the Harmony Formation, and the Havallah Sequence of Northwestern Nevada – An interrelated Paleozoic assemblage in the home of the Sonoma Orogeny: USGS Prof. Paper 1757, 21 p.

Lupe, R., and Silberling, N.J., 1985, Genetic relationship between lower Mesozoic continental strata of the Colorado Plateau and marine strata of the western Great Basin: significance for accretionary history of Cordilleran lithotectonic terranes, in

Howell, D. G., ed., Tectonostratigraphic terranes of the Circum-Pacific region: Circum-Pacific Council for Energy and Mineral Resources, Earth Science Series, no. 1, p. 263-271.

Martin, A.J., Wyld, S.J., Wright, J.E., and Bradford, J.H., Depositional environments and structural setting of the Lower Cretaceous King Lear Formation, northwest Nevada: Implications for regional tectonic evolution: submitted 2008 to Geological Society of America Bulletin.

Miller, E.L., Gans, P.B., Wright, J.E., and Sutter, J.F., 1988, Metamorphic history of the east-central Basin and Range province: Tectonic setting and relationship to magmatism, in Ernst, W. G., ed., Metamorphism and crustal evolution, western coterminous United States, Rubey Vol. 7: Prentice-Hall, Englewood Cliffs, New Jersey, p. 649-682.

Miller, E.L., Miller, M.M., Stevens, C.H., Wright, J.E., Madrid, R., 1992, Late Paleozoic paleogeographic and tectonic evolution of the western U.S. Cordillera *in* Burchfiel, B. C., Lipman, P. W., and Zoback, M. L., editors., The Cordilleran Orogen: Conterminous U. S. Geological Society of America, The Geology of North America, v. G-3, pp. 57-105.

Nichols, K.M., and Silberling, N.J., 1977, Stratigraphy and Depositional history of the Star Peak Group (Triassic), northwestern Nevada: Geological Society of America Special Paper 178, 73 pp.

Oldow, J.S., 1984, Evolution of a late Mesozoic back-arc fold and thrust belt, northwestern Great Basin, U. S. A.: Tectonophysics, v. 102, p. 245-274.

Passchier, C.W., Trouw, R.A., 2005, Microtectonics: Second Edition.

Roberts, R.J., Hotz, P.E., Gilluly, J., and Ferguson, H.G., 1958, Paleozoic rocks of north-central Nevada: American Association of Petroleum Geologists Bulletin, v. 42, no. 12, p. 2813-2857.

Silberling, N.J., Roberts, R.J., 1962, Pre-Tertiary Stratigraphy and Structure of Northwestern Nevada: USGS NO. 72.

Smith, D.L., Miller, E.L., Wyld, S.J., and Wright, J.E., 1993, Progression and timing of Mesozoic crustal shortening in the northern Great Basin, Western U.S.A., in Dunne, G.C., and McDougall, K.A., eds., Mesozoic paleogeography of the Western United States II, Field Trip Guidebook. Pacific Section, Society of Economic Paleontologists and Mineralogists, Volume 71, p. 389-405

Speed, R.C., 1978, Paleogeographic and plate tectonic evolution of the early Mesozoic marine province of the western Great Basin, in Howell, D. G., and McDougall, K. A., eds., Mesozoic paleogeography of the western U. S.: Pacific Section, Society of Economic Paleontologists and Mineralogists, Pacific Coast Paleogeography Symposium 2, p.253-270.

Speed, R.C., 1974, Evaporite-carbonate rocks of the Jurassic Lovelock Formation, West Humboldt Range, Nevada: Geological Society of America Bulletin, v. 85, p. 105-118.

Speed, R.C., Sleep, N.H., 1982, Antler Orogenry and foreland basin; a model: Geological Society of America Bulletin, Vol. 93, Issue 9, pp. 815-828.

Speed, R., Elison, M.W., and Heck, F.R., 1988, Phanerozoic tectonic evolution of the Great Basin, in Ernst, W. G., ed., Metamorphism and crustal evolution, western coterminous United States, Rubey Vol. 7: Prentice-Hall, Englewood Cliffs, New Jersey, p. 572-605.

Stewart, J.H., 1980, Geology of Nevada: A discussion to accompany the Geologic map of Nevada: Nevada Bureau of mines and Geology Special Publication 4.

Stahl, S.D., 1987, Pre-Cenozoic structural geology and tectonic history of the Sonoma Range, north-central Nevada [Ph.D. thesis]: Evanstone, Illinois, Northwestern University, 286 p.

Stahl, S.D., 1989, Recognition of Jurassic transport of rocks of the Roberts Mountains allochthon: Evidence from the Sonoma Range, north-central Nevada: Geology, v. 17, p. 645-648.

Wallace, R.E., Silberling, N.J., 1964, Westward tectonic overriding during Mesozoic time in north-central Nevada: USGS, Prof. Paper 501-C, pages C10-C13.

Whitebread, D.H., 1978 Preliminary geologic map of the Dun Glen Quadrangle: U.S. Geological Survey Open-File Report 78-407, scale 1:48,000.

Whitebread, D.H., 1994 Geologic map of the Dun Glen quadrangle: U.S. Geological Survey Miscellaneous Investigations Map I-2409, scale 1:48,000.

Wyld, S.J., 2002, Structural evolution of a Mesozoic back-arc fold-thrust belt in the U.S. Cordillera; new evidence from northern Nevada: Geological Society of America Bulletin, v. 114, p. 1452-1468.

Wyld, S.J., 2000, Triassic evolution of the arc and backarc of northwestern Nevada, and evidence for extensional tectonism, in Soreghan, M. J., and Gehrels, G. E., eds., Paleozoic and Triassic Paleogeography and tectonics of western Nevada and northern California: Boulder, CO, Geological Society of America Special Paper 347, p. 1-23.

Wyld, S.J., and Wright, J.E., 2000, Timing of deformation in the Mesozoic Luning-Fencemaker fold-thrust belt, Nevada: Geological Society of America Abstracts with Programs, v. 32, no. 7, p. A169-A170.

Wyld, S.J., Rogers, J.W., and Wright, J.E., 2001, Structural evolution within the Luning-Fencemaker fold-thrust belt, Nevada: Progression from back-arc basin collapse to intra-arc shortening: Journal of Structural Geology, v. 23, no. 12, 1971-1995.

Wyld, S.J., Rogers, J.W., and Copeland, P., 2003, Metamorphic evolution of the Luning-Fencemaker fold-thrust belt, Nevada: Illite crystallinity, metamorphic petrology, and 40 Ar/39 Ar geochronology: Journal of Geology, v. 111, p. 17-38.

APPENDIX A: Plate 1

APPENDIX B: Plate 2

LEGEND

Stratigraphic Units

Cenozoic

Quaternary alluvium

Diabase dikes

Inskip Canyon stock - Hornblende, pyroxene monzodiorite.

Quartz, plagioclase, biotite porphyry dikes

Jurassic?

Lee Peak pluton - Hornblende, biotite granodiorite to granite.

Wadley Mine stocks - Hornblende granodiorite.

Rockhill Canyon stock - Hornblende Granite

Rawhide metagabbro - Pyroxene, hornblende metagabbro.

Triassic

Early Triassic through Late Triassic

Auld Lang Syne Group

Auld Lang Syne Group - Basal terrane, mostly sandstone, siltstone, and shale.

Star Peak Group

Star Peak Group - Shelf terrane, mostly carbonate.

Koipato Group

Rochester Rhyolite - Felsic volcanic tuffs, flows, and conglomerate.

Triassic?

Lee Peak Window Units

Window Phyllite - Inferred equivalent to Lower Auld Lang Syne group. Primarily phyllite, with minor sandstone, quartzite and limestone.

Window Marble - Inferred equivalent to Star Peak group. White to dark grey, fine to coarse grained limestone and marble.

Paleozoic

Mississippian - Permian

Havallah Sequence

Havallah Sequence - Interbedded chert and siliceous argillite, fine/medium sandstone/quartzite, phyllite, greenschist.

Buena Vista Unit

Buena Vista Unit- Characterized by thinly bedded/laminated siltstone, shale, argillite, and limestone. Minor dismembered limestone beds.

Ordovician

Valmy Formation

Quartzite Member - Dominated by massively bedded fine/medium grained mature quartzite, minor siliceous argillite, black chert, and greenstone.

Argillite Member - Siliceous argillite and black chert with minor limestone, phyllite, and greenstone.

Greenstone Member- Greenstone, pillow basalts with limy matrix, volcanic breccia, and volcano-clastics.

Mississippian

Inskip Formation

Upper Member - siliceous argillite, fine sandstone, greenstone, with minor quartzite, limestone, graphitic layers.

Conglomerate - Found within both members.

Lower Member - Defined by immature poorly sorted medium grained sandstones/wackes with with large (3mm) grains of quartz /quartzite. Also consists of quartzite, conglomerates, siliceous argillite, and fine sandstone.

LEGEND

Symbols

Bedding

Non-mylonitic foliation

Buena Vista shear zone

Boundary of shear zone

Mineral and stretching lineation

Mylonitic foliation

Faults

Dashed where inferred, dotted where concealed

Normal fault
bumps on the hanging wall

High angle fault of uncertain displacement marked by cataclasite breccia

strike slip fault

Thrust Fault
teeth on hanging wall

Reverse Fault
boxes on hanging wall

Folded fault with uncertain displacement

Zone of silicic alteration

U-Pb Zircon sample locality

Igneous

Detrital

Limit of Mapping

Limit of Mapping

Rockhill Canyon Fault

Rockhill Canyon Stock

Lee Peak Fault

Lee Peak Fault

Lee Peak Pluton

Rawhide Metagabbro

Wadley Mine Stocks

Inskip Canyon Stock

Range Front Fault

Buena Vista shear zone

Buena Vista Valley

Lee Peak Fault

Lee Peak Fault

Limit of mapping

A

A'

B

B'

C

C'

Fossil Location
(Whitebread, D.H., 1978)

- early Early Ordovician, conodonts (Harris)
- Early Ordovician, conodonts (J. W. Huddle)
- Mississippian, middle Osagean, conodonts (Harris)
- Mississippian, conodonts (Harris)
- probably Mississippian, conodonts (Harris)
- Late Mississippian. (reworked?), conodonts (Repetski)
- mid-Mississippian? thru Pennslyvanian?, conodonts (Repetski)
- Permian, Wordian, conodonts (Wardlaw)
- Permian, Leonardian, conodonts (Wardlaw)

The East Range, Nevada

SCALE 1:24 000

0 1 2 3 4 5
KILOMETERS

1 .5 0 1
MILES

CONTOUR INERVAL 40 FEET

N

James Nutaitis

The East Range, Nevada

SCALE 1:24 000

0 1 2 3 4 5

KILOMETERS

1 .5 0 1

MILES

Cross-Sections

James Nutaitis

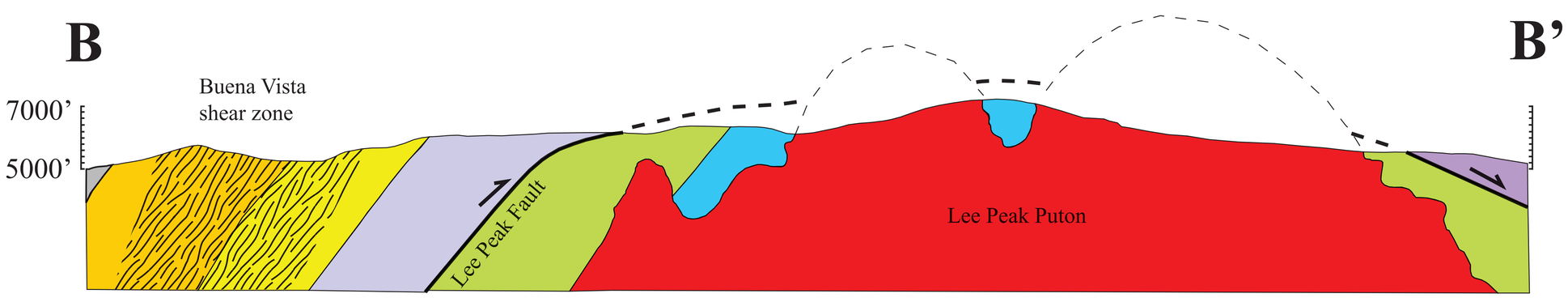

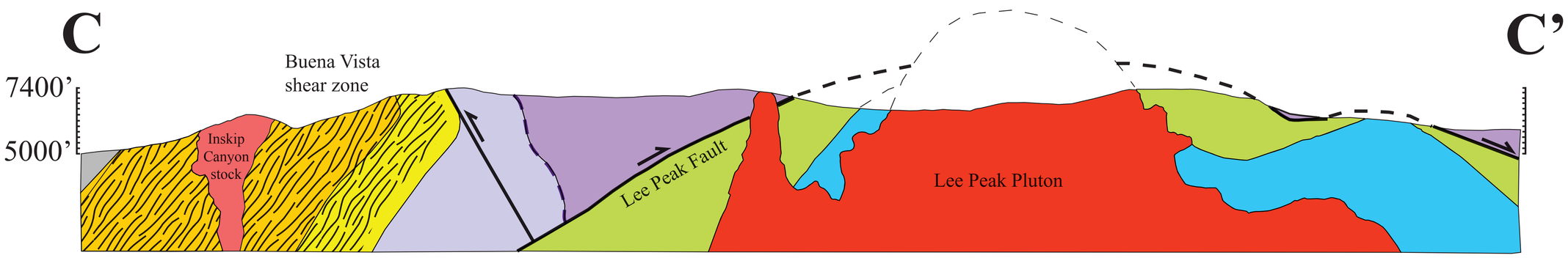

LEGEND

Stratigraphic Units

Mesozoic

Early Triassic
- Koipato Group

Triassic?
- Lee Peak window
- (unlabeled)

Paleozoic

Mississippian - Permian
- Havallah Sequence
- Buena Vista unit

Ordovician
- Valmy Formation
- (unlabeled)
- (unlabeled)

Mississippian
- Inskip Formation
- (unlabeled)
- (unlabeled)

Intrusive Rocks

Cenozoic

- Inskip Canyon stock

Mesozoic

Jurassic
- Lee Peak pluton
- Rockhill Canyon stock

LEGEND

Symbols

Faults

Dashed where inferred, dotted where concealed

Fault with arrow showing relative displacement

Denotes relative motion of strike-slip fault
- approaching wall
- receding wall

Folded fault with uncertain displacement

Buena Vista shear zone